UAB
Universitat Autònoma de Barcelona

THE CHARACTERISATION OF A BALLISTIC FRACTURE PATTERN IN HUMAN LONG BONES

Nathalie Corinne Schwab

ADVERTIMENT. L'accés als continguts d'aquesta tesi queda condicionat a l'acceptació de les condicions d'ús establertes per la següent llicència Creative Commons: https://creativecommons.org/licenses/?lang=ca

ADVERTENCIA. El acceso a los contenidos de esta tesis queda condicionado a la aceptación de las condiciones de uso establecidas por la siguiente licencia Creative Commons: https://creativecommons.org/licenses/?lang=es

WARNING. The access to the contents of this doctoral thesis it is limited to the acceptance of the use conditions set by the following Creative Commons license: https://creativecommons.org/licenses/?lang=en

Universitat Autònoma de Barcelona

PhD dissertation
by

Nathalie Corinne Schwab

THE CHARACTERISATION OF A BALLISTIC FRACTURE PATTERN IN HUMAN LONG BONES

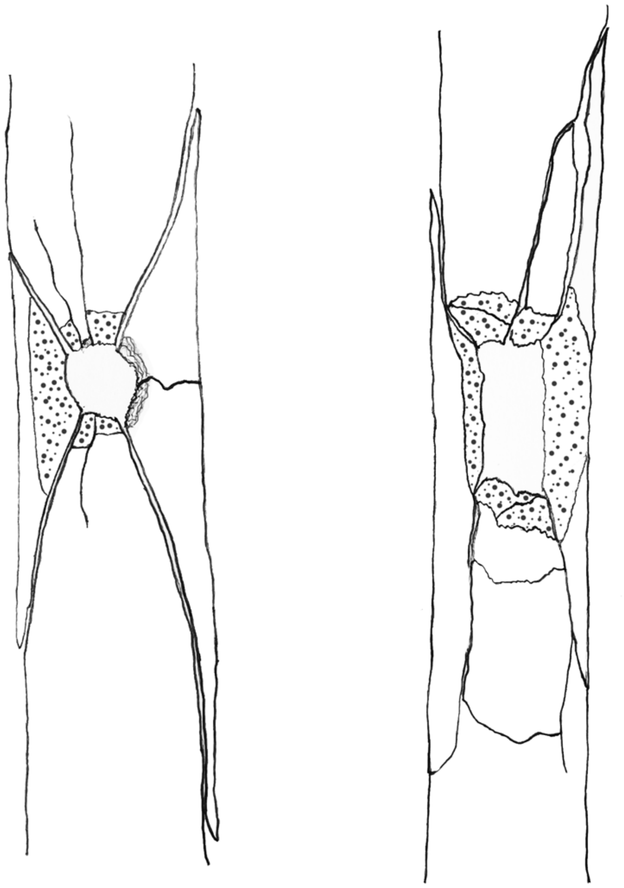

Supervisors: Dr. Ignasi Galtés and Dr. Xavier Jordana
Tutor: Dr. Ignasi Galtés

PhD Program in Biodiversity, Biological Anthropology Unit,
Department of Animal Biology, Plant Biology and Ecology, Faculty of Biosciences

2024

Für meine geliebte Tochter,
lass Dir von niemandem sagen, dass Du etwas nicht kannst.

ACKNOWLEDGEMENTS

First and foremost, I would like to express my deepest gratitude to my two PhD directors, Dr. Ignasi Galtés and Dr. Xavier Jordana - what a perfect match! Your invaluable guidance, insightful feedback, and unwavering support throughout my doctoral journey have been instrumental in the completion of this work. Your expertise and dedication have inspired me to strive for excellence and have considerably enriched my academic experience.

Above all, I am incredibly grateful to Dr. Ignasi Galtés for the opportunity you gave me by accepting my request for a joint research project. Your openness and willingness to start a scientific project with me laid the foundation for this thesis. Thank you for sharing your genuine enthusiasm for forensic science and for always being present whenever needed. I can truly say you are my role model and I am grateful we have met. To Dr. Xavier Jordana, I am in particular thankful for the dedicated involvement of your analytical and logical mind alongside your outstanding statistical skills. By sharing your invaluable perspective on the research, you have enriched my work, lending it depth and precision.

Furthermore, I am profoundly grateful to the Mossos d'Esquadra for their unconditional collaboration, which has been essential for the successful execution of the experiments. It was an enormous pleasure to work with you Joan Soler, Jordi Monreal, Manel Vega, Xavier Garrido and the whole ballistic team. *Un bon dia comença amb un bon esmorzar!*

Many thanks go to the Donor Centre - Barcelona Tissue Bank, Banc de Sang i Teixits de Catalunya, for providing the human bones and thereby making this research possible and so valuable. In this context, my special thanks go to Pedro Brillas for his motivation and effort to help collecting, handling and preparing the human bones for the experiments.

I would also like to thank the Catalonian Institute of Legal Medicine and Forensic Science (IMLCFC) for providing the space and facilities to conduct my research, which were essential for the success of this work.

Further, I want to express gratitude to my alma mater, the University of Basel in Switzerland for their financial support. Their generous funding from the “Research Fund for Excellent Junior Researchers” has enabled me to pursue my research and achieve my academic goals.

Additionally, I am deeply appreciative to Professor Christian De Geyter. Your expertise, mentorship and support during the preparation of the grant application provided a solid foundation for my academic development.

I also wish to thank Professor Eva Scheurer and Professor Roland Hausmann for their encouragement and support in my professional and academic development as a forensic pathologist.

My deepest appreciation goes to my parents, whose unwavering belief in me has been a constant source of strength and motivation. Your presence, encouragement and faith in my abilities have been cornerstones along the way. Thank you for your endless support!

To my dear husband Northon, I am extremely grateful we have met during this journey. I want to express a heartfelt thank you for always listening to me, for believing in me and encouraging me to achieve my goals. Your patience, love, and understanding have been my anchor through the highs and lows of this journey.

I am immensely grateful to my dear friends for their mental support and companionship during this journey. A very special thank you goes to Isabel Boissonnas, Nataliia Sotska and Fabienne Iten.

I would also like to remember and thank Judith Schneider for her endless encouragement and for always believing in me. Her memory continues to inspire and motivate me to pursue my dreams with determination and courage.

Lastly to my beloved daughter Naomi. Your birth has been a source of joy and inspiration, reminding me of the importance of perseverance and dedication. Thank you for bringing light and happiness into my life. May you always follow your dreams!

ABSTRACT

Introduction: In badly preserved cadavers and skeletal human remains, assessing the cause and circumstances of death constitutes a major challenge. When forensic evidence cannot be taken from the skin and soft tissue, the information may only be deduced from more resistant elements such as bone. Whereas cranial gunshot injuries have been well studied, reliable data on the fracture patterns in ballistic long bone trauma remains scarce. Yet, the correct interpretation of long bone fractures can be highly relevant for a better understanding of the circumstances surrounding death. More knowledge on the ballistic fracture pattern in human long bones is needed to render the forensic trauma interpretation and reconstruction more reliable.

Objectives: The main aim of this thesis was to gain more knowledge on the ballistic fracture pattern in human long bones. In addition, alternative surrogate and animal models were tested for their suitability to substitute human bones in gunshot trauma experiments.

Material and methods: For this study real human bones, bone surrogates and animal bones were subjected to ballistic trauma. All biological bones were fresh and dissected from the soft tissue. In total, 29 human bones, 16 femurs and 13 humeri, were collected from deceased adult body donors. As an alternative surrogate model two different polyurethane cylinders from Synbone®, 10 of each, were selected. As an alternative animal model, 4 femurs from female red deereviden were included. Each 10 human femurs and humeri, alongside all alternative models were embedded in Clear Ballistics Gel® to simulate soft tissue. The remaining 6 femurs and 3 humeri were shot without a soft tissue simulant. The shaft centre of all specimens was perpendicularly shot with a 9 mm Luger full metal jacket bullet at an impact velocity of 360 m/s from a distance of 2 m. The fractures were reconstructed and examined macroscopically. The fracture characteristics were defined for each sample group and compared between each other. In doing so, the alternative models were evaluated using the human bones. The characteristics found in the human bones were further analysed for potential correlations with bone properties such as cortical thickness, shaft diameter and bone length. In addition, they were tested for any correlation to the presence of Clear Ballistics Gel®.

Results: A distinct ballistic fracture pattern in human long bones was characterised. Hereby, the cortical characteristics could be divided into entrance, exit and general traits. With regard to the comparison between the human and alternative models, consistently comminuted fractures with a stellate pattern at the impact side was observed. However, despite some general similarities, neither of the two alternative models completely reproduced the fracture characteristics seen in the human bones. Comparing the two alternative models, the surrogate model revealed more significant differences to the human fracture than the animal model. With regard to comparisons among the human samples, some traits showed different occurrence values in relation to bone properties and the presence of Clear Ballistics Gel®.

Discussion and conclusion: This thesis reveals new insights in the ballistic fracture pattern of long bones. Concerning the usage of alternative models for ballistic experiments, the findings call caution in extrapolating fracture characteristics to human bones. The deer femurs did mainly not permit an as precise fracture reconstruction as the human bones due to a massive fragmentation. The Synbone® surrogates showed different traits leading to the assumption of a different failure mechanism than real bone. The findings underpin the challenge in deploying an accurate alternative trauma model in order to replace human material for ballistic experiments.

A distinctive ballistic fracture pattern was characterised based on the experiments with the human bones. The results not only allow the interpretation of a gunshot injury, but also provide important information for event reconstructions due to the discrimination between bullet entrance and exit. All evaluated cortical traits were reproduced in both humeri and femurs. This might lead to the assumption that they may be valid for other long bones, too. Nonetheless, some of the traits' occurrence values correlated with bone properties such as cortical thickness, shaft diameter or bone length. The presence of ballistic gel also influenced some characteristics, emphasising the relevance of using a soft tissue simulant in osseous gunshot experiments.

The new evidence presented in this thesis may contribute to a clearer guidance to identify gunshot trauma in human long bones. This can be particularly valuable for forensic anthropologists and pathologists when investigating bone trauma in badly preserved cadavers or skeletonised remains that lack correlations with soft tissue findings. Nevertheless, due to the dynamic nature of gunshot incidents, more research is needed to evaluate to which extent the ballistic fracture pattern alters when ballistic variables and bone characteristics change.

TABLE OF CONTENTS

1. INTRODUCTION

1.1. The relevance of gunshot trauma in the forensic field

The investigation of death and the surrounding circumstances in medicolegal situations is an interdisciplinary duty among various investigative authorities. Forensic pathology and anthropology are specialties that apply medical and biological scientific expertise to law, both civil and criminal, as well as to international humanitarian and human rights law aiming at supporting justice. One of the main tasks of forensic pathologists and anthropologists is to recognise, analyse and reconstruct traumatic findings. In doing so, they intend to create a record of the events occurred and provide important evidence in case of committed crimes. Yet, the type of human tissue the specialist must deal with, can vary fundamentally. Whilst forensic pathologists investigate corpses at a different degree of preservation, forensic anthropologists traditionally analyse skeletonised human remains. In some cases, such as the interpretation and reconstruction of injuries in badly preserved bodies, it is becoming more frequently a multidisciplinary task in which the expertise from both, forensic pathologists and anthropologists, can complement each other. When forensic pathologists carry out the postmortem examination, they routinely do not have the time to collect, clean, assemble and thoroughly analyse fractured bones [1]. Such an in-depth and time intensive approach to interpret skeletal trauma usually requires the expertise of a forensic anthropologist.

In both scientific fields, the investigation of firearm injuries is a frequent and relevant challenge. Gunshot trauma is not only widespread in armed conflicts, but also in the frame of civil violence [2–5]. With the expanding industrial production of firearms since the 19th century, gunshot trauma is increasing worldwide, also in Europe [4, 6–10]. In 2017, it was estimated that over 1 billion weapons were in circulation, of which 857 million were in civilian possession [11, 12]. This corresponds to an increase of 32% compared to the estimates from 2006 [12]. As a health consequence, gunshot trauma essentially affects the population's mortality and morbidity. Firearm violence has thus been recognised as a global public health issue with a growing tendency [13]. In 2016, between 195'000 and 276'000 people were reported to have died from gunshot injuries, the majority of which were homicides [12]. Other authors estimate the number of annual deaths caused by firearms to be around 400’000 to 500’000 [4, 14]. In 2019, it was revealed that globally around 44% of all homicides are associated with firearm offences [14].

1.2. Ballistic principles of gunshot injuries

Gunshot injuries are produced by a fast-acting force, such as a projectile discharged from a firearm [1]. To better comprehend how ballistic wounds are caused, some basic knowledge on firearms and ammunition is mandatory. Theoretically, firearms can be subdivided into many different categories based on aspects like the general structure and design, the mode of operation, the detailed construction of the barrel, the mechanism of firing and reloading cartridges, the historical evolution, etc. [15, 16]. To complicate matters, the classification and nomenclature differ in the literature. Attempting to cover all available varieties of firearms and ammunition, including the exotica, would go beyond the scope of this thesis. Principally, most authorities acknowledge the facilitated classification of modern weapons into small arms (handguns) and long arms. Handguns, namely pistols and revolvers, can be fired whilst held in one hand. The barrel is rather short and the velocity of a fired bullet is typically between 250 m/s and 400 m/s [17]. Long arms, for example rifles and shotguns, are designed to be operated with two hands. The barrels are long which has an increasing influence on the bullet’s speed during the shot. Typical bullet velocities in shots from rifles range from 600 m/s to 1000 m/s [17]. Next to the firearm, the ammunition has a relevant impact on the development and severity of gunshot injuries. Although the requirements that pistol and rifle ammunition fulfil differ greatly, their principal composition is similar [15]. Both, classical handgun and rifle cartridges consist of a casing that contains a primer, a propellant (gunpowder) and a single projectile [18]. In a loaded firearm, a shot is released by pulling the trigger. The primer is struck by a so-called hammer, explodes and ignites the propellant. The expanding combustion gases provide the propulsion to drive the projectile out of the barrel to hit the target. It is important to know that the composition and construction of the projectile itself varies too [15, 16]. Not all possible materials and designs can be introduced here, but the most commonly used bullets consist of a lead core and are either conclusion or semi-jacketed. The former are also referred to as full metal-jacket (FMJ) projectiles.

Their soft lead core is surrounded by a robust metal casing resulting in a stable, non-expanding, deep-penetrating projectile which is considered very reliable. In comparison, semi-jacked projectiles are only partially surrounded by the metal casing. They have an exposed lead point resulting in an immediate deformation and expansion upon impact and can severely fragmentate in the body.

The science of mechanics dealing with the flight, behaviour and effects of projectiles discharged from firearms is referred to as ballistics. This scientific subject can be subdivided into three main topics: internal, external and terminal ballistics. Internal ballistics considers the effects on the projectile within the firearm. External ballistics deals with the behaviour of the bullet during the flight between the muzzle and the target. Terminal ballistics focus on the interactions between the bullet and the target. In case the target is a body, usually the term wound ballistics is used referring to the analysis of the projectile's behaviour within body tissue and its causing injuries.

Understandably, wound ballistics is the area that forensic pathologists and anthropologists deal with the most. The extent of ballistic injuries depends on the characteristics and interaction of both, projectile and tissue [19]. The impact kinetic energy of a bullet is given by its mass and velocity ($Ke = 0.5\ mv^2$). Compared to other types of trauma such as blunt or sharp force, the impact velocity in gunshot trauma is much higher and usually given in metres per second, rather than kilometres per hour [1]. Besides the mass and velocity, the shape, deformation, orientation as well as yaw of the projectile have to be considered in order to understand how destructive energy is transferred to the tissue [20]. The latter is the manner in which a projectile tumbles sideways during the flight. With increasing speed, the bullet is more stable because it spins faster and the yaw decreases. In a typical gunshot with bullet penetration, the projectile crushes the surface and enters the body [1]. Its path continuous in the body and forms a wound channel by disrupting the tissue. In doing so, typically a permanent and a temporary cavity is formed [18, 21]. During the macroscopic wound inspection of a body, the first is a visible, approximately linear defect correspondent to the bullet's trajectory. It is provoked by the projectile's shearing and compressive forces which do not permit the tissue to fall back into the wound path [22]. In comparison, the temporary cavity is the much greater tissue damage, especially with increasing bullet velocities, yet more difficult to visualise. Next to the amount of the released kinetic energy, it is based on the tissue's elastic behaviour and cohesiveness upon projectile penetration [18]. Hereby, the tissue is forced to expand, but retracts promptly as the bullet passes [22]. Dependent on the projectile's kinetic energy, it either leaves the body and creates an exit wound or becomes embedded in the body.

1.3. The forensic interpretation of gunshot wounds

Soft tissue injuries typically show characteristic features at first sight, permitting conclusions on the applied mechanical force [23]. The examination of soft tissue in ballistic wounds not only enables the differentiation from other type of trauma but yields further essential information for the forensic event reconstruction [23]. Specifically in gunshot trauma, the wound characteristics allow the discrimination between bullet entrance and exit. Besides that, they can indicate further important clues such as information on the shooting distance or impact angle.

It is however important to understand, that the examination of a well-preserved body differs widely from the examination of corpses in poor condition such as those which are severely decomposed, burnt, scavenged, mummified, saponified, mutilated or otherwise damaged [24]. In badly preserved bodies evidence taken from the skin and soft tissue often remains inconclusive.

Consequently, the reconstruction of trauma and death may only be deduced from elements more resistant to destruction such as bone. The resistance of bone can be attributed to its special tissue structure. In comparison to soft tissue, bone has a high mineral content besides its organic component [25]. Even though signs of trauma usually persist in bone, to date, reliable forensic conclusions have been quite limited [26–28].

The literature reveals that most of the gunshot injuries affect the bone [29]. And still, compared to the well accepted wound characteristics of soft tissue, the data on osseous gunshot characteristics is comparatively weaker. As a consequence, it can be fairly difficult to clearly distinguish ballistic injuries from other types of bone trauma. This addresses for instance the distinction between gunshot wounds and perforations caused by arrows, spears or other pointed objects [30]. Although firearms usually generate higher kinetic energies, the risk of misinterpretations have been reported [30–32]. Furthermore, it can be a challenge to securely distinguish gunshot trauma from blunt force trauma, despite the considerable difference in the underlying biomechanical mechanism [33, 34]. This problem arises in particular when the skeletal remains are shattered or incomplete.

1.4. Ballistic long bone trauma

There is a discrepancy in the literature between the amount of ballistic data for the different bone types. Scientific studies concerning gunshot trauma have mainly been carried out to analyse cranial fractures, whereas gunshot injuries to long bones were given less attention [35–37]. Since one of the main tasks of forensic pathologists and anthropologists is to determine the cause of death, one may explain this difference in interest with the extremely deadly potential of cranial gunshots. Besides that, ballistic long bone trauma also appears to be more difficult to analyse than cranial fractures due to the relatively small diameter of long bones resulting in small fragments with close proximity [38].

Nonetheless, the literature reveals that at least 50% of all gunshot injuries affect the extremities and that they often result in fractures of the long bones [29, 39–41]. In this regard, it has been claimed that the femoral shaft fracture is the most common injury among all ballistic long bone fractures [41]. On the one hand, the life-threatening consequences of a shot to the limbs, especially if left untreated, should not be underestimated [42]. For instance, in particular shots towards the upper arm and thigh have been considered as potentially deadly. In those cases, it was recognised that comminuted fractures of the humeral and femoral shaft would often affect the brachial and femoral artery respectively, resulting in severe blood loss and haemorrhagic shock [42]. On the other hand, the correct interpretation of long bone fractures can be highly relevant for a better understanding of the circumstances surrounding death. With regard to forensic event reconstructions, they can provide important information about the position or movements of a body during the incident [43]. For example, gunshot wounds in the upper extremities may be caused during a defensive posture, sustained by covering other body parts or the vitals [43].

Despite the relevance of ballistic long bone trauma, there is little data in the literature than can be used for the forensic trauma reconstruction. In 1915, Bland-Sutton described five types of ballistic fractures in human long bones [44]: a projectile impacting a long bone can result in a transverse fracture, completely pierce the diaphysis, stay embedded in the bone, strike the diaphysis and produce a stellate or butterfly pattern, and/or shatter the bone into small fragments. On the one hand, this work solely describes potential ballistic fracture types from a general point of view without providing an in-depth analysis of detailed characteristics. On the other hand, an actualisation based on current ballistics is required because firearms and projectiles have changed since 1915. Thereafter, the majority of the experimental research using human long bones has focused on the fracture pathophysiology and risk prediction in relation to different ballistic variables [5, 45–48]. In the sixties, Huelke et al. used steel spheres with various sizes and velocities to quantify the energy transmitted by the projectiles [46–48]. In the eighties, Ragsdale & Josselson targeted on cancellous rich bone areas of distal femurs and proximal tibias, which do not allow the best analysis of cortical bone behaviour [49]. Robens and Küsswetter showed findings in X-rays after gunshot to the metaphyseal part of tibias [50]. Also Coudane et al. studied bone lesions with X-rays after producing gunshot injuries to the limbs of two dead bodies [51]. More recently, Dougherty, Sherman and Bir investigated indirect gunshot impact on diaphyseal femurs and tibia [5]. Bir et al. analysed the fracture risk prediction based on velocity, producing both direct and indirect ballistic fractures in human femurs and long bone polyurethane surrogates [45].

Aside from these few interventional studies, research on ballistic trauma to human long bones has essentially remained observational [38, 41, 52–54]. The limitation of descriptive studies, however, is that information on ballistic variables, such as the used firearm and ammunition, the impact speed and angle as well as other variables usually remain unrevealed.

Apart from forensic investigations, ballistic long bone trauma has been subject of clinical medical research [3, 41, 53–59]. However, these studies usually have a different purpose. Their relevance relates to clinical aspects like the treatment, healing process and general prognosis of ballistic injuries. In contrast, the detailed description of the fracture characteristics useful for forensic trauma interpretation and event reconstruction is generally out of the scope of clinical medical studies.

In a more recent review from 2022, Veenstra et al. studied publications providing data on ballistic fractures observed in long bones [60]. The work revealed different types of fractures as a result of gunshot trauma, including linear, oblique, butterfly and comminuted fractures.

Complicating the characterisation of ballistic fracture patterns, it must be considered that long bones have an inhomogeneous distribution of cortical and cancellous bone tissue. The diaphysis resembles a cylinder of thick cortical bone, with a rather low cancellous bone component inside the shaft. In comparison, the metaphysis and epiphysis are more cancellous rich areas, with a quite thin cortical wall. In this regard, it has been suggested that this variation in the ratio between cortical and cancellous bone has an effect on fracture patterns in long bones [61].

1.5. The need for more knowledge on ballistic fracture patterns in long bones

The main issue of the literature on ballistic long bone trauma is that detailed fracture characteristics, such as cortical traits are barely provided. This renders a correct forensic interpretation and reconstruction of osseus gunshot wounds and the differentiation from other types of trauma somewhat difficult. This is why more specific data, that forensic pathologists and anthropologists can rely on during the bone trauma analysis, is highly needed. This in turn gives rise to the need for further research in this area.

In this context, it should be noted that forensic research has traditionally been characterised by data obtained from single case reports [62]. Although they constitute a starting point for hypothesis-based systematic research in forensic science, they have a rather low scientific evidence level. The preference for this format may result from financial and infrastructural restraints and in particular from ethical barriers rendering experimental simulation of anecdotal single events difficult or impossible [62, 63]. As a consequence, experimental research in the forensic field is generally scarce. Nevertheless, high-quality experimental studies are essentially needed to generate a standardised knowledge base for the forensic interpretation of findings and to adapt current quality standards to present-day technical development [62].

With respect to ballistic long bone trauma, a crucial method to gain further knowledge on the detailed fracture patterns are thus experimental studies. In doing so, the fractures can be reproduced under controlled conditions and the fracture mechanism can be better understood. Naturally, the use of real human bones is the most reliable experimental model for this purpose. In addition, the bones should be fresh in order to reproduce as realistic fracture patterns as possible [25, 64–66]. In this context, fresh bones are considered moist or wet, because they contain water as well as organic components such as lipids and collagen [65]. These components influence the biomechanical properties, as they give the bone a certain elasticity in addition to its mineral rigidity. Yet, one has to consider that acquiring fresh human material for experimental research is not easy due to ethical barriers along with complex tissue handling and preservation. This explains why there is growing interest in finding a valid alternative model for such trauma experiments.

A suitable analogue to replace human tissue for ballistic trauma recreations should feature a similar energy dispersion and fracture mode, despite the microstructural particularity of different materials. In the past, both surrogate material and animal bones have been used for experimental ballistic research. Initially, bone surrogates produced by Synbone® AG (Switzerland) were developed for surgical training. Due to the demand for an appropriate bone analogue for forensic testing and event recreation, the company has designed special models to react in the same way as bone during ballistic impact [67]. The surrogates are made from polyurethane and are formed into different models to simulate gunshot trauma in various types of bone. Synbone® produces anatomical bone models and simplified cylinders. According to the manufacturer, the latter were especially designed for ballistic testing. Few articles have been published using both, the anatomical models and simplified cylinders for gunshot experiments [45, 68, 69]. For instance, Bir et al. analysed the fracture risk prediction based on the bullet velocity producing direct and indirect gunshot trauma [45]. Alongside human and Synbone® femurs, they also assessed a polyurethan femur from another manufacturer named Sawbone®. Interestingly, the authors claimed similar fracture patterns in Synbone® surrogates and human femurs, whilst the Sawbones® fractures were too dissimilar to the human ones. Kneubuehl and Thali compared ballistic impacts between Synbone® cylinders and porcine femurs and tibias, revealing that the bullet's energy loss, bullet deformation, bone fragmentation and the penetrating wound channel were similar [69]. In an experimental study from Henwood et al., it was shown that the Synbone® cylinders behaved more like porcine bone than the anatomical Synbone® models [68]. In contrast to the latter, the Synbone® cylinders and porcine bones presented comminuted fracture and a similar amount of the energy lost by the projectile upon impact. The authors claimed that the Synbone® cylinders may be used for ballistic impact tests to some extent, but drawing conclusions on fragment sizes or fracture propagation patterns were not recommended. However, these models were validated in comparison with porcine bone and not human bone.

Animal bones have played an important role in forensic experimental research too. As mentioned in the studies from Kneubuehl and Thali [69] and from Henwood et al. [68], porcine bones are a preferred animal model. The latter authors inflicted in another study gunshot trauma to pig shoulders and assessed whether the osseus entrance wound allows to determining the type of projectile with respect to its material structure and calibre [70]. Furthermore, also Zhang et al. used porcine bones [71]. The authors analysed the transient indirect effect of rifle projectiles on bone in gelatine-bone composite targets.

However, it is well known that there is no animal long bone that consistently resembles the human. In terms of morphology and biomechanical properties, Kieser et al. found deer femurs were the least dissimilar from human femurs compared to pig and sheep bones [72]. In experimental studies, the same authors have used female deer femurs to produce remote and indirect ballistic fractures, whereby in both cases wedge-shaped fractures were reported [73–75].

Nevertheless, in summary, detailed ballistic fracture patterns in different models have not been clearly defined yet. Thus, the question as to whether alternative surrogate and animal models are suitable to reproduce the fracture patterns of human long bones remains to be answered. This is a highly relevant query in forensic experimental research as the application of inappropriate alternative models can lead to useless, irrelevant, or even misleading information [76, 77].

2. OBJECTIVES

The main purpose of this research is to enhance the current knowledge on the fracture characteristics of ballistic long bone trauma in order to improve the distinction from other types of trauma. Providing guidance for the assessment of ballistic long bone trauma could be of great interest for forensic pathologists and anthropologists when interpreting and reconstructing gunshot events.

With this general purpose the following specific objectives have been defined:

1. To establish a valuable setup for long bone gunshot experiments.
2. To macroscopically characterise a distinct ballistic fracture pattern in human long bones.
3. To test the suitability of alternative trauma models for gunshot experiments such as synthetic and animal bones.
4. To assess the influence of bone features and the presence of soft tissue on the human fracture pattern.

3. STRUCTURE OF THE DISSERTATION

This is a publication-based dissertation that consists of two comprehensive original communications that have been published in internationally renowned scientific journals:

1. Schwab, N., Jordana, X., Soler, J., Garrido, X., Brillas, P., Savio, A., Lavín, S., Ortega-Sánchez, M., Galtés, I. (2023). Can Synbone® cylinders and deer femurs reproduce ballistic fracture patterns observed in human long bones?. *Journal of Materials Science*, *58*(11), 4970-4986. https://doi.org/10.1007/s10853-023-08333-6

2. Schwab, N., Jordana, X., Monreal, J., Garrido, X., Soler, J., Vega, M., Brillas, P., Galtés, I. (2024). Ballistic long bone fracture pattern: an experimental study. *International Journal of Legal Medicine*, 1-16. https://doi.org/10.1007/s00414-024-03191-6

The first publication evaluates different gunshot long bone models and addresses the objectives 1, 2 and 3. The second publication focuses on the characterisation of a ballistic fracture pattern in human long bones useful for the forensic trauma interpretation and addresses the objectives 1, 2 and 4.

4. MATERIALS AND METHODS

4.1. Samples

For this study real human bones, bone surrogates and animal bones were subjected to ballistic trauma. The general sample characteristics are summarised in Table 1.

Table 1 Sample group description (Fem = femur, Hum = humerus, Gel = samples embedded in ballistic gel, no Gel = samples without ballistic gel) revealing the gender and age if specified, the length, the shaft diameter and the cortical thickness (the numbers represent the mean and standard deviation, and below the *min - max value*).

Model type	Sample group	N	♂	♀	Age	Bone length (cm)	Shaft diameter (cm)	Cortical thickness (mm)
Human	Fem Gel	10	10	0	62 (5.4)	45.9 (2.8)	2.9 (0.3)	6.2 (0.8)
					55 - 71	*43.0 - 52.0*	*2.5 - 3.3*	*5.0 - 7.0*
Human	Fem no Gel	6	2	4	66 (4.9)	44.9 (2.4)	3.0 (0.1)	4.3 (1.5)
					62 -72	*41.8 - 46.9*	*2.9 - 3.0*	*3.0 - 6.5*
Human	Hum Gel	10	10	0	61 (5.0)	32.5 (1.9)	2.1 (0.2)	3.6 (0.8)
					55 - 71	*30.6 - 36.6*	*1.9 - 2.4*	*3.0 - 5.0*
Human	Hum no Gel	3	1	2	61 (4.0)	31.0 (0.8)	1.8 (0.5)	3.7 (1.5)
					56 - 63	*30.5 - 31.9*	*1.5 - 2.3*	*3.0 - 5.0*
Synbone®	Fem cylinder	10				27.0	3.0	5.0
Synbone®	Hum cylinder	10				27.0	3.0	3.0
Animal	Deer femur	4		4		22.4 (0.7)	1.9 (0.1)	3.8 (0.3)
						21.6 - 23.3	*1.8 - 2.0*	*3.5 - 4.0*

4.1.1. Human bones

In total 29 fresh human bones, 16 femurs and 13 humeri, were used for this study. All bones were provided by the Donor Centre - Barcelona Tissue Bank, Banc de Sang i Teixits de Catalunya. They were donated from a total of 14 cadavers, 12 males and 2 females. Informed consent was obtained from their next of kin. Donor age at death was between 55 and 72 years. All bones were collected with a postmortem time interval of up to 24 hours. They were entirely dissected from the limbs while parts of the muscles remained attached in order to prevent desiccation (Figure 1a). The samples were individually wrapped in plastic bags and stored in the freezer at the

Institut de Medicina Legal i Ciències Forenses de Catalunya (IMLCFC) and at the Universitat Autònoma de Barcelona (UAB) until further use. Prior to the experiments, the bones were completely thawed. The remaining soft tissue was removed up to the periosteum with the usage of surgical tools, wooden spatula and paper (Figure 1b). Subsequently, each bone was macroscopically investigated to exclude pathologies or damage. Each bone was measured for maximum length and mid-shaft diameter. The centre of the anterior shaft aspect was highlighted with a permanent marker to indicate the point of target. As the diaphysis has a high corticalis-spongiosa-ratio, it allows the best analysis of cortical bone behaviour and hence is more informative than cancellous rich areas near the epiphysis.

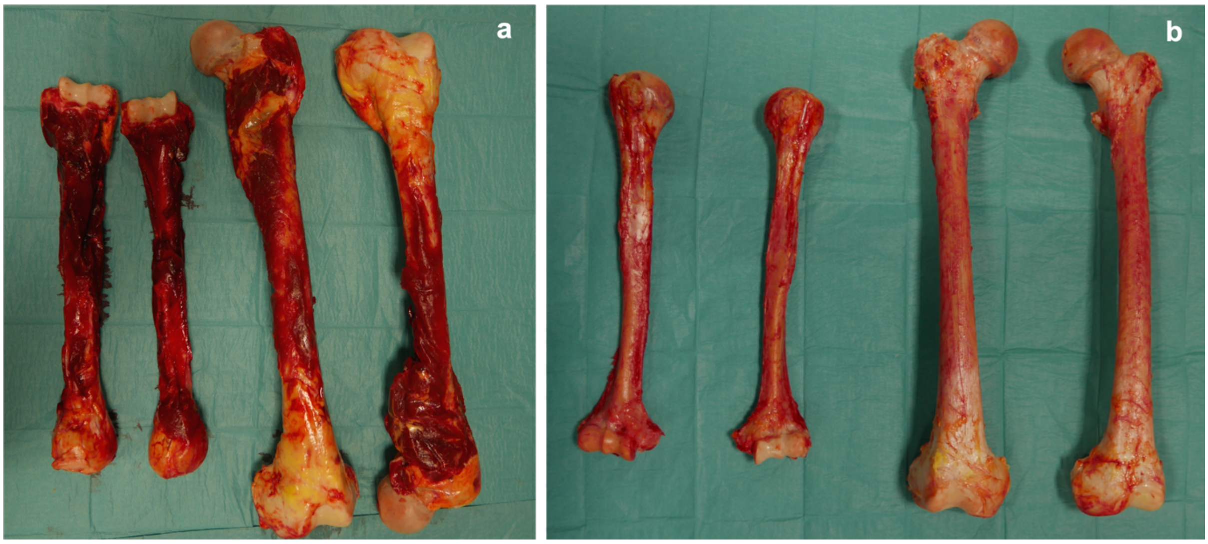

Fig. 1 Human humeri and femurs **a** with soft tissue and **b** without soft tissue.

4.1.2. Synthetic bones

Cylindrical surrogates from the manufacturer Synbone® were chosen for this study. These geometrically simplified models simulate a long bone shaft and were especially developed for ballistic testing. They are made out of polyurethane and are covered with a rubber skin simulating the periosteum of real bone. Two different types, of each ten, were selected (Figure 2). Model PR0108.G is hereafter referred to as femur cylinder as its wall thickness is similar to the human femur. Model PR0109.G is hereafter referred to as humerus cylinder as its wall thickness is similar to the human humerus. The point of target was highlighted with a permanent marker in the centre of the cylinder.

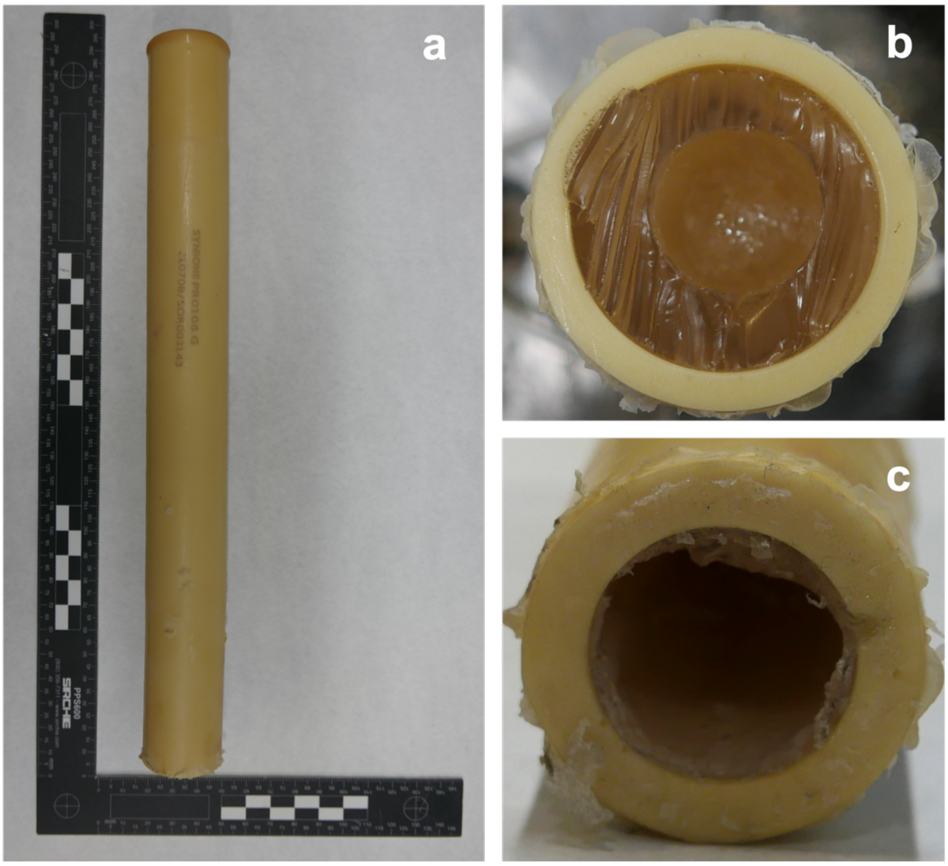

Fig. 2 a Example of a Synbone® cylinder, transversal view of a **b** humerus cylinder and **c** femur cylinder.

4.1.3. Animal bones

The Faculty of Veterinary of the UAB provided four healthy, entire, undamaged, fresh femurs from wild-shot, young adult, female red deer (*Cervus elaphus*). The animals were shot for hunting reasons. The femurs were dissected with little soft tissue attached, leaving the periosteum intact (Figure 3). They were individually wrapped in plastic bags and kept in the freezer of the IMLCFC until further use. Analogous to the human bones, the deer femurs were measured for maximum length and mid-shaft diameter. The centre of the anterior shaft aspect was highlighted with a permanent marker to indicate the point of target.

Fig. 3 Partially skeletonised leg of a red deer with the femur on the right side.

4.2. Gunshot experiments

In collaboration with the Mossos d'Esquadra, Catalan police, the experiments were carried out in their scientific laboratory (Laboratoris de Policia Científica, Divisió de Policia Científica dels Mossos d'Esquadra). All staff were instructed in appropriate handling technique and complied with ethical principles.

4.2.1. Production of gel blocks

In order to simulate soft tissue, the samples were embedded in ballistic gel, with the exception of 9 human bones. A product from the Canadian brand Clear Ballistics was used (Clear Ballistics Gel®), which is supplied as a ready mixed, solid block that requires to be melted at 100°C for 4 to 5 hours before individual application. The Clear Ballistics polymer blocks are known for its convenient preparation and exceptional transparency and clearness compared to the standard simulant which is 10% ordnance gelatine [78]. Despite the possibility of reusing this gel, in this study, consistently new gel was employed for the samples.

To surround the samples with Clear Ballistics Gel®, metal moulds were priorly designed (Figure 4 and 5). Those moulds were cylindrical with a diameter of 10 cm. The bones were positioned with the anterior face located 2 cm deep behind the mould’s front surface. The liquid gel was poured into the moulds until the bone shaft was entirely surrounded. Subsequently, the gel was left to solidify overnight at room temperature. The surrogates were analogously embedded in the gel. In addition, the hollow interior of the cylinders was also filled with the gel in order to simulate bone marrow and its exploding reaction to gunshot [69]. Due to the different anatomy of the animal bones a different mould had to be used in order to guarantee an anterior gel thickness of 2 cm. The decision of a 2 cm thick gel layer on the target side was made in accordance with other authors who conducted ballistic experiments [45, 69].

Fig. 4 View from above on four cylindrical metal moulds.

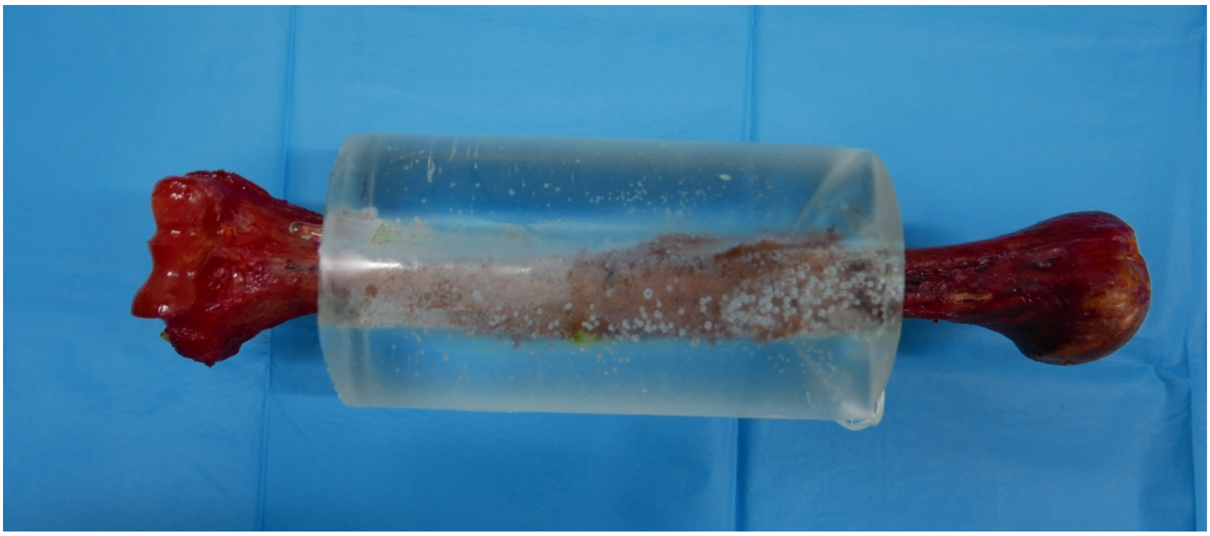

Fig. 5 In ballistic gel embedded shaft of a human humerus.

It was observed that after embedding the models in Clear Ballistics Gel®, numerous very small air bubbles aligned around the shafts. This hampered seriously the analysis of the fracture propagation on the high-speed images later on. Consequently, 9 out of 29 human samples, 6 femurs and 3 humeri, were included to the study and shot without the soft tissue simulant for a better visualisation of the cracking mechanism.

4.2.2. Orthograde fixation of the samples

Each specimen was securely fixed upright using a self-constructed stabilisation device. This device was firmly attached to a table (Figure 6). It consisted of a rigid metal plate on the bottom and an adjustable metal plate on the top. The latter could be moved up or down along a steel bar that connected both plates. By the help of two metal cup stabilizers, on each plate one, the sample extremes were held securely.

Fig. 6 Fixation table and partially depicted light barrier system in the scientific laboratory.

4.2.3. Shooting procedure

The specimens were placed 2 m before the muzzle of a 9 mm Luger test barrel (Drello Bal 1025 FU-R). While the mechanics of test barrels differ to a certain extent from real firearms, they enable precise, reproducible shots and are commonly employed as a method in experimentation. The bullet impact velocity produced by the test barrel was 360 m/s, simulating a shot from a handgun. An optical laser was used to define the point of shooting. This was possible in all samples, as the transparency of the ballistic gel allows exact targeting. For the shots, a NonTox 9 mm Luger full metal jacket projectile from Sellier&Bellot® was used (Figure 7). This ammunition was chosen as the 9 mm Luger full metal jacket projectile is the worldwide most common military handgun cartridge [18]. The mass of the bullet is 7.98 g. On each sample one single projectile was fired in an orthograde manner, whereby the bullet nose struck the middle of the anterior face of the shaft. The exit velocity of the projectile upon impact was measured using a light barrier (Drello LS 11-03) with a computerised system (Drello VC 4043-09). The performance was recorded with a high-speed camera (Phantom V2012). Figure 8 illustrates the experimental set up.

Fig. 7 NonTox 9 mm Luger full metal jacket projectile from Sellier&Bellot®.

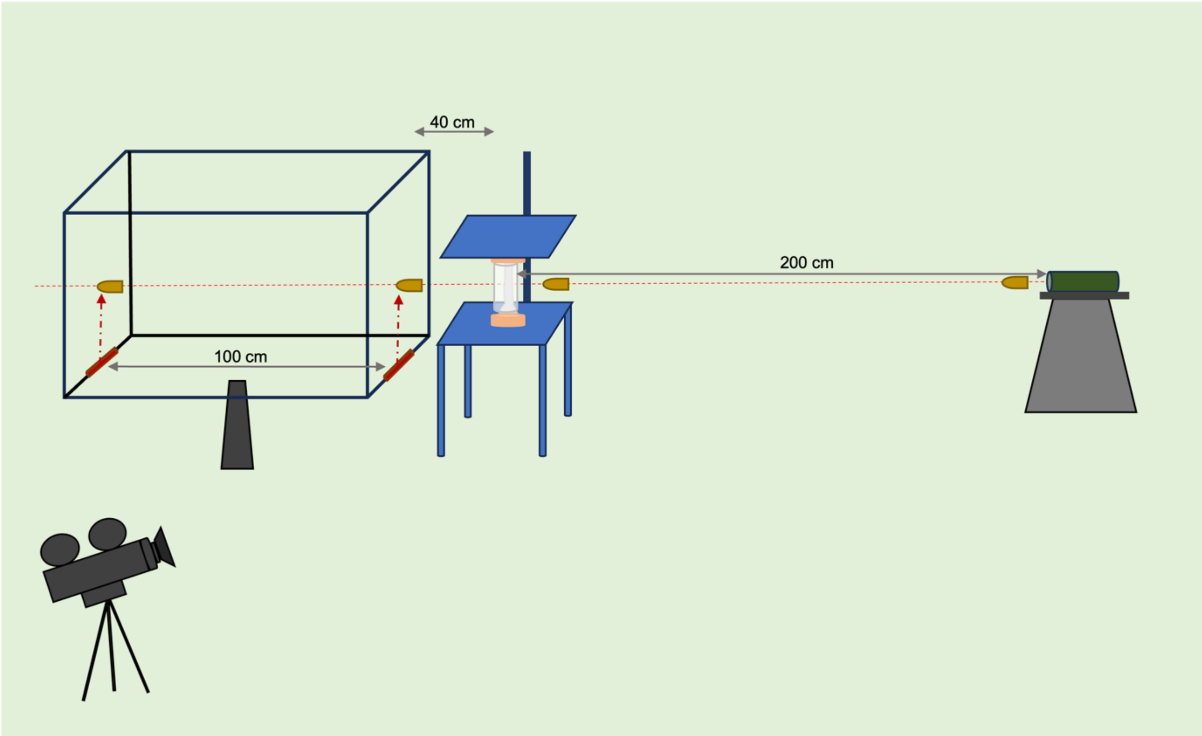

Fig. 8 Experimental set up: Test barrel (green) on the right side, fixation table (blue) with metal cup stabilisers (orange) and bone-gel-sample (light grey). Light barrier with two sensors (red) that measure the time the bullet takes from the first to the second sensor. High-speed camera on the bottom left. Distances: 200 cm between muzzle and bone, 40 cm between bone and light barrier, 100 cm between the first and second sensor of the light barrier. The dashed red line indicates the trajectory of the projectile (yellow-brown).

4.3. Fragment preparation prior to reconstruction

After the shooting, the fractured samples were placed in individual plastic bags and brought to the anthropological laboratory of the IMLCFC. The gel blocks were opened with a scalpel to remove the bone fragments.

4.3.1. Preparing human and animal bones

In order to clear away the remaining soft tissue from the human and animal bones, they were macerated at 100°C in a water detergent solution (one cup of commercial degreasing detergent in 5 litres of plain water) [64]. In doing so, the bone fragments of each specimen were placed in a hand-made bag out of heat-resistant fabric. To guarantee free floating in the boiling liquid and prevent contact to the hot bottom of the pot, the bags were hanged on a stick over the pot. After 2 to 5 hours of cooking, the bones were scrubbed smoothly with a wooden spatula and paper to clear away the periosteum. Subsequently, the bones were rinsed with water and left to dry at room temperature. Figure 9 shows an example of cleaned bone fragments from a shot human femur.

Fig. 9 Bone fragments from a shot human femur after the cleaning process.

4.3.2. Preparing Synbone® surrogates

In contrast to the biological tissue, the synthetic periosteum of the Synbone® surrogates could be smoothly peeled off the fragments without the need of further interventions (Figure 10).

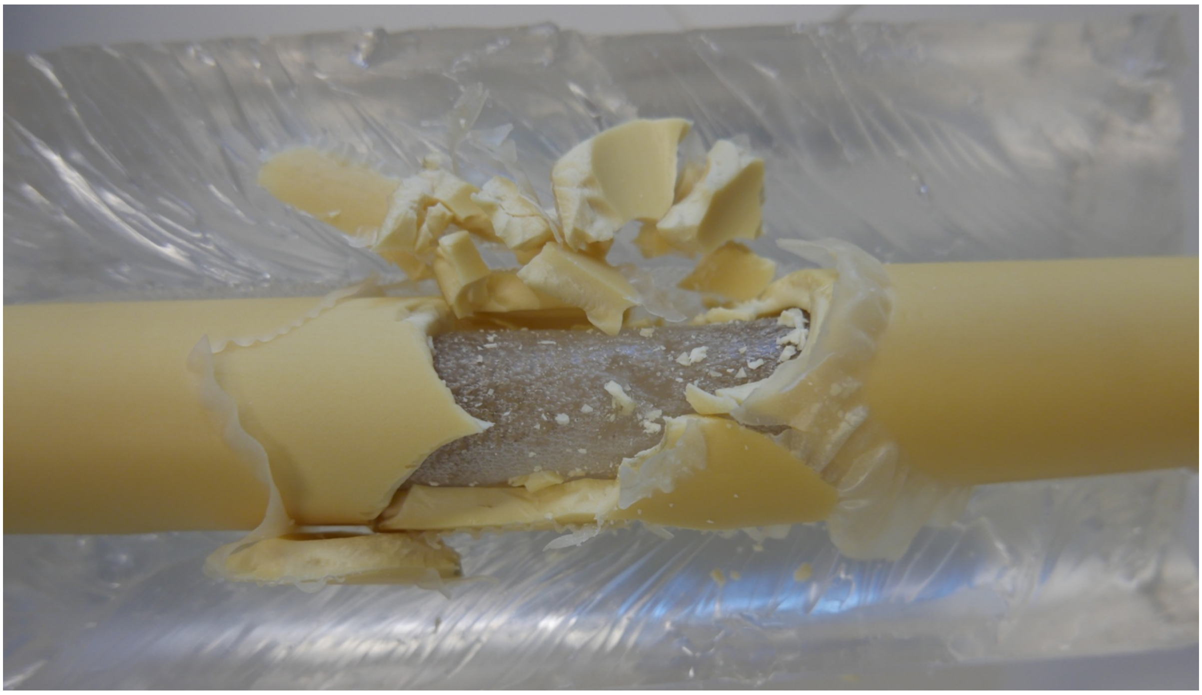

Fig. 10 Fragments of a shot femur cylinder from Synbone® after opening the gel block from the front side. Also visible are the synthetic periosteum and the gel in the cylinder's hollow interior.

4.4. Reconstruction of the fracture

The fragments of each specimen were reassembled with a superglue to better visualise the fracture patterns. This technique is often required and well accepted in the forensic anthropological investigation of fractures [1, 77]. The fracture surfaces and margins were assessed before the application of adhesives.

4.5. Sample assessment

4.5.1. Qualitative fracture variables

All samples were macroscopically examined to define the fracture type and cortical fracture traits. The former was determined by the appearance of the bullet impact side. The latter were subdivided into entrance, exit and general cortical traits.

4.5.2. Quantitative fracture variables

For the quantitative analyses, the cortical thickness at the level of the bullet impact, the maximal longitudinal fracture extent and the horizontal and vertical diameter of the bullets' entrance and exit hole were measured with a calliper. The measurement of the post-impact velocity of the projectiles allowed the calculation of the kinetic energy lost in each sample ($Ke = 0.5\ mv^2$). For the comparison between human, synthetic and animal bone models also the different forms of radiating fracture lines around the bullet entry were counted: longitudinal (lines running along the longitudinal axis towards the epiphysis / cylinder ends), oblique (lines running at an angle to the longitudinal axis of the samples) and transverse (lines running horizontally from the entry point to the posterior aspect of the samples). Any fracture line longer than 5 mm was counted.

4.5.3. High-speed videos

The analysis of the high-speed videos was carried out on human bones shot without Clear Ballistics Gel®. As mentioned before, only those samples permitted an accurate evaluation of the fracture propagation upon gunshot.

4.5.4. Sample group comparison

All carefully gathered data was recorded and archived in a data sheet. The following two sections explain which sample groups have been compared for each part of the study. Figure 11 shows a schematic overview of the two research parts.

For the first part of this study, the fracture characteristics between the human, the surrogate and the animal models were compared [79]. In doing so, results gathered from a preliminary human sample group totalling 14 bones, 7 femurs and humeri each, were used. The alternative sample groups counted all 20 Synbone® cylinders and all 4 deer femurs. The details on materials and methods can be consulted in the respective publication (see *Results* chapter 1).

For the second part of this study, the human sample number was increased in order to acquire more knowledge on the fracture pattern and its underlying mechanism [80]. The fracture characteristics in all 29 human bones were analysed. The human samples were grouped into femurs with and without gel, 10 and 6 respectively, and humeri with and without gel, 10 and 3 respectively. All details on materials and methods can be consulted in the respective publication (see *Results* chapter 2).

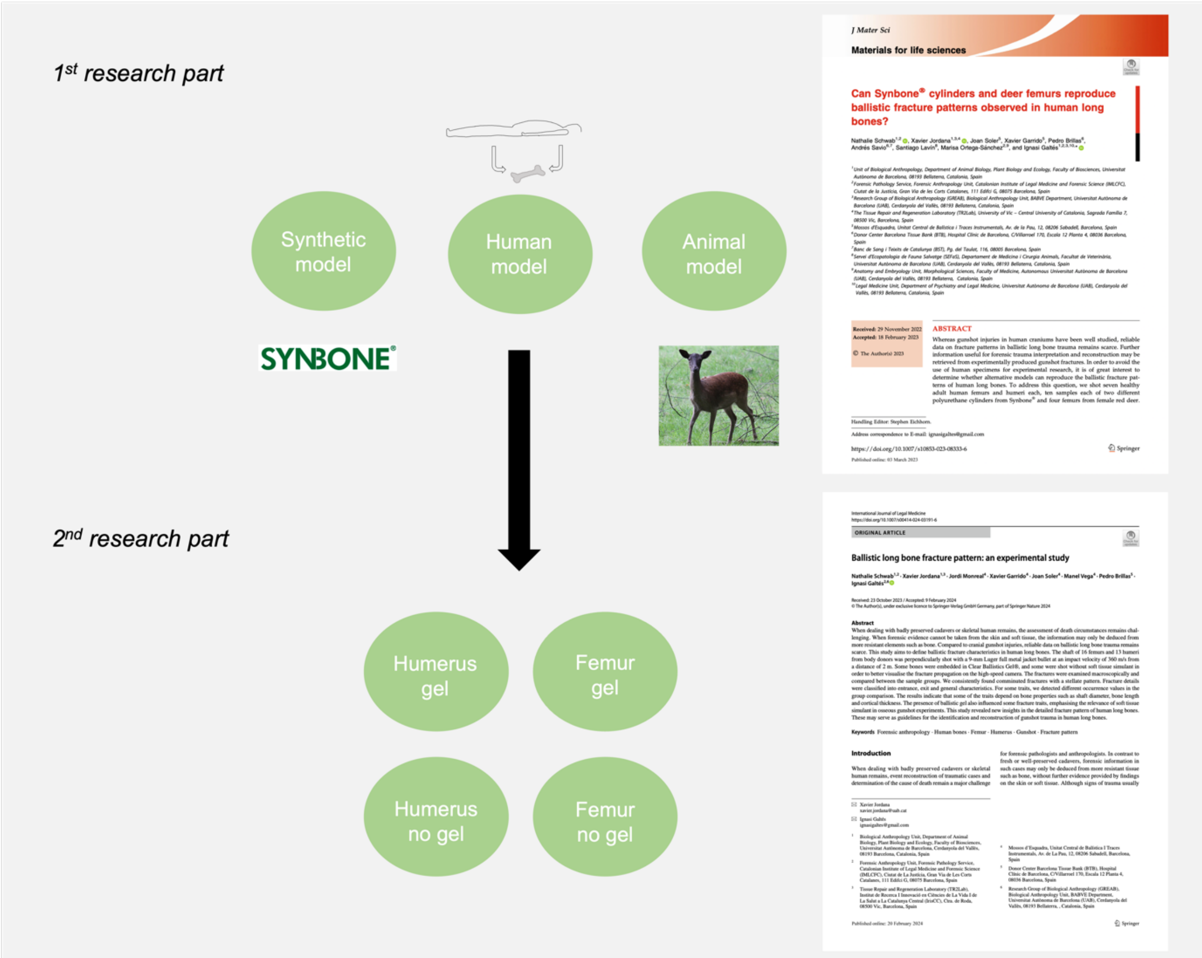

Fig. 11 Schematic overview of both research parts resulting in two publications. The green boxes illustrate the compared sample groups.

4.6. Statistical analyses

The statistical analysis applied for the first part of the research [79] included Pearson's Chi-squared test in order to determine significant differences in the frequencies of the entry, exit and general cortical traits between the sample groups. Contingency coefficients were calculated to correlate the traits with the sample groups. The multivariate correspondence analysis was used to examine correlations and clusters between the fracture traits in the sample groups. The quantitative variables such as entry and exit hole size, fracture extent, percentage of transverse fracture lines and energy loss values were tested for normality and equal variance using Shapiro Wilk and Levene's test. An analysis of variance using One-Way ANOVA was performed.

Games-Howell post hoc test was applied to compare the quantitative variables between the sample groups. Significance level was set at 0.05.

For the statistical analysis of the second part of this research [80] logistic regression and two-way ANOVA were performed to test the effect of Clear Ballistics Gel® and the type of bone (femur and humerus) in the occurrence of fracture characteristics. The significance levels were set at 0.05. A multivariate correspondence analysis was done to demonstrate correlations between the fracture traits (qualitative and quantitative), experimental groups (type of bone and use of Clear Ballistics Gel®) and bone properties (bone length, shaft diameter and cortical thickness).

4.7. Ethical aspects

This study followed the ethical precepts of the Declaration of Helsinki (Fortaleza, Brazil, Oct 2013) and was approved by the local ethics committee (Bellvitge University Hospital, L'Hospitalet de Llobregat, Barcelona; Ref. PR416/20). Human samples were processed according to the guidance for clinical use (EEC regulations 2004/23/CE and 2006/17/CE) and to the legal requirements of Spain (Law 14/2007, RD 1716/2011 and RD 9/2014). All human bone samples were donated anonymously and obtained under informed consent. All samples are stored in the private collection at the Institut de Medicina Legal i Ciències Forenses de Catalunya (IMLCFC) in Barcelona, Spain (Registro Nacional de Biobancos. Ref. C.0004241).

5. RESULTS

5.1. Can Synbone® cylinders and deer femurs reproduce ballistic fracture patterns observed in human long bones?

Authors

Schwab, N., Jordana, X., Soler, J., Garrido, X., Brillas, P., Savio, A., Lavín, S., Ortega-Sánchez, M., Galtés, I.

Journal

Journal of Materials Science. Impact factor and quartile ranking: 4.5, Q2.

Date of publication

18 February 2023

Addressed objectives

This first publication evaluates different gunshot long bone models and addresses the previously defined objectives 1, 2 and 3:

1. To establish a valuable setup for long bone gunshot experiments.
2. To macroscopically characterise a distinct ballistic fracture pattern in human long bones.
3. To test the suitability of alternative trauma models for gunshot experiments such as synthetic and animal bones.

J Mater Sci

Materials for life sciences

Can Synbone® cylinders and deer femurs reproduce ballistic fracture patterns observed in human long bones?

Nathalie Schwab[1,2], Xavier Jordana[1,3,4], Joan Soler[5], Xavier Garrido[5], Pedro Brillas[6], Andrés Savio[6,7], Santiago Lavín[8], Marisa Ortega-Sánchez[2,9], and Ignasi Galtés[1,2,3,10,*]

[1] *Unit of Biological Anthropology, Department of Animal Biology, Plant Biology and Ecology, Faculty of Biosciences, Universitat Autònoma de Barcelona, 08193 Bellaterra, Catalonia, Spain*
[2] *Forensic Pathology Service, Forensic Anthropology Unit, Catalonian Institute of Legal Medicine and Forensic Science (IMLCFC), Ciutat de la Justícia, Gran Via de les Corts Catalanes, 111 Edifci G, 08075 Barcelona, Spain*
[3] *Research Group of Biological Anthropology (GREAB), Biological Anthropology Unit, BABVE Department, Universitat Autònoma de Barcelona (UAB), Cerdanyola del Vallès, 08193 Bellaterra, Catalonia, Spain*
[4] *The Tissue Repair and Regeneration Laboratory (TR2Lab), University of Vic – Central University of Catalonia, Sagrada Família 7, 08500 Vic, Barcelona, Spain*
[5] *Mossos d'Esquadra, Unitat Central de Balística i Traces Instrumentals, Av. de la Pau, 12, 08206 Sabadell, Barcelona, Spain*
[6] *Donor Center Barcelona Tissue Bank (BTB), Hospital Clínic de Barcelona, C/Villarroel 170, Escala 12 Planta 4, 08036 Barcelona, Spain*
[7] *Banc de Sang i Teixits de Catalunya (BST), Pg. del Taulat, 116, 08005 Barcelona, Spain*
[8] *Servei d'Ecopatologia de Fauna Salvatge (SEFaS), Departament de Medicina i Cirurgia Animals, Facultat de Veterinària, Universitat Autònoma de Barcelona (UAB), Cerdanyola del Vallès, 08193 Bellaterra, Catalonia, Spain*
[9] *Anatomy and Embryology Unit, Morphological Sciences, Faculty of Medicine, Autonomous Universitat Autònoma de Barcelona (UAB), Cerdanyola del Vallès, 08193 Bellaterra, Catalonia, Spain*
[10] *Legal Medicine Unit, Department of Psychiatry and Legal Medicine, Universitat Autònoma de Barcelona (UAB), Cerdanyola del Vallès, 08193 Bellaterra, Catalonia, Spain*

Received: 29 November 2022
Accepted: 18 February 2023

© The Author(s) 2023

ABSTRACT

Whereas gunshot injuries in human craniums have been well studied, reliable data on fracture patterns in ballistic long bone trauma remains scarce. Further information useful for forensic trauma interpretation and reconstruction may be retrieved from experimentally produced gunshot fractures. In order to avoid the use of human specimens for experimental research, it is of great interest to determine whether alternative models can reproduce the ballistic fracture patterns of human long bones. To address this question, we shot seven healthy adult human femurs and humeri each, ten samples each of two different polyurethane cylinders from Synbone® and four femurs from female red deer.

Handling Editor: Stephen Eichhorn.

Address correspondence to E-mail: ignasigaltes@gmail.com

https://doi.org/10.1007/s10853-023-08333-6

Springer

Published online: 03 March 2023

The specimens were embedded in ballistic gelatin and perpendicularly shot from a distance of 2 m, using a 9-mm full metal jacket projectile at an impact velocity of 360 m/s. The macroscopical appearance of the detailed fracture pattern considering entry, exit and general cortical traits as well as the bullet's energy lost upon impact were compared between the models. Despite some general similarities, neither of the two alternative models entirely reproduced the fracture patterns of human long bones. Comparing the two alternative models, the surrogate model revealed more significant differences to the human fracture than the animal model. This leads to the conclusion that the polyurethane material provides a different failure mechanism than real bone, underpinning the challenge in deploying an accurate analog.

Introduction

The analysis and reconstruction of gunshot wounds are frequent challenges in forensic medicine. Soft tissue injuries often show characteristic features, which allow conclusions about the applied mechanical force [1]. Examination of a well-preserved body differs widely from examination of corpses in poor condition such as those which are severely decomposed, burnt, scavenged, mummified or saponified [2]. Forensic evidence obtained from soft tissue in such conditions often remains inconclusive. The reconstruction of trauma and death may only be deduced from elements more resistant to destruction such as bone. Although signs of trauma almost always persist in bone, to date, reliable forensic conclusions have been very limited [3–5]. In particular, when fractured skeletal remains are shattered or incomplete, it can be challenging to clearly distinguish blunt force trauma from gunshot trauma [6, 7].

Forensic research on gunshot bone trauma has mainly focused on cranial injuries [8–10]. In contrast, only a few studies have dealt with gunshot trauma in long bones. In 1915, five types of ballistic fractures in human long bones have been described [11]. A bullet grazing a long bone may (1) produce a transverse fracture, (2) completely pierce the shaft, (3) become embedded in the bone, (4) strike the shaft and produce stellate or butterfly fractures and/or (5) break the bone into small fragments. Since then, most of the experimental studies with human bones focused on the fracture pathophysiology and risk prediction related to ballistic variables [12–16]. Apart from that research on ballistic trauma in human long bones mainly remained descriptive [17–21]. A recent review has summarized publications on ballistic fracture patterns observed in human long bones [22]. Therein, different types of fractures such as linear, oblique, comminuted and butterfly fractures are collated following direct gunshot trauma. However, detailed data on cortical fracture patterns of gunshot trauma in human long bones useful for forensic trauma interpretation and recreation are barely provided. To fill this gap of knowledge and incorporate confidence in gunshot trauma evaluation, experimental studies to reproduce ballistic fractures under controlled conditions are needed.

Since acquiring human material for experimental forensic research is not easy due to ethical barriers as well as complex tissue handling and preservation, there is growing interest in finding an alternative model for trauma experiments. A suitable analogue to replace human tissue for ballistic trauma recreations should feature a similar energy dispersion and fracture mode, despite the microstructural particularity of different materials.

In the past, both surrogate material and animal bones have been used for experimental ballistic research. Initially, polyurethane surrogates produced by Synbone® AG (Switzerland) were developed for surgical training. Due to the demand for an appropriate bone analogue for forensic testing and event recreation, the company has designed special models to react in the same way as bone during ballistic impact [23]. The surrogates are made from polyurethane and formed into different models to simulate gunshot trauma in various types of bone. Focusing on ballistic long bone trauma, few articles have been published using anatomical models or simplified cylinders from Synbone® [12, 24, 25]. According to Synbone® the latter were especially designed for ballistic testing. In an experimental study from Henwood et al. [25], it was shown that the Synbone® cylinders behaved more like porcine bone than the anatomical Synbone® models. In contrast to the latter, the prior two presented comminuted fracture and a similar amount of the energy lost by the projectile upon impact. The authors claimed that the Synbone® cylinders may be used for ballistic impact tests to some extent, but drawing conclusions on fragment sizes or fracture propagation patterns were not recommended. However, these models were validated in comparison with porcine bone and not human bone.

Animal bones have played an important role in forensic experimental research too [24, 26–29]. However, there are morphological and biomechanical differences and no animal long bone consistently resembles the human. In terms of morphology and biomechanical properties, Kieser et al. [30] found deer femurs were the least dissimilar from human femurs compared to pig and sheep bones. In experimental studies, the same authors have used female deer femurs to produce remote and indirect ballistic fractures, whereby in both cases wedge-shaped fractures were reported [26, 27].

Nevertheless, in summary, detailed ballistic fracture patterns in different models have not been clearly defined yet. Thus, the query as to whether alternative surrogate and animal models are suitable to reproduce the fracture patterns of human long bones remains to be answered. To address this question, we experimentally inflicted gunshot trauma to human femurs and humeri, Synbone® surrogates and deer femurs. Qualitative and quantitative evaluation was made on all samples to compare the macroscopic fracture patterns.

Materials and methods

Samples and sample preparation

Human bones

The Donor Center-Barcelona Tissue Bank, department of Banc de Sang i Teixits de Catalunya provided 14 healthy, entire, unfractured, fresh human bones from cadavers with informed consent from their relatives. Seven femurs and humeri each were collected from a total of six male aged between 55 and 71 years.

With a postmortem time interval of up to 24 h the bones were dissected from the limbs, defleshed and stored in the freezer until further use. The human femurs had an average length of 46.1 cm (43–52 cm), an average mid-diaphyseal width of 2.9 cm (2.5–3.3 cm) and an average cortical thickness of 5.8 mm (5–6.5 mm). The human humeri had an average length of 32.6 cm (30.8–36.6 cm), an average mid-diaphyseal width of 2.1 cm (1.9–2.3 cm) and an average cortical thickness of 3.1 mm (3–4 mm).

Synbone® surrogates

Two different types of polyurethane cylinders from Synbone®, each ten, were selected. Both types have a length of 27 cm, an outer diameter of 3 cm, a hollow interior and are covered with a rubber skin simulating periosteum. Model PR0109.G is hereafter referred to as humerus cylinder and has a wall thickness of 3 mm, which is similar to the human humerus. Model PR0108.G is hereafter referred to as femur cylinder and has a wall thickness of 5 mm, which is similar to the human femur.

Animal bones

The Faculty of Veterinary of the Universitat Autònoma de Barcelona (UAB) provided four healthy, entire, undamaged, fresh femurs from wild-shot, young adult, female red deer (*Cervus elaphus*). The animals were shot for hunting reasons. The femurs were dissected with very little soft tissue attached, leaving the periosteum intact. They had an average length of 22.4 cm (21.6–23.3 cm), an average mid-diaphyseal width of 1.9 cm (1.8–2 cm) and an average cortical thickness of 3.8 mm (3.5–4 mm). They were stored in the freezer until further use.

Preparation of the ballistic gelatin blocks

All specimens were embedded in ballistic gelatin to simulate transparent soft tissue. We used gelatin from Clear Ballistics (Canada), which is supplied as a ready mixed, solid block that needs to be melted at 100 °C for 4–5 h before it can be individually applied. The liquid gelatin was poured into molds with the samples and left to solidify at air temperature overnight. The thickness of the gelatin on the target side was 2 cm for each specimen. In case of the Synbone® cylinders, also the hollow interior was filled with gelatin to simulate bone marrow and its exploding reaction to gunshot [31, 32].

Shooting procedure

The 9 mm Luger test barrel (Drello Bal 1025 FU-R) was used to fire a 9 mm Luger full metal jacket projectile to each specimen. The impact velocity of the projectile was 360 m/s, simulating a shot from a handgun. The specimen blocks were placed 2 m before the muzzle. In order to ensure a perpendicular impact, we constructed a device that held the specimens at the ends to stabilize them upright. An optical laser was used to define the impact point in the middle of the shaft. For velocity measurement of the projectile upon impact, a light barrier (Drello LS 11-03) with a computerized system (Drello VC 4043-09) was used.

Sample assessment

After the shooting, the fractured samples were removed from the gelatin blocks. The synthetic periosteum of the Synbone® surrogates could be smoothly peeled off. In order to clean the human and animal bones, they were cooked at 100 °C in a water detergent solution (one cup of commercial degreasing detergent in 5 L of plain water) [33]. After 2–5 h of cooking, the bones were cleaned and left to dry. After the cleaning process, the fragments of each specimen were reassembled with a superglue to better visualize the fracture patterns.

All samples were macroscopically examined to define the fracture type and cortical fracture patterns. The latter was subdivided in entrance, exit and general cortical traits. We determined the fracture type by the appearance of the impact side. Furthermore, we counted the different forms of radiating fracture lines around the bullet entry: longitudinal (lines running along the longitudinal axis toward the epiphysis/cylinder ends), oblique (lines running at an angle to the longitudinal axis of the samples) and transverse (lines running horizontally from the entry point to the posterior aspect of the samples). Any fracture line longer than 5 mm was counted. For further quantitative analysis, the cortical thickness at the level of the impact, the maximal longitudinal fracture extent and the horizontal and vertical diameter of the bullets' entrance and exit hole were measured with a calliper. The measurement of the post-impact velocity of the projectiles allowed the calculation of the kinetic energy lost in each sample ($Ke = 0.5\ mv^2$). The mass (m) of the projectile was 7.98 g. After collection of all data, they were compared within the sample categories.

Statistics

Pearson's Chi-squared test was carried out to determine significant differences in the frequencies of the entry, exit and general cortical traits between the sample groups. Contingency coefficients were calculated to correlate the traits with the sample groups. The multivariate correspondence analysis was used to examine correlations and clusters between the fracture traits in the sample groups.

The quantitative variables such as entry and exit hole size, fracture extent, percentage of transverse fracture lines and energy loss values were tested for normality and equal variance using Shapiro Wilk and Levene's test. An analysis of variance using One-Way ANOVA was performed. Games-Howell post hoc test was applied to compare the quantitative variables between the sample groups. Significance level was set at 0.05.

Ethics

This study followed the ethical precepts of the Declaration of Helsinki (Fortaleza, Brazil, Oct 2013) and was approved by the local ethics committee (Bellvitge University Hospital, L'Hospitalet de Llobregat, Barcelona; Ref. PR416/20). Human samples were processed according to guidance for clinical use (EEC regulations 2004/23/CE and 2006/17/CE) and to the legal requirements of Spain (Law 14/2007, RD 1716/2011 and RD 9/2014). All human bone samples were donated anonymously and obtained under informed consent. The respective samples are stored in the private collection at the Catalonian Institute of Legal Medicine and Forensic Science (IMLCFC) in Barcelona, Spain (Registro Nacional de Biobancos. Ref. C.0004241).

Results

Qualitative fracture characteristics

All samples were completely perforated by the bullet and presented comminuted fractures. In the human bones and Synbone® cylinders the complete specimen length, the entrance and exit holes could be reconstructed. In contrast, the animal bones exhibited a massive fragmentation, particularly on the lateral aspects of the bullet perforation. This hampered the shaft assembling, allowing only a partial reconstruction of the entry and exit hole. All samples presented a various number of radiating fractures lines creating a stellate pattern at the impact side. Explanations of the assessed cortical traits are given below. We divided them into entrance, exit and general traits as shown in Table 1 (the wall of the surrogates will still be referred to as cortical for the sake of simplified readability). To the best of our knowledge, some of these traits have not yet been reported in the literature. In all sample groups we found the impact side provided more cortical characteristics to identify gunshot trauma than the exit.

Entrance traits (Figs. 1, 3)

A *round entry hole* is the bullets initial entry defect that visually appears round.

A *V-shape* of the bone is present proximal and/or distal of the entry hole. The tip of the V points toward the impact and the margins are defined by oblique fracture lines.

Y-branching is present proximal and/or distal of the entry hole. It is a bifurcation of the longitudinal fracture line into two oblique lines that run toward both lateral aspects.

Tip fragmentation is a superficial, external loss of cortical fragment(s) at the tip of the bone around the bullet entry. The transition to the intact cortical bone is sharply defined by quite chiseled edges. Tip fragmentation on bone pieces next to each other appears as a stepped circular margin around the entry.

Table 1 Cortical traits analyzed in all sample groups subdivided in entrance traits, exit traits, and general traits, with the respective x^2 test's *p*-value and contingency coefficient (CC)

	Human femur		Human humerus		Synbone® femur cylinder		Synbone® humerus cylinder		Deer femur		*p* value	CC
N	7		7		10		10		4			
Entrance traits												
Round hole	7	100%	7	100%	10	100%	10	100%	0	0%	< 0.001	0.707
V-shape	7	100%	7	100%	4	40%	7	70%	4	100%	0.011	0.506
Y-branching	0	0%	1	14%	7	70%	6	60%	0	0%	0.005	0.532
Tip fragmentation	6	86%	6	86%	6	60%	3	30%	4	100%	0.034	0.463
Wing flake	4	57%	2	29%	0	0%	0	0%	0	0%	0.006	0.524
Wing flake defect	6	86%	2	29%	0	0%	0	0%	0	0%	< 0.001	0.624
Ring defect	7	100%	7	100%	0	0%	1	10%	0	0%	< 0.001	0.688
Depressed ring	0	0%	0	0%	10	100%	10	100%	0	0%	< 0.001	0.707
Bullet wipe	0	0%	0	0%	10	100%	10	100%	0	0%	< 0.001	0.707
Internal beveling	7	100%	7	100%	10	100%	10	100%	4	100%		
Radiating Fx lines	7	100%	7	100%	10	100%	10	100%	4	100%		
Exit traits												
Round hole	1	14%	0	0%	2	20%	8	80%	0	0%	0.001	0.570
Square hole	6	86%	7	100%	8	80%	2	20%	0	0%	< 0.001	0.597
Layered breakage	7	100%	6	86%	0	0%	0	0%	0	0%	< 0.001	0.707
External beveling	7	100%	7	100%	9	90%	10	100%	4	100%	0.579	0.265
Radiating Fx lines	7	100%	7	100%	10	100%	10	100%	4	100%		
General traits												
Plastic deformation	7	100%	7	100%	0	0%	0	0%	4	100%	< 0.001	0.707
Wall splitting	2	29%	0	0%	9	90%	6	60%	0	0%	< 0.001	0.576

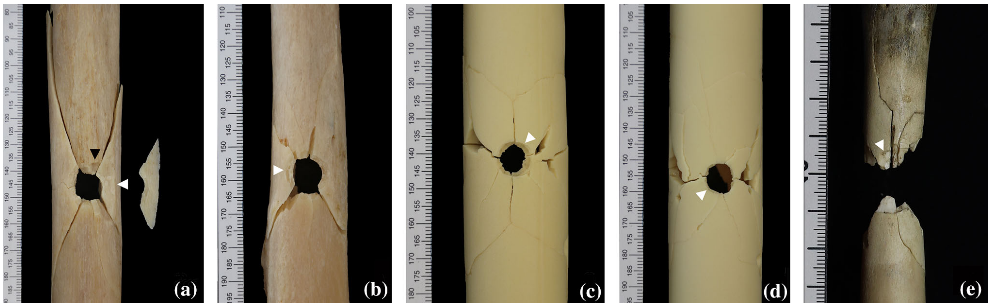

Figure 1 Stellate fracture at the impact side of a **a** human femur with a round entry hole surrounded by a partial ring defect, tip fragmentation (black arrow head), wing flake defect (white arrow head), wing flake and V-shape, **b** human humerus with a round entry hole surrounded by a partial ring defect (white arrow head) and V-shape, **c** Synbone® femur cylinder with a round entry hole surrounded by a depressed ring and bullet wipe (white arrow head) and Y-branching, **d** Synbone® humerus cylinder with a round entry hole surrounded by a depressed ring and bullet wipe (white arrow head) and V-shape, **e** deer femur with tip fragmentation (white arrow head) an V-shape.

A *wing flake* is a loose trapezoidal chip of cortical bone that resembles spread wings. It originates from the lateral aspect(s) of the entry hole.

A *wing flake defect* is the imprint of a wing flake that is left on the lateral aspect(s) of the entry hole.

A *ring defect* is a circular or partial circular loss of superficial cortical bone on the margin of the entry hole. Its appearance reminds of an abrasion ring. It may be interrupted by other entrance patterns such as tip fragmentation.

A *depressed ring* is a circular or partial circular depression of the entry hole margin.

A *bullet wipe* appears as a gray ring around the entry hole.

Internal beveling is a funnel shape in the cortical wall with the larger part on the internal aspect.

Radiating fracture lines run from the entry hole toward the epiphyses and the posterior aspect of the sample.

A significant difference was found for round entrance hole that was produced in all human bones and Synbone® surrogates, while in the deer femurs it could not be reconstructed. V-shape was featured by all human and animal bones and thus significantly more frequent than in Synbone® surrogates. Y-branching was significantly more often present in Synbone® surrogates than in human humeri, while in human and deer femurs it was never observed. Tip fragmentation was featured by all deer femurs and the majority of human bones and thus significantly more frequent than in the Synbone® surrogates. Also statistically significant were the findings wing flake and wing flake defect that exclusively occurred in human bones. Ring defect was statistically significant present in all human bones and in only one humerus cylinder from Synbone®, while in femur cylinders and deer femurs it was never observed. Finally, all Synbone® surrogates significatively featured depressed ring and bullet wipe, while in human and animal bones both traits were absent. No statistical significances were found for internal beveling and radiating fracture lines that both occurred in every specimen.

Exit traits (Figs. 2, 3)

Round exit hole is the bullets exit defect that visually appears round.

Square exit hole is the bullets exit defect that visually appears edgy or square.

Layered breakage is a layered pattern on the fracture surface of the cortical bone.

External beveling is a funnel shape in the cortical wall with the larger part on the external aspect.

Radiating fracture lines run from the exit defect toward the epiphyses and the anterior aspect of the sample.

Concerning the exit traits, all human humeri and the majority of the human femurs and femur cylinders showed a square exit hole. This is statistically significant compared to the humerus cylinders that mostly featured a round exit hole. As noted, the exit hole in deer bones could not entirely be

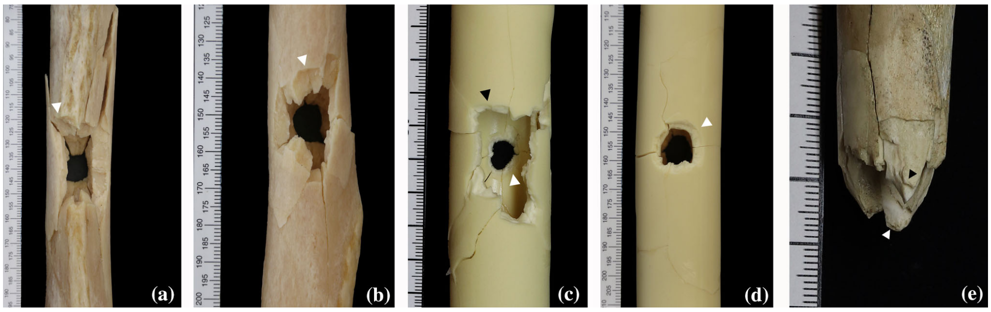

Figure 2 The exit side of a **a** human femur with a square exit hole and external beveling (white arrow head), **b** human humerus with a square exit hole and external beveling (white arrow head), **c** Synbone® femur cylinder with a square exit hole, external beveling (black arrow head) and internal beveling (white arrow head), **d** Synbone® humerus cylinder with a round exit hole and external beveling (white arrow head), **e** deer femur with external beveling (black arrow head) and internal beveling (white arrow head).

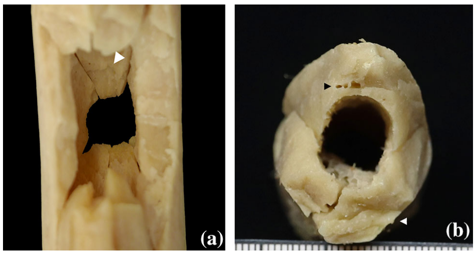

Figure 3 **a** The exit side of a human femur with the view on internal entrance beveling (white arrow head), and **b** axial view on the fracture surface of a human femur showing wall splitting (black arrow head) at the impact side and layered breakage (white arrow head) at the exit side.

reconstructed. Layered breakage occurred in all human femurs and the majority of human humeri. This finding is statistically significant, since it was never featured by the Synbone® surrogates and the animal bones. No significant differences were found for external beveling and radiating fracture lines. External beveling was present in all specimens with the exception of one femur cylinder from Synbone®. Radiating fracture lines were present in all samples.

General traits

Plastic deformation is a persistent deformation of bone.

Wall splitting is a separation of bone within the cortical wall (Figs. 3, 4).

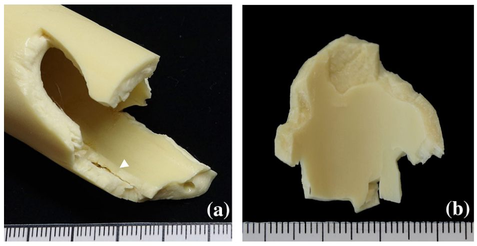

Figure 4 **a** Oblique-lateral view on a Synbone® femur cylinder with wall splitting (white arrow head) and a void lacuna in the material, and **b** demonstrates the irregular fragment shape of a Synbone® humerus cylinder.

Plastic deformation was present in all human and animal samples. This finding is significantly significant, since in the Synbone® surrogates it never occurred. Wall splitting was significantly more frequent in both Synbone® models compared to human femurs. In human humeri and deer femurs it was never observed.

Multivariate analysis

All qualitative variables were used for a multivariate correspondence analysis (Fig. 5). The results showed that human bones and Synbone® surrogates feature distinctive fracture patterns. A closer inspection shows two clusters of fracture patterns, one typically found in human bones and the other in Synbone® surrogates. The cluster of typical ballistic traits

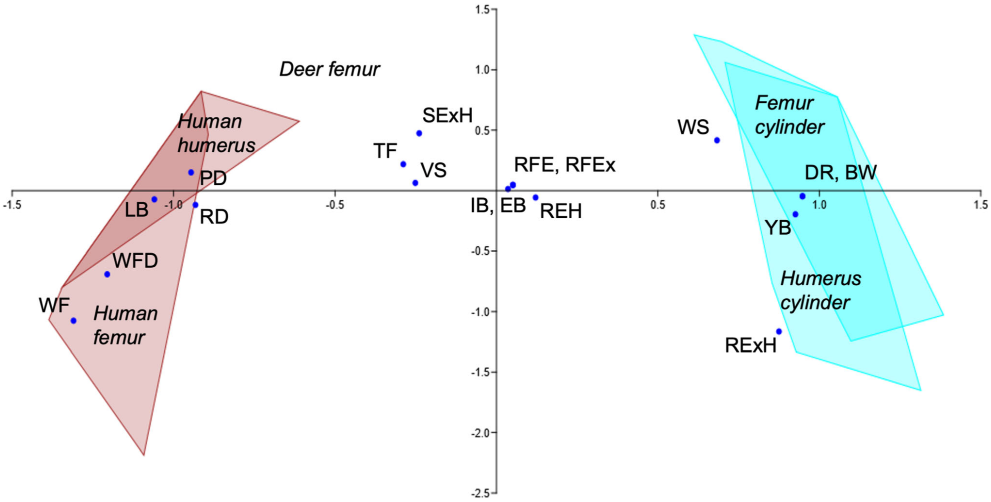

Figure 5 The multivariate correspondence analysis with the qualitative cortical traits evaluated in all sample groups (REH = round entrance hole, VS = V-shape, YB = Y-branching, TF = tip fragmentation, WF = wing flake, WFD = wing flake defect, RD = ring defect, DR = depressed ring, BW = bullet wipe, IB = internal beveling, RFE = radiating fracture lines entrance, RExH = round exit hole, SExH = square exit hole, LB = layered breakage, EB = external beveling, RFEx = radiating fracture lines exit, PD = plastic deformation, WS = wall splitting). The first component represents 52% of the total variance and the second component 14%, cumulative both axes represent 66%.

observed in human bones consists of ring defect, wing flake, wing flake defect, layered breakage and plastic deformation. The cluster of typical ballistic traits observed in Synbone® surrogated consists of depressed ring, bullet wipe, Y-branching, round exit hole and wall splitting. The cluster of cortical traits featured by the animal model is more similar to the cluster reproduced in human bones.

Quantitative fracture characteristics

The entry and exit hole diameters, fracture extent, and the presence of transverse fracture lines could only be evaluated for the human and Synbone® specimens (Table 2; Fig. 6). The largest mean fracture extent was found in human femurs. Statistically significant differences were found compared to the human humeri and femur cylinders. Furthermore, among the humerus cylinders a considerable variation of the fracture extent was observed.

The entry and exit holes were measured in their vertical and horizontal diameter. Compared to the projectile's diameter, the mean vertical entry hole diameter in human bones and humerus cylinders was larger, while in femur cylinders it was smaller. Comparing the sample groups, the mean vertical diameter in the femur cylinders were significantly smaller than in the other three sample groups. The mean horizontal entry hole diameter in human bones was larger, while in Synbone® surrogates it was smaller than the projectile's diameter. Comparing the sample groups, the mean horizontal diameter in human bones was significantly bigger than in the Synbone® surrogates. Among the Synbone® surrogates the horizontal diameter in humerus cylinders were significantly bigger than in femur cylinders. The mean vertical exit hole diameter in human humeri was significantly bigger than in all other three sample groups. The mean horizontal diameter was significantly bigger in femur cylinders compared to human bones and in humerus cylinders compared to human humeri.

The percentage of transverse, oblique and longitudinal fracture lines compared to all entrance associated radiating fracture lines are shown in Table 2. Statistical differences were found for the percentage of transverse fracture lines that was significantly

Table 2 Descriptive statistics of the entry and exit hole size (VD = vertical diameter, HD = horizontal diameter), fracture extent, percentage of the transversal, oblique and longitudinal fracture lines out of the entrance associated fracture lines in human bones and Synbone® surrogates

Quantitative variables	Group	*N*	Mean	SD	Min	Max
Entry hole VD (mm)	FH	7	10.4	1	9	11.5
	HH	7	10	0.7	9	11
	FS	10	8.3	0.4	8	9
	HS	10	9.8	0.5	9	11
Entry hole HD (mm)	FH	7	10.4	0.5	10	11
	HH	7	9.8	0.9	9	11
	FS	10	6.8	0.3	6.5	7
	HS	10	8.6	0.5	8	9
Exit hole VD (mm)	FH	7	16	3.9	12.5	23
	HH	7	24.7	10	13.5	40.5
	FS	10	15.4	4.3	8.5	22
	HS	10	14.2	4.4	11	24.5
Exit hole HD (mm)	FH	7	11.2	1.6	9	13
	HH	7	9.5	1.7	8	12.5
	FS	10	13.8	1.8	11	16
	HS	10	12.9	2.1	10	15.5
Fracture extent (cm)	FH	7	14.2	2.6	11.2	17.9
	HH	7	9.5	1.8	6.5	12.0
	FS	10	10.2	2.4	6.9	15.1
	HS	10	11.1	3.8	6.7	16.6
Transverse Fx lines (%)	FH	7	8.7	8.4	0	17
	HH	7	10.3	10.9	0	29
	FS	10	24.5	4.3	18	33
	HS	10	22.2	8.4	11	33
Oblique Fx lines (%)	FH	7	83.7	16.9	50	100
	HH	7	73.4	11.4	57	86
	FS	10	64.1	10.5	50	78
	HS	10	68.3	10.7	50	88
Longitudinal Fx lines (%)	FH	7	7.6	13.6	0	33
	HH	7	16.3	12.8	0	33
	FS	10	11.5	10.9	0	25
	HS	10	9.6	9.8	0	25
Energy loss (J)	FH	4	352.4	29.9	316.9	389.1
	HH	6	232.4	29.8	193.8	265.7
	FS	10	168.3	10.7	153.4	188.7
	HS	10	124.8	12	108.9	151.1
	FA	4	245.5	32.4	215.2	278.6

Also shown is the projectile's energy lost upon impact in all five sample groups (*FH*, human femur, *HH*, human humerus, *FS*, femur cylinder, *HS*, humerus cylinder, *FA*, deer femur)

higher in both Synbone® surrogates compared to human femurs (Fig. 6). No significant differences were found for the presence of oblique and longitudinal fracture lines.

The projectile's exit velocity was detected in all samples, except in three human femurs and one humerus due to interferences. Table 2 and Fig. 7 show the calculated energy loss upon impact in all sample groups. The mean energy loss in the human femur was significantly higher than in the rest of sample groups. Energy loss in the human humeri was significantly higher than in both Synbone® surrogates. Energy loss in the deer femurs was most similar to human humeri. It was significantly higher than in the humerus cylinders from Synbone®. Furthermore, also between the two Synbone® models, the energy loss in femur cylinders were significantly higher than in humerus cylinders.

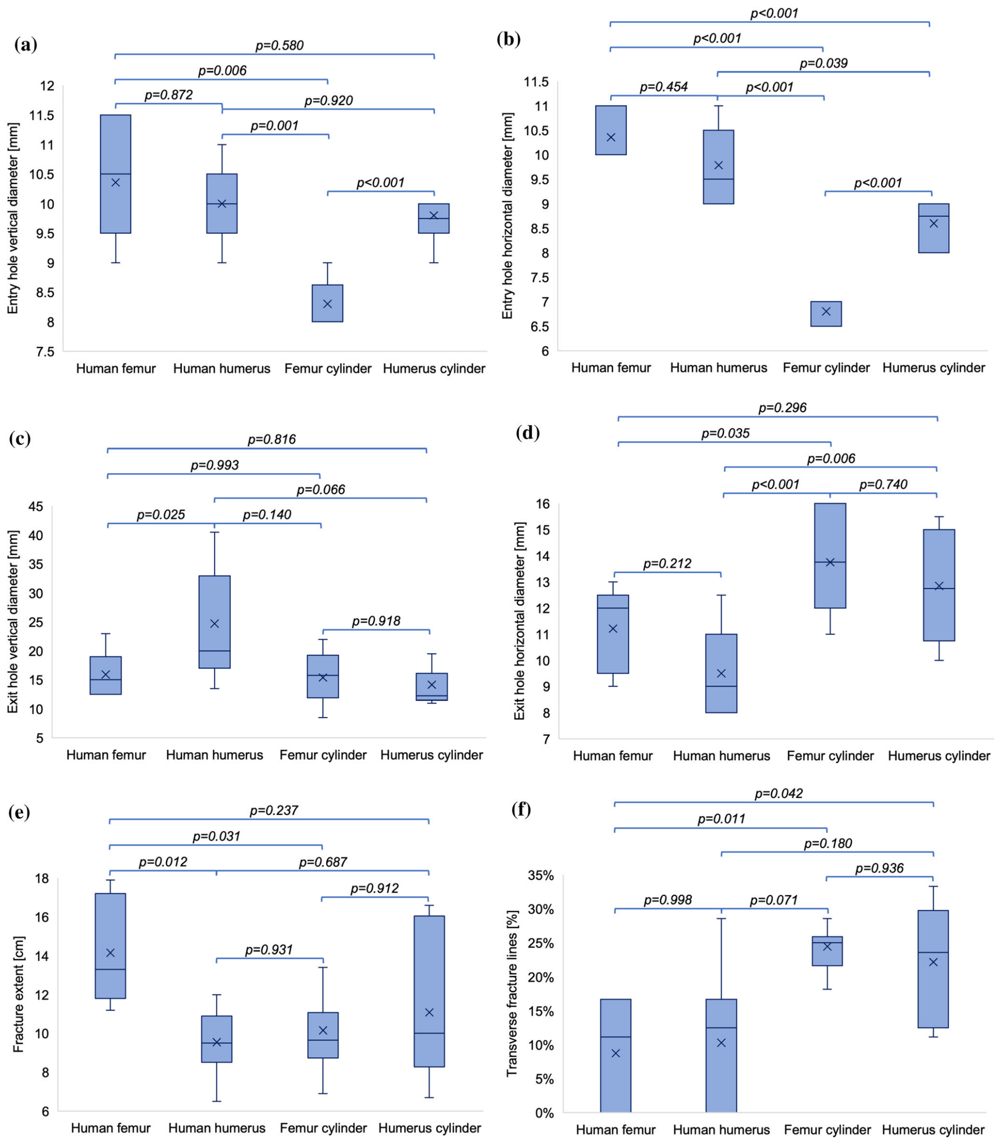

Figure 6 Box plots representing the **a** vertical and **b** horizontal entry hole diameter, the **c** vertical and **d** horizontal exit hole diameter, the **e** fracture extent, and **f** the percentage of transverse fracture lines out of the entrance associated fracture lines in human bones and Synbone® surrogates (*p*-values for the pairwise comparison).

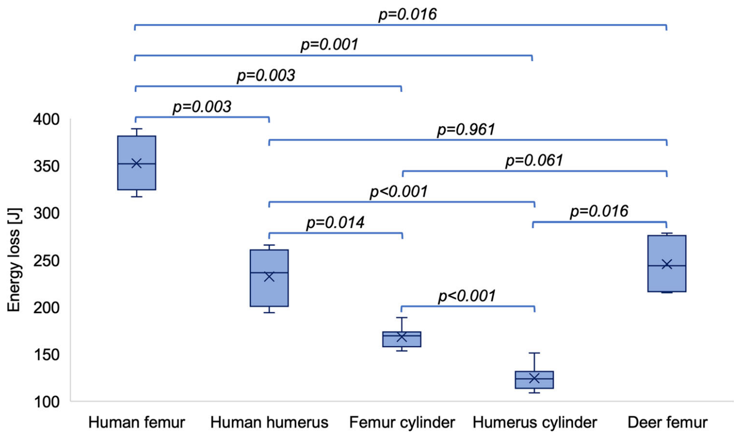

Figure 7 Box plots representing the projectiles' energy lost upon impact in all five sample groups (*p*-values for the pairwise comparison).

Discussion

Alternative models for trauma experiments are of great interest due to the restricted possibilities of using human specimens for forensic research. Despite different tissue and material, a suitable alternative is thought to exhibit properties such as elasticity, strength and energy absorption similar to human tissue [32]. Moreover, useful models should ensure reproducibility [12]. To date, this is the first experimental study designed to provide conclusions on whether Synbone® cylinders and deer femurs are suitable to macroscopically reproduce detailed ballistic fracture patterns in human long bones. For this purpose, we shot with real ammunition and used real human bones as a comparison alongside the alternative synthetic and animal models.

The macroscopical generalization of the fractures

On the first sight, the ballistic fractures in each sample group appeared similar. All samples presented comminuted fracture, which is consistent with the review by Veenstra et al [22]. revealing comminuted fracture is the most frequent diaphyseal fracture in gunshot trauma. In order to characterize the fracture type more accurately, we considered the appearance at the impact side. Stellate fracture was identified in all sample groups, as it has also been observed by other authors [11, 21, 28, 34]. All models allowed the assessment of the impact direction and bullet trajectory, since entrance and exit side could be identified and distinguished from each other. Interestingly, some authors revealed that the exit hole is not always present in long bones because the bullet entry fragments the bone before the projectile reaches the other side of the shaft [21, 35]. This observation could not be made in our study. In all sample groups, we found a beveled exit with radiating fracture lines allowing the conclusion that they were directly produced by the projectile. Certainly, the entrance associated fracture lines that reach the posterior aspect may influence the shape of the exit fracture, taking into account the Puppe rule that fracture lines stop at preexisting ones [36]. As a standard feature to distinguish between entrance and exit, it is well known that bone bevels out in the direction in which the projectile travels [34]. In cranial bones, the entry wound classically presents an internal beveling, whereas external beveling is a typical characteristic of the exit wound [37, 38]. In our study, internal beveling of the entrance defect and the already mentioned external beveling of the exit defect were reproduced in all sample groups. Furthermore, in all sample groups the exit fractures were dominated by a vast fragmentation and thus larger than the bullet entry as it has already been reported in human long bones [39]. In accordance with claims about the particular importance of the entry wound assessment [40], we found the impact side in all sample groups provided more characteristic traits to identify gunshot trauma than the exit side.

The fracture macroscopy in detail

A detailed fracture pattern analysis showed that both the surrogate and animal models differed significantly from human bones. When comparing the two alternative models, the clusters of entry, exit, and general cortical traits in the animal model were found to be more similar to human bone than the Synbone® surrogates.

In a ballistic study comparing human craniums with Synbone® plates and spheres, Smith et al. [41] noted similar entry but different exit wound features between the models. Unlike these findings, in our long bone models especially the entrance fracture presented differences between the sample groups. We observed traits that revealed to be distinct for human bones and described them as wing flake, wing flake defect and ring defect. The aspect of V-shape, as already observed by Martrille et al. [21], and tip fragmentation, a term we defined in this study, were reproduced in all sample groups. However, both traits appeared significantly more often in human and animal bones than in Synbone® surrogates. Y-branching, depressed ring and bullet wipe revealed to be characteristic Synbone® entrance traits. According to the literature, the presence or absence of a depressed ring may help to identify the type of ammunition in terms of fully jacket or lead bullets [25, 42]. However, this finding may not be applicable in human bones, since we could not reproduce it there. Another unique Synbone® finding is the bullet wipe that may be associated with the presence of a depressed ring. With other words, in Synbone® we found the anterior surface around the bullet entry depressed but mostly intact. In contrast, in human and animal bones we always saw a loss of cortical bone around the bullet entry. The main difference on the impact side of the deer femurs was that especially the medial and lateral aspects of the bullet entry were shattered and could not be reassembled. This did not allow us the same precise evaluation of the entrance traits compared to human bones and Synbone® surrogates.

With respect to the exit fracture, we also found some dissimilarities between the three models. Layered breakage revealed to exclusively occur in human bones. Interestingly, this trait has formerly been associated to the compression side of blunt force trauma in fresh human long bones [33]. The Synbone® femur cylinders mostly presented a square hole like in human bones, whereas the majority of the humerus cylinders showed a round exit hole. The deer bones did not allow the assessment of the exit shape.

In terms of general cortical traits, exclusively the real bones featured plastic deformation which is referred as to the persistent deformation of bone prior fracturing [34]. In contrast, wall splitting revealed to be a distinct Synbone® trait.

Focusing on caliber estimation, studies on cranial bones have revealed that the minimum diameter of the entry hole allows the discrimination between "small" and "large" calibers, whereas a precise determination is difficult [43–45]. In our study, we found significant differences between the entry size in the models. The human bones reproduced bigger entry holes, while the Synbone® surrogates featured mostly smaller entry holes than the projectile used. This may be explained by the different entry hole traits, ring defect in human bones versus depressed ring in Synbone® surrogates. While the first represents a cortical loss of bone, the latter can be regarded as an inward folding of the material. Again, the deer bones could not be used to evaluate the entry hole size.

The energy loss of the projectile upon impact

Our results on the bullet's energy lost upon impact indicates that the resistance to the projectile is significantly lower in Synbone® cylinders than in human and deer bones. Interestingly, this result differs from the finding that Synbone® surrogates feature a similar resistance to porcine bone [24, 25].

In accordance with the literature, the distinct fracture patterns found in our study may essentially be attributed to differences in the underlying material [25, 41]. In respect of the microstructural differences, it has been expressed that polyurethane is not a suitable alternative for studies investigating bone trauma below a very general and superficial level [41]. Thus, other authors have argued that animal bones remain an essential alternative model for human bone trauma [46].

Surrogate material such as polyurethane does not feature the microstructural complexity of real bone based on its components and their arrangement in space [47]. Despite some histological differences between the species [48, 49], all bones consist of a mineral phase (hydroxyapatite) embedded in an organic matrix (mainly type I collagen). The former makes the bone rigid and stiff, while the latter contributes to its toughness and gives it a certain flexibility reducing brittleness and allowing some resistance to fracture [50]. Also, the water content is critical to the mechanical behavior [34]. Bone is a fluid-imbibed material and its water is not only present in the vascular system and canaliculi, but also structurally bound in the collagen matrix [51]. It was found that drying out of a bone is related to a loss of elasticity and plasticity [33, 52]. In this context, fracture characteristics have been linked to the elasticity, cohesiveness and density of bone [53]. It is known that the less flexible the tissue the greater the damage because more energy is transferred to the stretch mechanism [54, 55].

But, not only intrinsic factors influence the bone's fracture biomechanics. It is thought that in response to different mechanical stressors bone reacts differently. In blunt force trauma, bone has been observed to behave like a ductile material by deforming prior to fracturing [33]. In contrast, in gunshot trauma, bone typically behaves as a stiff and brittle material and tends to fracture instantly before deformation can occur [56]. These authors, however, do not provide information on the impact speed. In our study, simulating a shot from a pistol, we could find plastic deformation in all human and deer bones. Indeed, this finding finds support by the observation of Martrille et al. [21] who also reported on the occurrence of plasticity prior fracturing in gunshot trauma. In the Synbone® models we could not find plastic deformation. A potential explanation is that the surrogates may are more brittle than real bone. Further support for this is given by our finding that transverse fractures occurred more frequently in the Synbone® surrogates than human bones. In the literature, transverse lines are typical associated to fractures in dry, brittle bone [57].

In our study, the deer femurs were massively fragmented into very small pieces and chips. The fracture could not be as efficiently reconstructed and thus not all parts as precisely evaluated as human bones and Synbone® cylinders. We considered this as a main drawback of the animal model. Interestingly, this finding differs from results by Kieser et al. [28] who found radiating fracture lines producing a butterfly-shaped fracture at the impact side of the anterior mid-shaft of fresh mature female deer femurs. Compared to our study, their findings resemble more the fracture pattern found in our human bones than in our deer bones. We assume that this difference may be particularly traced back to the impact energy of 0.013–5.35 J of the spherical steel projectiles used in the experiments by Kieser, compared to the impact energy of 517.97 J in our study. This assumption may be supported by the literature reporting bone behaves more like brittle material under high velocity impacts [58, 59]. Since the grade of comminution is not only associated to the amount of transferred energy but also to a small target size [34], an additional influence might be related to the smaller size of the deer bones used in our study (Iberian subspecies from Catalonia, Spain). They featured an average length of 22.4 cm and an average diaphyseal width of 1.9. We assume they were smaller than the ones used by Kieser et al. [27] from New Zealand, who reported in an earlier study an average bone length of 27.6 cm and a mid-diaphyseal width of 2.7 cm. The relation between the grade of comminution and a small target size may further be supported by our experience that human humeri compared to human femurs shattered in smaller fragments and hence were more difficult to assemble. Kieser et al. reported deer femurs being a suitable model to substitute human femurs. The deer femurs used in our study were considerably smaller and from this point of view they might rather substitute human humeri. This can find further support by our observation that energy loss in human humeri and deer femurs were quite similar. With respect to the material properties, the deer bones seem to have a comparable toughness as human humeri.

Ultimately, an additional explanation for the different fracture patterns found in our study may constitute the geometrical variability of the models, in particular dissimilar cortical thickness and the complex shape of real bone. In accordance with Smith et al. [41], these factors also influence the resistance through thinner and thicker bone areas and thus fracture propagation. As noted, there is no animal bone that geometrically resembles a human femur or humeri. In case of the Synbone® surrogates, there exist anatomical models, however the ones especially developed for ballistic testing were geometrically simplified. These simplified cylinders have been developed to reduce the effect of heterogeneous tissues during research and hence should guarantee reproducibility. In this context, however, we could observe some differences in the detailed fracture patterns among the Synbone® models. Some entrance traits such as V-shape, Y-branching, Tip fragmentation and ring defect only occurred irregularly. Also the exit hole reveled to appear round or square shaped. Furthermore, we found a considerable variability of the fracture extent among of the humerus cylinders. In contrast to the findings of Henwood et al. [25], however, we did not observe fractures reaching the cut edges of the cylinders. Since fracture lines run along the least resistance [9], a potential explanation for the observed inconsistencies among the Synbone® models may lay in a certain degree of heterogeneity of the polyurethane wall. As an indicator for this heterogeneity, we found void lacunas of up to 2.5 mm in some samples. This assumption finds further support by our observation of irregular fragment shapes in the Synbone® models. Henwood et al. [25] made an analogous observation, reporting on a sudden change of fracture direction in Synbone® surrogates that could not be observed in real bones from pigs. The authors claimed that the fracture lines change the direction when they reached a different pore density. However, they also express some reluctance to accept this interpretation because not all fracture lines showed a response to the change in pore density.

Limitations

A limitation of the research presented in our study may concern the sample size, in particular the number of animal bones. However, within this groups we found a 100% congruence of the presence or absence of the evaluated fracture patterns. Furthermore, the results of this study represent fracture patterns in the diaphysis, produced by a 9 mm full metal jacket projectile with an impact speed of 360 m/s. Gunshot trauma in more cancellous rich areas such as the epiphyses as well as different bullet types and impact velocities may produce different fracture patterns. Since the scope of this study was only a macroscopical evaluation, it might be useful to investigate the material behavior of each model from a microstructural point of view.

Conclusion

The ballistic fracture patterns produced in the Synbone® surrogates and animal bones tested in this study were a fair general approximation of those seen in human long bones. However, a detailed analysis revealed a range of dissimilarities that calls caution in extrapolating ballistic fracture patterns of alternative models to human long bones. The Synbone® surrogates did not present all the observed human fracture traits and in addition, they presented different characteristics. This leads to the conclusion that the polyurethane material provides an alternate failure mechanism than real bone. The animal model tested in our study revealed to be more suitable than Synbone®, in terms of both qualitative and quantitative fracture characteristics. However, the main drawback of the deer femurs was the massive fragmentation that did not allow us the same precise fracture reconstruction as in human bone and Synbone® surrogates. Our study shows that special caution is needed when validating surrogate material with animal bone instead of human bone. We further emphasize the continued need for innovation in new model systems such as computational modeling. However, before alternative models can be validated, further experiments with real human long bones seem to be required to define a distinct ballistic fracture pattern.

Acknowledgements

Funding support for the current project was provided by the Research Fund for Excellent Junior Researchers of the University of Basel, Switzerland. A very special thank goes to Professor Christian De Geyter, Professor Eva Scheurer and Professor Roland Hausmann. We are extremely grateful for the collaboration with the Mossos d'Esquadra for providing the facilities, the material and the personal staff.

Authors' contribution

Conceptualization was contributed by NS and IG; Methodology was contributed by NS, JS, XG, PB, AS, and MO-S; Formal analysis and investigation were contributed by NS, IG, and XJ; Writing—original draft preparation was contributed by NS; Writing—

review and editing was contributed by IG, XJ, and NS; Visualization was contributed by NS, IG, and XJ; Supervision was contributed by IG and XJ.

Funding

Open Access Funding provided by Universitat Autonoma de Barcelona.

Data availability

The data generated during and/or analyzed during the current study are available from the corresponding author on reasonable request.

Declarations

Conflict of interest The authors have no conflicts of interest to declare that are relevant to the content of this article.

Ethics approval This study followed the ethical precepts of the Declaration of Helsinki (Fortaleza, Brazil, Oct 2013) and was approved by local ethics committee (Bellvitge University Hospital, L'Hospitalet de Llobregat, Barcelona; Ref. PR416/20). Human samples were processed according to guidance for clinical use (EEC regulations 2004/23/CE and 2006/17/CE) and to the legal requirements Spain (Law 14/2007, RD 1716/2011 and RD 9/2014). All human bone samples were donated anonymously and obtained under informed consent. The respective samples are stored in the private collection at the IMLCFC (Barcelona, Spain) (Registro Nacional de Biobancos. Ref. C.0004241).

Open Access This article is licensed under a Creative Commons Attribution 4.0 International License, which permits use, sharing, adaptation, distribution and reproduction in any medium or format, as long as you give appropriate credit to the original author(s) and the source, provide a link to the Creative Commons licence, and indicate if changes were made. The images or other third party material in this article are included in the article's Creative Commons licence, unless indicated otherwise in a credit line to the material. If material is not included in the article's Creative Commons licence and your intended use is not permitted by statutory regulation or exceeds the permitted use, you will need to obtain permission directly from the copyright holder. To view a copy of this licence, visit http://creativecommons.org/licenses/by/4.0/.

References

[1] Saukko P, Knight B (2015) Knight's forensic pathology. CRC Press, Boca Raton

[2] Sorg MH, Haglund WD (eds) (1996) Forensic taphonomy: the postmortem fate of human remains. CRC Press, Boca Raton

[3] Andrews P, Fernández-Jalvo Y (2012) How to approach perimortem injury and other modifications. Forensic microscopy for skeletal tissues. Humana Press, Totowa, pp 191–225

[4] Cappella A, Castoldi E, Sforza C, Cattaneo C (2014) An osteological revisitation of autopsies: comparing anthropological findings on exhumed skeletons to their respective autopsy reports in seven cases. Forensic Sci Int 244:315-e1

[5] Sauer NJ (1998) The timing of injuries and manner of death: distinguishing among antemortem, perimortem and postmortem trauma. Forensic Osteol: Adv Identif Hum Remains 2:321–331

[6] Hart GO (2005) Fracture pattern interpretation in the skull: differentiating blunt force from ballistics trauma using concentric fractures. J Forensic Sci 50(6):1–6

[7] Symes SA, Ericka N, L'Abbé ENC, Wolff I, Dirkmaat DC (2012) 17 interpreting traumatic. Companion Forensic Anthropol 39:340

[8] O'BC S, Berryman HE, Lahren CH (1987) Cranial fracture patterns and estimate of direction from low velocity gunshot wounds. J Forensic Sci 32(5):1416–1421

[9] Berryman HE, Symes SA (1998) Recognizing gunshot and blunt cranial trauma through fracture interpretation. Forensic Osteol: Adv Identif Hum Remains 2:333–352

[10] Smith OC, Pope EJ, Symes SA (2015) Look until you see: identification of trauma in skeletal material. Hard evidence. Routledge, Abingdon, pp 190–204

[11] Bland-Sutton J (1915) Observations on injuries of the bones of the limbs by the S Bullet. BMJ Mil Health 24(4):314–323

[12] Bir C, Andrecovich C, DeMaio M, Dougherty PJ (2016) Evaluation of bone surrogates for indirect and direct ballistic fractures. Forensic Sci Int 261:1–7

[13] Huelke DF, Buege LJ, Harger JH (1967) Bone fractures produced by high velocity impacts. Am J Anat 120(1):123–131

[14] Huelke DF, Harger JH, Buege LJ, Dingman HG, Harger DR (1968) An experimental study in bio-ballistics: femoral fractures produced by projectiles. J Biomech 1(2):97–105
[15] Huelke DF, Harger JH, Buege LJ, Dingman HG (1968) An experimental study in bio-ballistics: femoral fractures produced by projectiles—II shaft impacts. J Biomech 1(4):313–321
[16] Dougherty PJ, Sherman D, Dau N, Bir C (2011) Ballistic fractures: indirect fracture to bone. J Trauma Acute Care Surg 71(5):1381–1384
[17] Berryman HE, Gunther WM (2000) Keyhole defect production in tubular bone. J Forensic Sci 45(2):483–487
[18] Dougherty PJ, Vaidya R, Silverton CD, Bartlett C, Najibi S (2009) Joint and long-bone gunshot injuries. JBJS 91(4):980–997
[19] Long WT, Chang W, Brien EW (2003) Grading system for gunshot injuries to the femoral diaphysis in civilians. Clin Orthop Relat Res 1976–2007(408):92–100
[20] Ryan JR, Hensel RT, Salciccioli GG, Pedersen HE (1981) Fractures of the femur secondary to low-velocity gunshot wounds. J Trauma 21(2):160–162
[21] Martrille L, Symes SA (2019) Interpretation of long bones ballistic trauma. Forensic Sci Int 302:109890
[22] Veenstra A, Kerkhoff W, Oostra RJ, Galtés I (2022) Gunshot trauma in human long bones: towards practical diagnostic guidance for forensic anthropologists. Forensic Sci Med Pathol 18:1–9
[23] Synbone® (2022) Portfolio for ballistic testing. https://www.synbone.com/product-category/biomechanics-generics/forensic-and-ballistic/forensic-and-ballistic-rod/?shop_currency=CHF. Accessed 10 Oct 2022
[24] Kneubuehl BP, Thali MJ (2003) The evaluation of a synthetic long bone structure as a substitute for human tissue in gunshot experiments. Forensic Sci Int 138(1–3):44–49
[25] Henwood BJ, Appleby-Thomas G (2020) The suitability of Synbone® as a tissue analogue in ballistic impacts. J Mater Sci 55:3022–3033. https://doi.org/10.1007/s10853-019-04231-y
[26] Kieser DC, Carr DJ, Leclair SCJ, Horsfall I, Theis JC, Swain MV, Kieser JA (2013) Gunshot induced indirect femoral fracture: mechanism of injury and fracture morphology. BMJ Mil Health 159(4):294–299
[27] Kieser DC, Carr DJ, Leclair SC, Horsfall I, Theis JC, Swain MV, Kieser JA (2013) Clothing increases the risk of indirect ballistic fractures. J Orthop Surg Res 8(1):1–7
[28] Kieser DC, Riddell R, Kieser JA, Theis JC, Swain MV (2014) Bone micro-fracture observations from direct impact of slow velocity projectiles. J Arch Mil Med 2(1):1–6
[29] Zhang X, Xu C, Wen Y, Luo S (2015) The experimental and numerical study of indirect effect of a rifle bullet on the bone. Forensic Sci Int 257:473–480
[30] Kieser DC, Kanade S, Waddell NJ, Kieser JA, Theis JC, Swain MV (2014) The deer femur—a morphological and biomechanical animal model of the human femur. Bio-Med Mater Eng 24(4):1693–1703
[31] Jussila J (2005) Wound ballistic simulation: assessment of the legitimacy of law enforcement firearms ammunitionby means of wound ballistic simulation. Academic Dissertation, University of Helsinki
[32] Kneubuehl BP, Coupland RM, Rothschild MA, Thali MJ (2011) Wound ballistics: basics and applications. Translation of the 3rd German edition. Springer, Berlin
[33] Scheirs S, Malgosa A, Sanchez-Molina D, Ortega-Sánchez M, Velázquez-Ameijide J, Arregui-Dalmases C, Medallo-Muñiz J, Galtés I (2017) New insights in the analysis of blunt force trauma in human bones. Preliminary results. Int J Legal Med 131(3):867–875
[34] Kieser J, Taylor M, Carr D (2012) Forensic biomechanics. Wiley, Hoboken
[35] Smith OC, Pope EJ, Symes SA (2015) Look until you see: identification of trauma in skeletal material. In: Hard evidence. Routledge
[36] Madea B, Staak M (1988) Determination of the sequence of gunshot wounds of the skull. J Forensic Sci Soc 28(5–6):321–328
[37] Quatrehomme G, Işcan MY (1998) Analysis of beveling in gunshot entrance wounds. Forensic Sci Int 93(1):45–60
[38] Quatrehomme G, İşcan MY (1997) Bevelling in exit gunshot wounds in bones. Forensic Sci Int 89(1–2):93–101
[39] Huelke D, Darling J (1964) Bone fractures produced by bullets. J Forensic Sci 9(4):461–469
[40] DiMaio VJ (2015) Gunshot wounds: practical aspects of firearms, ballistics, and forensic techniques. CRC Press, Boca Raton
[41] Smith MJ, James S, Pover T, Ball N, Barnetson V, Foster B, Guy C, Rickman J, Walton V (2015) Fantastic plastic? Experimental evaluation of polyurethane bone substitutes as proxies for human bone in trauma simulations. Legal Med 17(5):427–435
[42] Henwood B, Oost T, Fairgrieve S (2019) Bullet caliber and type categorization from gunshot wounds in *Sus scrofa* (Linnaeus) long bone. J Forensic Sci. https://doi.org/10.1111/1556-4029.14004
[43] Berryman H, Smith O, Symes S (1995) Diameter of cranial gunshot wounds as a function of bullet caliber. J Forensic Sci 40(5):751–4
[44] Ross A (1996) Caliber estimation from cranial entrance defect measurements. J Forensic Sci 41(4):629–33

[45] Paschall A, Ross A (2017) Bone mineral density and wounding capacity of handguns: implications for estimation of caliber. Int J Legal Med 131(1):161–6
[46] Muschler GF, Raut VP, Patterson TE, Wenke JC, Hollinger JO (2010) The design and use of animal models for translational research in bone tissue engineering and regenerative medicine. Tissue Eng Part B Rev 16(1):123–145
[47] Augat P, Schorlemmer S (2006) The role of cortical bone and its microstructure in bone strength. Age Ageing 35(suppl_2):ii27–ii31
[48] Hillier ML, Bell LS (2007) Differentiating human bone from animal bone: a review of histological methods. J Forensic Sci 52(2):249–263
[49] Dominguez VM, Crowder CM (2012) The utility of osteon shape and circularity for differentiating human and non-human Haversian bone. Am J Phys Anthropol 149(1):84–91
[50] Wang X, Shen X, Li X, Agrawal CM (2002) Age-related changes in the collagen network and toughness of bone. Bone 31(1):1–7
[51] Nyman JS, Roy A, Shen X, Acuna RL, Tyler JH, Wang X (2006) The influence of water removal on the strength and toughness of cortical bone. J Biomech 39(5):931–938
[52] Pineri MH, Escoubes M, Roche G (1978) Water–collagen interactions: calorimetric and mechanical experiments. Biopolym: Orig Res Biomol 17(12):2799–2815
[53] Schmitt KU, Niederer PF, Cronin DS, Morrison B III, Muser MH, Walz F (2019) Trauma biomechanics: an introduction to injury biomechanics. Springer, Cham
[54] Sellier KG, Kneubuehl BP, Haag LC (1995) Wound ballistics and the scientific background. Am J Forensic Med Pathol 16(4):355
[55] Fackler ML (1996) Gunshot wound review. Ann Emerg Med 28(2):194–203
[56] Özkaya N, Nordin M (1999) Fundamental of biomechanics: equilibrium, motion and deformation, 2nd edn. Springer, New York, pp 17–21, 125–147, 206–210
[57] Wheatley BP (2008) Perimortem or postmortem bone fractures? An experimental study of fracture patterns in deer femora. J Forensic Sci 53(1):69–72
[58] Einhorn TA (1992) Bone strength: the bottom line. Calcif Tissue Int 51(5):333–339
[59] Cohen H, Kugel C, May H, Medlej B, Stein D, Slon V, Hershkovitz I, Brosh T (2016) The impact velocity and bone fracture pattern: forensic perspective. Forensic Sci Int 266:54–62

Publisher's Note Springer Nature remains neutral with regard to jurisdictional claims in published maps and institutional affiliations.

5.2. Ballistic long bone fracture pattern: an experimental study

Authors

Schwab, N., Jordana, X., Monreal, J., Garrido, X., Soler, J., Vega, M., Brillas, P., Galtés, I.

Journal

International Journal of Legal Medicine. Impact factor and quartile ranking: 2.1, Q2.

Date of publication

20 February 2024

Addressed objectives

This second publication focuses on the characterisation of a ballistic fracture pattern in human long bones useful for the forensic trauma interpretation and addresses the previously defined objectives 1, 2 and 4:

1. To establish a valuable setup for long bone gunshot experiments.
2. To macroscopically characterise a distinct ballistic fracture pattern in human long bones.
4. To assess the influence of bone features and the presence of soft tissue on the human fracture pattern.

This article is reproduced with permission from Springer Nature.

International Journal of Legal Medicine
https://doi.org/10.1007/s00414-024-03191-6

ORIGINAL ARTICLE

Ballistic long bone fracture pattern: an experimental study

Nathalie Schwab[1,2] · Xavier Jordana[1,3] · Jordi Monreal[4] · Xavier Garrido[4] · Joan Soler[4] · Manel Vega[4] · Pedro Brillas[5] · Ignasi Galtés[2,6]

Received: 23 October 2023 / Accepted: 9 February 2024
© The Author(s), under exclusive licence to Springer-Verlag GmbH Germany, part of Springer Nature 2024

Abstract

When dealing with badly preserved cadavers or skeletal human remains, the assessment of death circumstances remains challenging. When forensic evidence cannot be taken from the skin and soft tissue, the information may only be deduced from more resistant elements such as bone. Compared to cranial gunshot injuries, reliable data on ballistic long bone trauma remains scarce. This study aims to define ballistic fracture characteristics in human long bones. The shaft of 16 femurs and 13 humeri from body donors was perpendicularly shot with a 9-mm Luger full metal jacket bullet at an impact velocity of 360 m/s from a distance of 2 m. Some bones were embedded in Clear Ballistics Gel®, and some were shot without soft tissue simulant in order to better visualise the fracture propagation on the high-speed camera. The fractures were examined macroscopically and compared between the sample groups. We consistently found comminuted fractures with a stellate pattern. Fracture details were classified into entrance, exit and general characteristics. For some traits, we detected different occurrence values in the group comparison. The results indicate that some of the traits depend on bone properties such as shaft diameter, bone length and cortical thickness. The presence of ballistic gel also influenced some fracture traits, emphasising the relevance of soft tissue simulant in osseous gunshot experiments. This study revealed new insights in the detailed fracture pattern of human long bones. These may serve as guidelines for the identification and reconstruction of gunshot trauma in human long bones.

Keywords Forensic anthropology · Human bones · Femur · Humerus · Gunshot · Fracture pattern

Introduction

When dealing with badly preserved cadavers or skeletal human remains, event reconstruction of traumatic cases and determination of the cause of death remain a major challenge for forensic pathologists and anthropologists. In contrast to fresh or well-preserved cadavers, forensic information in such cases may only be deduced from more resistant tissue such as bone, without further evidence provided by findings on the skin or soft tissue. Although signs of trauma usually

✉ Xavier Jordana
xavier.jordana@uab.cat

✉ Ignasi Galtés
ignasigaltes@gmail.com

1 Biological Anthropology Unit, Department of Animal Biology, Plant Biology and Ecology, Faculty of Biosciences, Universitat Autònoma de Barcelona, Cerdanyola del Vallès, 08193 Barcelona, Catalonia, Spain

2 Forensic Anthropology Unit, Forensic Pathology Service, Catalonian Institute of Legal Medicine and Forensic Science (IMLCFC), Ciutat de La Justícia, Gran Via de Les Corts Catalanes, 111 Edifci G, 08075 Barcelona, Spain

3 Tissue Repair and Regeneration Laboratory (TR2Lab), Institut de Recerca I Innovació en Ciències de La Vida I de La Salut a La Catalunya Central (IrisCC), Ctra. de Roda, 08500 Vic, Barcelona, Spain

4 Mossos d'Esquadra, Unitat Central de Balística I Traces Instrumentals, Av. de La Pau, 12, 08206 Sabadell, Barcelona, Spain

5 Donor Center Barcelona Tissue Bank (BTB), Hospital Clínic de Barcelona, C/Villarroel 170, Escala 12 Planta 4, 08036 Barcelona, Spain

6 Research Group of Biological Anthropology (GREAB), Biological Anthropology Unit, BABVE Department, Universitat Autònoma de Barcelona (UAB), Cerdanyola del Vallès, 08193 Bellaterra, , Catalonia, Spain

Published online: 20 February 2024

persist in bone, reliable forensic conclusions can be considerably complicated, particularly when skeletal remains are shattered or the fractured bones incomplete [1, 2].

Gunshot trauma is widespread not only in armed conflicts, but also in the frame of civil violence [3–6]. Some authors report that at least 50% of the gunshot injuries affect the extremities, often resulting in fractures [7–10]. In this context, the femoral shaft fracture was observed most frequently among ballistic long bone trauma [9]. Despite the frequent occurrence of ballistic long bone trauma, there is only little reliable data in the literature on their fracture characteristics useful for forensic trauma reconstructions.

Studies concerning gunshot trauma have mainly been carried out to analyse cranial fractures [11–13]. There are only a few studies focusing on gunshot trauma in long bones. In 1915, Bland-Sutton described five types of ballistic fractures in human long bones [14]: a projectile impacting a long bone can result in a transverse fracture, completely pierce the diaphysis, stay embedded in the bone, strike the diaphysis and produce a stellate or butterfly pattern, and/or shatter the bone into small fragments. On one hand, this work solely describes the potential fracture type produced by a gunshot without providing details on cortical traits. On the other hand, an actualisation based on current ballistics is required as guns and projectiles have changed since 1915. Since then, however, the majority of the experimental research using human long bones focused on the fracture pathophysiology and risk prediction in relation to different ballistic variables [6, 15–18]. In the 1960s, Huelke et al. used steel spheres with various sizes and velocities to quantify the energy transmitted by the projectiles [16–18]. In the 1980s, Ragsdale and Josselson targeted on cancellous-rich bone areas of distal femurs and proximal tibias, which do not allow the best analysis of cortical bone behaviour [19]. Robens and Küsswetter showed findings in X-rays after a gunshot to the metaphyseal part of the tibias [20]. Also, Coudane et al. studied bone lesions with X-rays after producing gunshot injuries to the limbs of two dead bodies [21]. More recently, Dougherty, Sherman and Bir investigated indirect gunshot impact on diaphyseal femurs and tibia [6]. Bir et al. analysed the fracture risk prediction based on velocity producing both direct and indirect ballistic fractures in human femurs and long bone polyurethane surrogates [15]. Aside from these studies, research on ballistic trauma in human long bones essentially remained descriptive [9, 22–25]. In a more recent review from 2022, Veenstra et al. studied publications providing data on ballistic fractures observed in long bones [26]. The work revealed different types of fractures as a result of gunshot trauma such as linear, oblique, butterfly and comminuted fractures. However, the above-mentioned studies barely provide data on detailed cortical traits useful for gunshot trauma interpretation, reconstruction and differentiation from other types of trauma.

Further studies on this topic are needed to improve the quality and reliability of the forensic investigation of human long bone trauma. A crucial method to gain further knowledge on detailed ballistic trauma patterns including cortical traits are experimental studies, where the fractures can be reproduced under controlled conditions. In a recent paper, we presented some preliminary data on cortical traits observed in experimentally produced gunshot fractures in human long bones [27]. The purpose of that study was to test whether alternative long bone models such as polyurethane cylinders from Synbone® AG (Switzerland) and female red deer femurs can reproduce the same ballistic fracture patterns. It was revealed that neither the synthetic nor the animal model sufficiently reproduces the human fracture pattern, making these alternative models unsuitable to replace human bones for further fracture investigations.

In the current work, we aim to define a distinctive gunshot fracture pattern in human long bones. Specifically, we propose to reproduce, characterise and discuss the cortical traits related to ballistic long bone trauma and to acquire more knowledge on the underlying fracture mechanism. To this purpose, we have experimentally analysed a broad size of human long bones including femur and humerus. Two different types of long bones were selected to assess if there are considerable differences or if they show similar characteristics indicating that long bones generally produce a similar ballistic fracture pattern. We surrounded the specimens with Clear Ballistics Gel®, a synthetic simulant for soft tissue. In addition, some bones were shot without the gel in order to better visualise the fracture propagation on the high-speed videos. In doing so, we used the opportunity to assess potential differences in the fracture patterns between the specimens shot with and without the soft tissue simulant.

Materials and methods

A total of 29 fresh human healthy bones, 16 femurs and 13 humeri, were used to analyse the fracture type, the fracture propagation and the cortical traits upon gunshot.

Samples and sample preparation

All 29 bones were provided by the Donor Center-Barcelona Tissue Bank, Banc de Sang i Teixits de Catalunya. They were donated from a total of 14 cadavers, 12 males and 2 females. Donor age at death was between 55 and 72 years. All bones were collected with a postmortem time interval of up to 24 h. They were entirely dissected from the limbs and kept in the freezer until further use. Prior to the experiments, the bones were thawed and the remaining soft tissue was removed up to the periosteum with surgical tools. Subsequently, each bone was macroscopically investigated to exclude pathologies or damage.

To simulate soft tissue, 20 samples, 10 femurs and humeri each, were embedded in ballistic gel. We used a product from the Canadian brand Clear Ballistics, which is supplied as a ready mixed, solid block that requires to be melted at 100 °C for 4 to 5 h before individual application. Clear Ballistics polymer blocks are known for their convenient preparation and exceptional transparency and clearness compared to the standard simulant which is 10% ordnance gelatine [28]. Despite the possibility of reusing this gel, in this study, we consistently employed new gel for the samples. To surround the bones with the gel, we used cylindrical metal moulds with a total diameter of 10 cm. The bones were positioned with the anterior face located 2 cm deep behind the mould's front surface. The liquid gel was poured into the moulds until the bone shaft was entirely surrounded. Subsequently, the gel was left to solidify overnight at room temperature. We observed that air bubbles formed around the bones, which hampered a clear view on the bone surface. As a consequence, further nine samples, six femurs and three humeri, were shot without gel for a better visualisation of the cracking mechanism on the high-speed recordings. The sample characteristics are summarised in Table 1.

Shooting procedure

All bones were shot under the same condition. Figure 1 illustrates the experimental setup. We securely fixed each specimen upright using a self-constructed stabilisation device. This device was firmly attached to a table. It consisted of a rigid metal plate on the bottom and an adjustable metal plate on the top. The latter could be moved up or down along a steel bar that connected both plates. With the help of two metal cup stabilisers, on each plate one, the bone's epiphyses were held securely. The specimens were placed 2 m before the muzzle of a 9-mm Luger test barrel (Drello Bal 1025 FU-R). While the mechanics of test barrels differ to a certain extent from real firearms, they enable precise, reproducible shots and are commonly employed as a method of experimentation. The bullet impact velocity produced by the test barrel was 360 m/s,

Table 1 Sample group description (*Fem Gel*, = femur with gel; *Fem no Gel*, = femur without gel; *Hum Gel*, humerus with gel; *Hum no Gel*, humerus without gel), revealing the gender, age, bone length, shaft diameter and cortical thickness (mean and standard deviation)

Sample group	*N*	Male	Female	Age	Bone length (cm)	Shaft diameter (cm)	Cortical thickness (mm)
Fem Gel	10	10	0	62 (5.4)	45.9 (2.8)	2.9 (0.3)	6.2 (0.8)
Fem no Gel	6	2	4	66 (4.9)	44.9 (2.4)	3.0 (0.1)	4.3 (1.5)
Hum Gel	10	10	0	61 (5.0)	32.5 (1.9)	2.1 (0.2)	3.6 (0.8)
Hum no Gel	3	1	2	61 (4.0)	31.0 (0.8)	1.8 (0.5)	3.7 (1.5)

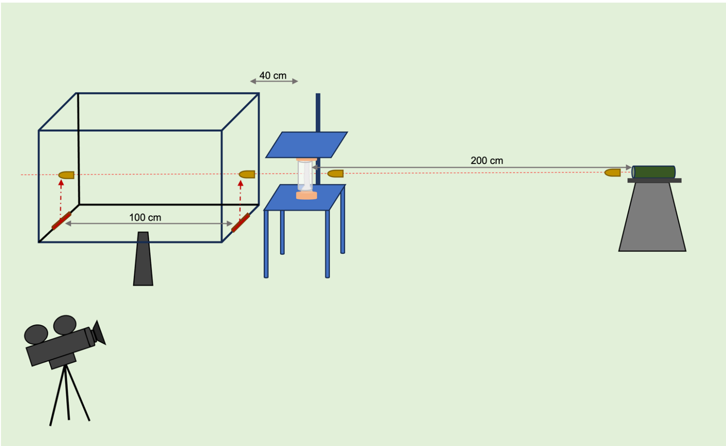

Fig. 1 Experimental setup: test barrel (green) on the right side, fixation table (blue) with metal cup stabilisers (orange) and bone-gel-sample (light grey). Light barrier with two sensors (red) that measure the time the bullet takes from the first to the second sensor. High-speed camera on the bottom left. Distances: 200 cm between muzzle and bone, 40 cm between bone and light barrier, 100 cm between the first and second sensor of the light barrier. The dashed red line indicates the trajectory of the projectile (yellow–brown)

simulating a shot from a handgun. An optical laser was used to define the point of shooting. This was possible in all samples, as the transparency of the ballistic gel allows exact targeting. For the shots, we used a NonTox 9-mm Luger full metal jacket projectile from Sellier & Bellot® ($m = 7.98$ g). On each sample, one single projectile was fired in an orthograde manner, whereby the bullet nose struck the middle of the anterior face of the shaft. As the diaphysis has a high corticalis-spongiosa ratio, it allows the best analysis of cortical bone behaviour and hence is more informative than cancellous-rich areas near the epiphysis (Antrag: 43). The exit velocity of the projectile upon impact was measured using a light barrier (Drello LS 11–03) with a computerised system (Drello VC 4043–09). The performance was recorded with a high-speed camera (Phantom V2012).

Sample assessment

The fragments of each shot specimen were collected and cleaned prior to analysis. In doing so, the bones were cooked at 100 °C for 2 to 5 h in a water detergent solution consisting of 5 L of plain water and 1 cup of commercial degreasing detergent [29]. Subsequently, the bones were scrubbed smoothly to clear away the periosteum. After the bones were left to dry, the fragments of each sample were reassembled using a superglue. This allowed us to better visualise the fracture patterns. The fractures were examined macroscopically. The fracture type was determined by its appearance on the impact side. The cortical traits were classified into entrance, exit and general features. For quantitative analyses, we used a calliper to measure the maximal longitudinal fracture extent and the horizontal and vertical diameter of the projectile's entrance and exit hole. The projectiles' post-impact velocity was used to calculate the kinetic energy lost in each bone ($Ke = 0.5\ mv^2$).

After the collection of all data, the ballistic fracture patterns were defined. In doing so, we grouped the samples into femurs with and without gel and humeri with and without gel. Logistic regression and two-way ANOVA (Tukey post hoc tests) were performed to statistically test the effect of ballistic gel and the type of bone (femur and humerus) in the occurrence of fracture characteristics. The significance level was set at 0.05. A multiple correspondence analysis was done to explore correlations between the fracture traits (qualitative and quantitative), experimental groups (type of bone and use of gel) and bone properties (length, shaft diameter and cortical thickness).

Results

Upon gunshot, all samples exhibited comminuted fracture accompanied by severe fragmentation into small bone chips. Nevertheless, assembling the bigger fragments allowed a more comprehensive fracture reconstruction and a sound macro-morphological assessment. Tables 2, 3 and 4 and Figs. 2, 3 and 4 present the qualitative cortical traits classified into entrance, exit and general features that characterise the ballistic fracture pattern in human long bones. In total, 24 qualitative and 6 quantitative variables were determined.

The entrance fracture pattern

Table 5 shows the occurrence of the cortical entrance traits in the sample groups. Figures 2 and 3 illustrate the entrance fracture with the detailed cortical traits. In each case, the entrance fracture featured a round entry hole with various radiating and concentric fractures. On the impact side, this visually resulted in a stellate pattern. Longitudinal concentric fractures around the entry hole were observed in all samples. They could typically be seen on the lateral shaft aspect. Transversal concentric fractures were less frequent. In the gel samples, they occurred in none of the femurs (0%) and in three out of ten humeri (30%). In the samples without gel, they occurred in two out of six femurs (33%) and in one out of three humeri (33%). Differences between sample groups were not statistically significant.

V-shape, ring defect, internal beveling and wing piece were featured by all samples. A lateral notch was found in all femurs with and without gel (100% each), in all humeri without gel (100%) and in nine out of ten humeri with gel (90%). There were no significant differences between the sample groups. Tip fragmentation was featured in all femurs and humeri without gel (100% each) and in nine out of ten femurs and humeri with gel, respectively (90% each). The difference between the samples, however, was not statistically significant. Wing flake was most common in gel femurs with seven out of ten positive cases (70%). In contrast, they were not found in any of the femurs without gel (0%). In gel humeri, they occurred in five out of ten cases (50%), and in humeri without gel in one out of three cases (33%). Logistic regression revealed a significant correlation between the presence of gel and the occurrence of wing flakes (p value = 0.031, odds ratio = 12.5). Wing flake defect was featured by all femurs with gel (100%) and three out of six femurs without gel (50%). In humeri, the trait was found in five out of ten with gel (50%) and in two out of three without gel (67%). Logistic regression did not reveal a significant difference, but yet showed that the occurrence of a wing flake defect is close to significantly greater in femurs than humeri (p value = 0.081, odds ratio = 0.19).

As quantitative entrance variables, we measured the vertical and horizontal entry hole diameter (Table 6, Fig. 5). The latter, however, could not be evaluated for all samples as a complete entry hole reconstruction was not always possible. The mean vertical entry hole diameter was the largest in femurs, both with (10.1 ± 1.0 mm) and without gel (10.1 ± 0.5 mm). In humeri with gel, it was 9.8 ± 0.7 mm,

Table 2 Trait definition at the entrance fracture

Round entry hole	The projectile's initial entry defect appearing visually round
Radiating fracture	Longitudinal, transversal or oblique fractures that radiate away from the entry hole
Concentric fracture	Curvilinear fractures facing with their concave aspect towards the entry hole. They were divided into transversal or longitudinal ones. The first occurs proximal/distal of the entry hole, the second on the sides of the entry hole
V-shape	Describes the shape of the bone proximal/distal to the entry hole. The tip of the v-shape points towards the bullet entry. The margins of the v-shape are built by oblique fracture lines
Tip fragmentation	A superficial, external loss of cortical fragment(s) at the tip of the bone around the entry hole. It only appears proximal/distal of the bullet entry. Typically, chiselled edges indicate a sharply defined transition to the intact cortical bone. In case oblique fractures separate the bone, tip fragmentation on bone parts next to each other creates the image of a stepped circular margin around the bullet entry
Ring defect	A circular or partial circular loss of superficial cortical bone on the entry hole's margin. Its presentation reminds of an abrasion ring. It can be interrupted by other entrance traits such as tip fragmentation
Wing flake	A loose trapezoidal flake of cortical bone resembling spread wings. The aspect facing the entry hole features part of the ring defect. In contrast to tip fragmentation, it comes from the lateral aspect(s) of the entry hole. It may be broken and thus incomplete
Wing flake defect	The superficial cortical defect on the lateral aspect(s) of the entry hole that is produced when the wing flake breaks out
Internal beveling	A funnel shape in the cortical wall with a larger extent on the internal side
Wing piece	A bone fragment originating from the lateral shaft aspect(s). Its shape is similar to the wing flake, but it is usually much bigger, and most importantly, it affects the hole cortical wall; only the extremes run out superficially. The aspect facing the entry hole may contain part of the ring defect or a wing flake defect. A wing piece can be entire, but also broken into two or more fragments. Less frequently, they may be still attached on one side of the shaft
Lateral notch	As the wing piece's extremes run out superficially, they leave behind a corresponding cortical defect on the lateral shaft aspect. On this fracture surface, there is a prominent notch visible

Table 3 Trait definition at the exit fracture

Square exit hole	The projectile's exit defect appears visually edgy or square
Radiating fracture	Transversal, longitudinal or oblique fractures that radiate away from the exit hole
Concentric fracture	Curvilinear fractures facing with their concave aspect towards the exit hole. They were divided into transversal or longitudinal ones. The first occurs proximal/distal of the exit hole, the second on the sides of the exit hole
Layered breakage	Is a layered pattern visible on the fracture surface
External beveling	A funnel shape in the cortical wall with a larger extent on the external side
Stepped breakout	A sequence of multiple transversal concentric fractures on the posterior shaft aspect resulting in a stepped breakout of fragments with similar shapes

Table 4 General trait definition

Plastic deformation	Is the persistent deformation of bone
Marginal chipping	Tiny, superficial cortical defects on the fracture margin
Fx surface scaling	Tiny cortical scaling on the fracture surface

and in humeri without gel the smallest with 9.2 ± 0.3 mm. There was no significant difference between the sample groups. The largest mean horizontal diameter was established for femurs with gel (10.1 ± 0.7 mm). In contrast, the smallest mean horizontal diameter was found in femurs without gel (8.3 ± 0.9 mm). In humeri with gel, it was 9.8 ± 0.9 mm. In humeri without gel, only one sample could be evaluated revealing a horizontal diameter of 9.5 mm. Two-way ANOVA showed significant differences in the size of the horizontal entry hole diameter between samples with and without gel (p value = 0.002, eta^2 = 0.39).

The exit fracture pattern

Table 5 shows the occurrence of all cortical exit traits in the sample groups. In all samples, we observed an exit hole with various radiating and concentric fractures. The transversal concentric fractures were present in all femurs and humeri with gel (100% each), in all humeri without gel (100%) and in five out of six femurs without gel (83%). There were no significant differences between the sample groups. Longitudinal concentric fractures were present in seven out of ten femurs and six out of ten humeri with gel (70% and 60% respectively). In

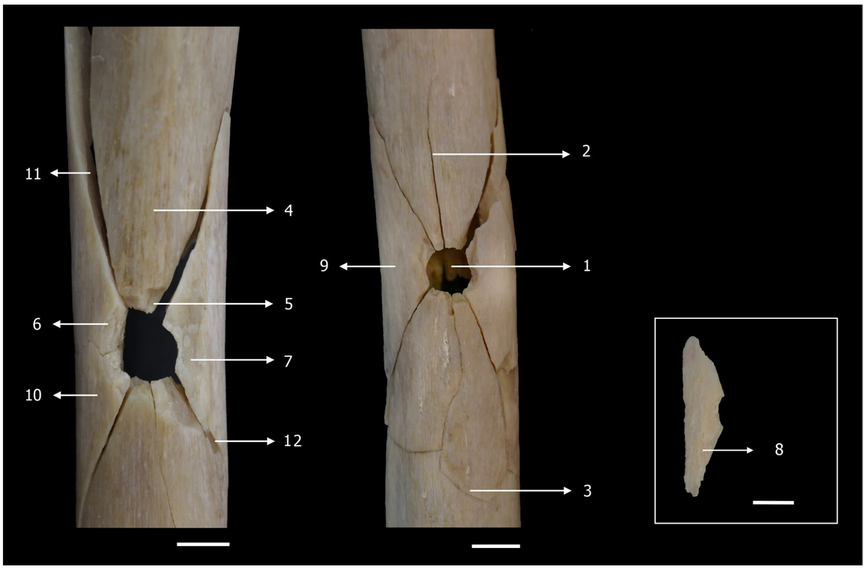

Fig. 2 Anterior view of two shot femurs (white bar = 1 cm). Entrance traits: round entry hole (1), radiating fracture (2), transversal concentric fracture (3), v-shape (4), tip fragmentation (5), ring defect (6), wing flake defect (7), wing flake (8), wing piece (9), transversally broken wing piece (10). General cortical traits: plastic deformation (11), marginal chipping (12)

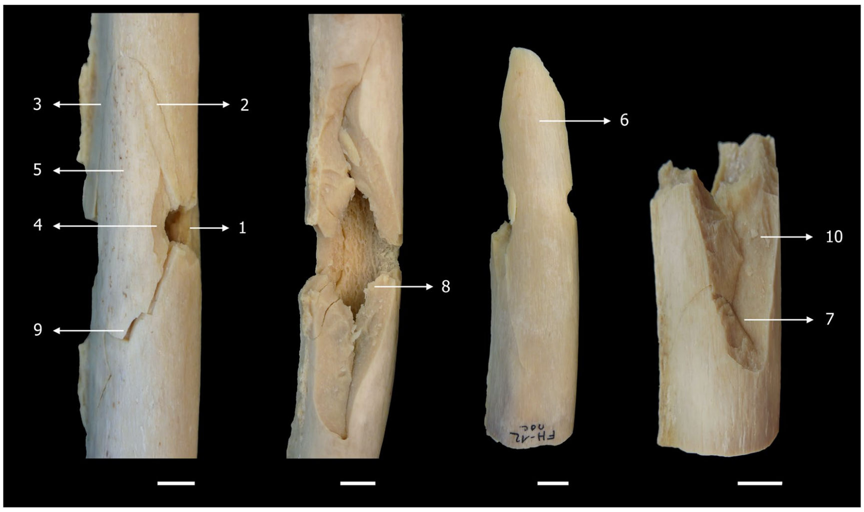

Fig. 3 Lateral view of four shot femurs (white bar = 1 cm). Entrance traits: round entry hole (1), radiating fracture (2), longitudinal concentric fracture (3), wing flake defect (4), wing piece (5), wing piece attached to the shaft (6), lateral notch (7), internal beveling (8). General cortical traits: plastic deformation (9), Fx surface scaling (10)

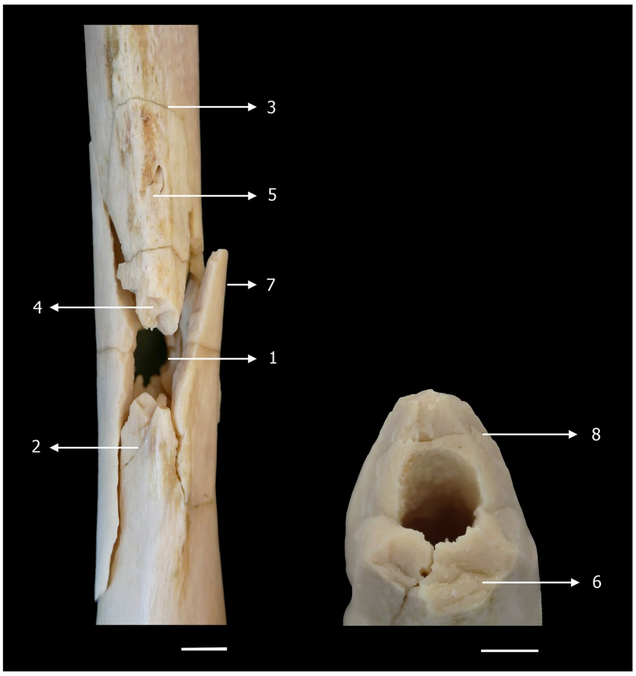

Fig. 4 Posterior view and superior view of two shot femurs (white bar = 1 cm). Exit traits: square exit hole (1), radiating fracture (2), transversal concentric fracture (3), external beveling (4), stepped breakout (5), layered breakage (6). General cortical traits: plastic deformation (7), Fx surface scaling (8)

the samples without gel, they were present in three out of six femurs (50%) and in none of the humeri (0%). There were no significant differences between the sample groups.

A square exit hole was found in all humeri with and without gel (100% each). In femurs, it was found in nine out of ten with gel (90%) and in five out of six without gel (83%). There were no significant differences between the sample groups. The two femurs, one with and one without gel, which did not have a square exit hole, presented a round exit hole. Stepped breakout was found in six out of ten femurs with gel (60%) and five out of six femurs without gel (83%). In humeri, it was less common with an occurrence of two out of ten with gel (20%) and a complete absence in the ones without gel (0%). Logistic regression revealed that the occurrence of stepped breakout is significantly greater in femurs than humeri (p value = 0.009, odds ratio = 0.08). Layered breakage occurred in nine out of ten femurs and eight out of ten humeri with gel (90% and 80% respectively). In the samples without gel, it occurred in four out of six femurs (67%) and in one out of three humeri (33%). The logistic regression showed no significant, but yet a close correlation between the presence of gel and layered breakage (p value = 0.075, odds ratio = 5.9). External beveling was detected in all femurs with and without gel (100% each) and in all humeri with gel (100%), but only in one out of three without gel (33%). However, statistically significant differences between sample groups were not found.

Quantitatively, the vertical and horizontal exit hole diameters were evaluated; however, the consistent measurement was hampered as the exit hole could not always be entirely reconstructed (Table 6 and Fig. 5). Notably, it was not possible with any of the no gel humeri. The mean vertical exit hole diameter was the largest in humeri with gel (21.6 ± 9.6 mm). In the femurs with gel, it was 18.2 ± 6.3 mm, and in femurs without gel the smallest with 15.0 ± 6.9 mm. There were no significant differences between the groups. The mean horizontal exit hole diameter was the largest in femurs with gel (10.5 ± 1.8 mm). In the humeri with gel, it was 9.5 ± 1.7 mm, and in femurs without gel the smallest with 7.9 ± 2.6 mm. Two-way ANOVA showed that the size of the horizontal exit hole diameter was significantly larger in samples with gel than without gel (p value = 0.026, $eta^2 = 0.234$).

The general fracture characteristics

Some general cortical traits could be detected without a relation to the entrance or exit fracture. All samples showed plastic deformation, marginal chipping and fracture surface

Table 5 Analysed cortical traits divided into entrance, exit and general traits (*p value < 0.05, **p value < 0.01)

	Femur gel		Femur no gel		Humerus gel		Humerus no gel	
N	10		6		10		3	
Entrance traits								
Round hole	10	100%	6	100%	10	100%	3	100%
V-shape	10	100%	6	100%	10	100%	3	100%
Tip fragmentation	9	90%	6	100%	9	90%	3	100%
Ring defect	10	100%	6	100%	10	100%	3	100%
Wing flake	7	70%	0	0%	5	50%	1	33%
Wing flake defect	10	100%	3	50%	5	50%	2	67%
Internal beveling	10	100%	6	100%	10	100%	3	100%
Wing piece	10	100%	6	100%	10	100%	3	100%
Lateral notch	10	100%	6	100%	9	90%	3	100%
Radiating fracture	10	100%	6	100%	10	100%	3	100%
Concentric fracture	10	100%	6	100%	10	100%	3	100%
Transversal	0	0%	2	33%	3	30%	1	33%
Longitudinal	10	100%	6	100%	10	100%	3	100%
Exit traits								
Square hole	9	90%	5	83%	10	100%	3	100%
External beveling	10	100%	6	100%	10	100%	1	33%
Layered breakage	9	90%	4	67%	8	80%	1	33%
Stepped breakout	6	60%	5	83%	2	20%	0	0%
Radiating fracture	10	100%	6	100%	10	100%	3	100%
Concentric fracture	10	100%	6	100%	10	100%	3	100%
Transversal	10	100%	5	83%	10	100%	3	100%
Longitudinal	7	70%	3	50%	6	60%	0	0%
General traits								
Plastic deformation	10	100%	6	100%	10	100%	3	100%
Marginal chipping	10	100%	6	100%	10	100%	3	100%
Fx surface scaling	10	100%	6	100%	10	100%	3	100%

scaling (Table 5). As shown in Table 6 and Fig. 5, the mean fracture extent was the largest in femurs with gel (14.9 ± 3.3 cm), followed by femurs without gel (14.3 ± 2.6). In humeri with gel, it was 9.2 ± 1.7 cm, and in humeri without gel the smallest with 8.3 ± 1.9 cm. Two-way ANOVA showed that the fracture extent was significantly larger in femurs than in humeri (p value < 0.001, eta^2 = 0.58).

Video analysis

Figure 6 shows a sequence of images from two high-speed videos. Despite the clarity and transparency of the Clear Ballistics Gel®, the densely arranged air bubbles around the bone significantly hindered the analysis of the fracture propagation in the recordings. In this regard, to assess the fracture propagation during gunshot, only the samples without gel allowed an accurate analysis. On the high-speed videos of these samples, we saw that the bullet penetrates the anterior and posterior wall of the shaft producing a direct entrance and exit fracture, respectively. As a further result, we found when the bullet penetrates the anterior wall, radiating fractures initiate on the front side. On the lateral aspect, concentric fractures develop just before the radiating fractures are fully extended. With fracture progression, the radiating and concentric fractures merge. In doing so, the lateral wing piece is formed and eventually blown out laterally as a consequence of the blast effect when the bullet penetrates the shaft.

The bullet's energy lost upon impact

The projectile's exit velocity was measured to calculate the energy lost upon impact (Table 6 and Fig. 5). However, the measurements were not successful in all samples due to interferences with the light barrier caused by bullet fragments and in case of no gel samples also bone fragments. The greatest mean energy loss was observed in femurs with gel (348.6 ± 69.7 J), whereas in femurs without gel, it was only 264.4 ± 99.1 J. In humeri with gel, it

Table 6 Descriptive statistics of the analysed quantitative (*VD*, vertical diameter; *HD*, horizontal diameter; *Fem Gel*, femur with gel; *Fem no Gel*, femur without gel; *Hum Gel*, humerus with gel; *Hum no Gel*, humerus without gel)

	Group	*N*	Mean	SD	Min	Max
Entry hole VD (mm)	Fem Gel	10	10.1	1.0	9.0	11.5
	Fem no Gel	6	10.1	0.5	9.5	11.0
	Hum Gel	10	9.8	0.7	9.0	11.0
	Hum no Gel	3	9.2	0.3	9.0	9.5
Entry hole HD (mm)	Fem Gel	10	10.1	0.7	9.0	11.0
	Fem no Gel	4	8.3	0.9	7.5	9.0
	Hum Gel	7	9.8	0.9	9.0	11.0
	Hum no Gel	1	9.5			
Exit hole VD (mm)	Fem Gel	10	18.2	6.3	12.5	29.0
	Fem no Gel	6	15.0	6.9	9.0	27.0
	Hum Gel	10	21.6	9.6	13.0	40.5
	Hum no Gel	0				
Exit hole HD (mm)	Fem Gel	10	10.5	1.8	7.5	13.0
	Fem no Gel	5	7.9	2.6	4.0	11.0
	Hum Gel	7	9.5	1.7	8.0	12.5
	Hum no Gel	0				
Fracture extent (cm)	Fem Gel	10	14.9	3.3	11.2	21.5
	Fem no Gel	6	14.3	2.6	11.2	16.6
	Hum Gel	10	9.2	1.7	6.5	12.0
	Hum no Gel	3	8.3	1.9	6.2	9.8
Energy loss (J)	Fem Gel	6	348.6	69.7	237.4	444.6
	Fem no Gel	4	264.4	99.1	157.5	375.1
	Hum Gel	8	261.1	61.3	193.8	379.2
	Hum no Gel	1	258.8			

was 261.1 ± 61.3 J), and in humeri without gel, we could only calculate the energy loss in one out of three samples, which was 258.8 J. Two-way ANOVA showed that the higher energy loss in gel femurs compared to the energy loss in gel humeri was close to significant (p value = 0.059, $eta^2 = 0.206$).

Multiple correspondence analysis

A multiple correspondence analysis was done in order to observe correlations among fracture characteristics, bone properties and sample groups (Fig. 7 and Table 7).

Dimension 1 (21% of the variance) shows that gel was especially important in the presence of both wing flake and wing flake defect, as well as the absence of transversal concentric fractures at the bullet entrance. To a lesser extent, gel also had an influence on the presence of external beveling. In contrast, the type of bone (humerus or femur) did not show a significant correlation with the fracture characteristics. Yet, a correlation between bone properties such as cortical thickness and shaft diameter with the occurrence of wing flake, wing flake defect, external beveling and a larger horizontal entry hole diameter has been found.

Dimension 2 (15% of the variance) shows a correlation between a squared exit hole and a higher vertical exit hole diameter, as well as a correlation between absent stepped breakout and absent transversal concentric fractures around the exit hole. The latter was expected, as the stepped breakout is formed by a repetition of transversal concentric fractures.

Ultimately, dimension 3 (14% of the variance) correlates bone properties such as the shaft diameter and bone length with fracture characteristics such as a larger vertical entry hole diameter, a not squared exit hole and a greater occurrence of longitudinal concentric fractures at the exit.

Discussion

In good preserved cadavers, skin and soft tissue injuries typically show characteristic features allowing conclusions on the applied mechanical force such as gunshot, blunt force, sharp force or other impacts [30]. In gunshot trauma, the ballistic characteristics of entrance and exit skin wounds are widely accepted and applied in routine forensic investigations, while less precise morphological information is given for bones. The interpretation and reconstruction of ballistic bone trauma is particularly challenging when dealing with long bones as conclusive

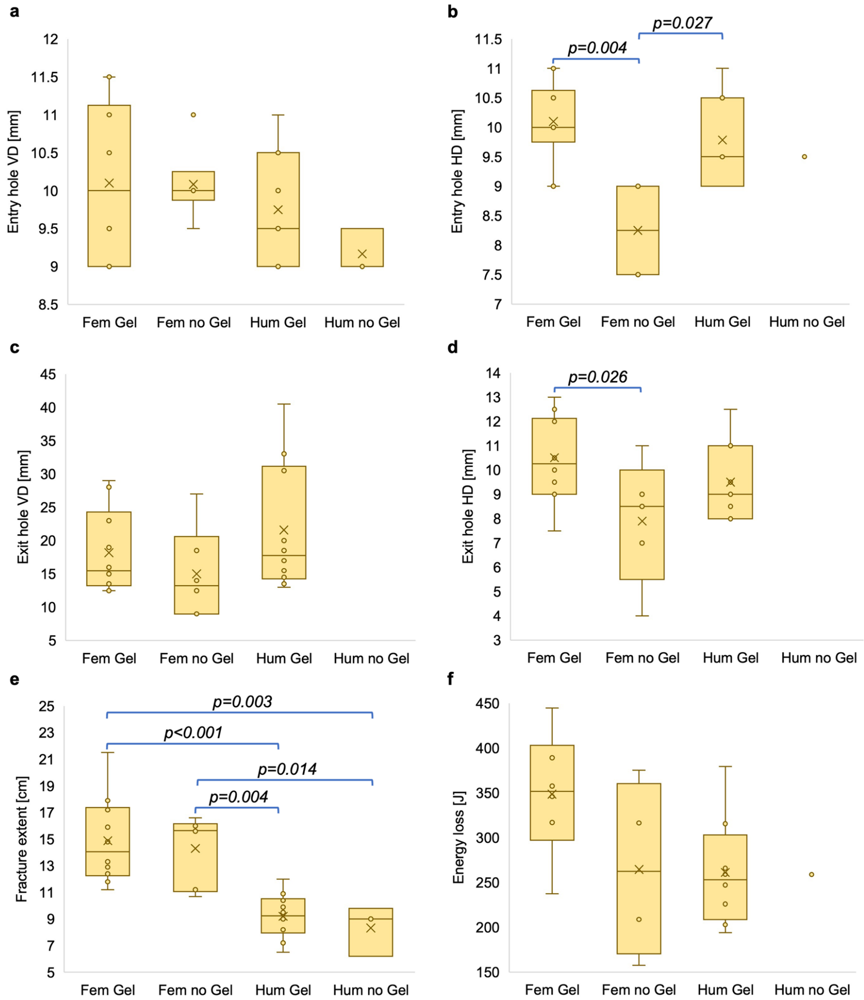

Fig. 5 Box plots representing the **a** vertical entry hole diameter, **b** horizontal entry hole diameter, **c** vertical exit hole diameter and **d** horizontal exit hole diameter, **e** fracture extent and **f** projectiles' energy lost upon impact (VD = vertical diameter, HD = horizontal diameter, Fem Gel = femur with gel, Fem no Gel = femur without gel, Hum Gel = humerus with gel, Hum no Gel = humerus without gel) (significant *p* values for the pairwise comparison)

data is scarce. To resolve such uncertainty, realistic experiments are of great importance. As we revealed in a previous study, the selection of alternative models is problematic because animal bones and bone surrogates are too dissimilar to human bones [27]. In this study, we shot ten femurs and ten humeri with ballistic gel and six femurs and three humeri without ballistic gel. We examined in a comprehensive way the macroscopic characteristics in order to provide supportive guidelines for the ballistic trauma interpretation. Consistently, a comminuted fracture was reproduced, which according to the literature is the most common type of diaphyseal gunshot trauma [26]. In line with the postulation that particularly the bullet impact region is of high conclusive value [27,

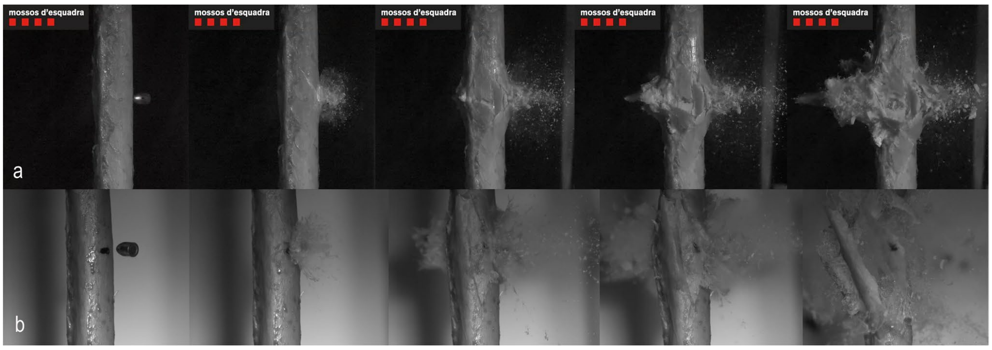

Fig. 6 Sequence of images from high-speed videos capturing the shot of two femurs without gel, from the **a** lateral-posterior perspective showing the bullet entry and exit and the blast effect, and **b** lateral-anterior perspective showing the formation of first radiating and then concentric fractures at the entrance and the blast out of the wing piece

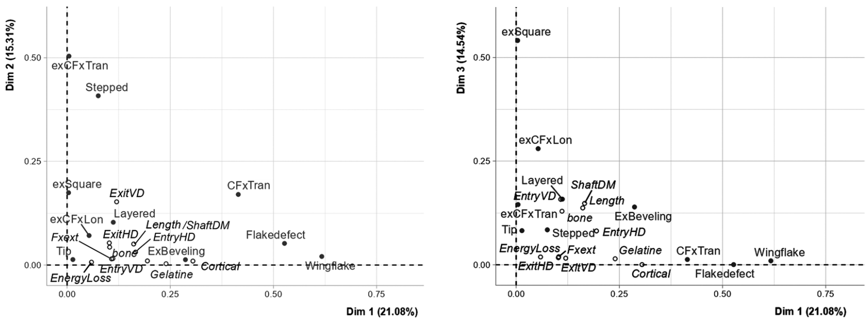

Fig. 7 Multiple correspondence analysis showing the three first dimensions. Representation of the variables: exCFxTran = transversal concentric fracture of the exit, Stepped = stepped breakout, exSquare = squared exit hole, exCFxLon = longitudinal concentric fracture of the exit, Fxext = fracture extent, Tip = tip fragmentation, ExitVD = vertical exit hole diameter, Layered = layered breakage, ExitHD = horizontal exit hole diameter, EntryVD = vertical entry hole diameter, EntryHD = horizontal entry hole diameter, ExBeveling = external beveling of the exit hole, CFxTran = transversal concentric fracture of the entry, Flakedefect = wing flake defect, Wingflake = wing flake, EnergyLoss = bullet's energy loss, bone = type of bone (femur or humerus), Gel = ballistic gel, Length = bone length, ShaftDM = shaft diameter, Cortical = cortical thickness

31], the entrance fracture provided more characteristics than the exit fracture. Figure 8 illustrates the scheme of paradigmatic diaphyseal gunshot fracture resulting from the gunshot scenario tested in this study. In all sample groups, we found a similar ballistic fracture pattern. However, the occurrence values of some traits differed between the groups. The results support the relevance of using a soft tissue simulant, but are not entirely in line with the assumption that the biomechanics behind gunshot trauma are similar in all tubular bones [32]. A detailed discussion of the traits and their correlation to ballistic gel and bone properties is provided in the following paragraphs.

Entrance fracture and fracture type

In the literature, the fracture type in ballistic long bone trauma is commonly classified as a stellate pattern, indicating that multiple fractures radiate from the entry hole [14, 25, 33, 34]. Other authors refer to butterfly fractures [14, 18, 34, 35]. Yet, there is a controversy in using this term as it implies a different fracture mechanic occurring classically in blunt force trauma [36]. There, a real butterfly fracture is thought to initiate on the tension side of the shaft, which is opposite to the impact side [37, 38]. In contrast, ballistic fractures initiate at the impact side. Hence, some authors also use the term false butterfly fracture to describe this reverse phenomenon [37,

Table 7 Description of the axes of the multiple correspondence analysis. Significant correlations of the traits with the three first dimensions are shown. Category: (+) trait presence or (-) trait absence of the qualitative traits. Representation of the variables: *Wingflake*, wing flake; *Flakedefect*, wing flake defect; *CFxTran*, transversal concentric fracture of the entry; *Cortical*, cortical thickness; *ExBeveling*, external beveling of the exit hole; *Gel*, ballistic gel; *EntryHD*, horizontal entry hole diameter; *ShaftDM*, shaft diameter; *Length*, bone length; *exCFxTran*, transversal concentric fracture of the exit; *Stepped*, stepped breakout; *exSquare*, squared exit hole; *ExitVD*, vertical exit hole diameter; *exCFxLon*, longitudinal concentric fracture of the exit; *EntryVD*, vertical entry hole diameter; *Layered*, layered breakage

Percentage of the variance	Trait	Category	R^2	*p* value
Dim 1 (21.08%)	Wingflake	+	0.61	0.001
	Flakedefect	+	0.52	0.001
	CFxTran	-	0.41	0.001
	Cortical		0.30	0.001
	ExBeveling	+	0.28	0.002
	Gel	+	0.23	0.007
	EntryHD		0.19	0.01
	ShaftDM		0.17	0.02
	Length		0.16	0.03
Dim 2 (15.31%)	exCFxTran	-	0.50	0.001
	Stepped	-	0.41	0.001
	exSquare	+	0.17	0.02
	CFxTran	-	0.17	0.02
	ExitVD		0.15	0.03
Dim 3 (14.54%)	exSquare	-	0.54	0.001
	exCFxLon	+	0.28	0.001
	EntryVD		0.16	0.03
	Layered	-	0.16	0.03
	ShaftDM		0.14	0.03
	exCFxTran	-	0.14	0.04
	ExBeveling	+	0.14	0.04
	Length		0.13	0.04

39]. Lower gunshot velocities have also been linked to other patterns such as spiral, oblique or bore-hole fractures [14, 20, 24, 34, 39]. In our study, the impact side revealed an entry hole with radiating and concentric fractures, similar to the findings by Martrille and Symes and Smith et al. [13, 25]. As these fracture components also appear in skulls, Smith et al. claimed that long bone and cranial gunshot trauma is comparable. In general, the formation of radiating and concentric heaving fractures is strongly related to large amounts of kinetic energy [1, 13, 25, 40]. Principally, radiating fractures without concentric ones can occur when they are sufficient to relieve the pressure [41]. In contrast, concentric fractures do not occur solely. In cranial gunshot trauma, they were related to the increased intracranial pressure and blast effect upon bullet penetration [41]. Long bones can also be considered hollow organs with a solid wall. Thus, increased pressure in the shaft and cavity formation are thought to be part of the ballistic fracture mechanism [42]. In cranial gunshot trauma, radiating and concentric fractures are usually visible at the impact side [1]. Authors described the concentric form after the radiating ones and end perpendicularly at them [1, 11]. The fracture image reminds of a spiderweb and thus is referred to as a spiderweb-like pattern [1]. In long bones, we saw concentric fractures are often not visible on the frontal view since they appear mostly lateral on the shaft. Hence, they are less commonly transversal ones on the anterior aspect. Soft tissue simulant was even revealed to reduce their appearance. In addition, we observed the concentric fractures typically merge with the radiating ones instead of ending perpendicularly at them. As a consequence, the definition of a classical spiderweb-like pattern may not be entirely accurate for ballistic long bone trauma. In summary, although the classification is not that trivial, we consider the stellate pattern to be the most suitable to describe the fracture type revealed in our study.

Beyond the fracture type, radiating and concentric fractures also formed distinctive cortical entry traits. The *v-shape* is formed by radiating fractures, defines the anterior silhouette of the shaft and indicates the bullet impact with its tip. We recognised this characteristic in a work from Baraybar and Gasior [43], who analysed long bone fractures of real gunshot victims. The *wing piece* is formed by the fusion of radiating and concentric fractures. It is mostly detached from the shaft, but easy to recognise among other fragments due to its characteristic shape. Martrille and Symes described it as a pie-shaped fragment that can be confused with the wings of a butterfly fracture [25]. On our high-speed videos, we saw the wing piece was laterally blasted off the shaft. This is in line with Di Maio, who explained when a bullet penetrates a bone, it creates a temporary cavity causing the bone fragments to be propelled laterally [31]. After the wing piece breaks out, a prominent *lateral notch* can be seen on the shaft.

Focusing on the entry hole, we consistently found a round shape as well reported in perpendicular impacts [25, 41]. On the interior surface, all specimens exhibited *internal beveling*, a cone shape due to bone shards knocked off in the bullet's flight direction [11, 31, 44–47]. The entry hole size did not precisely reflect the bullet diameter. Comparable findings exist for cranial gunshot wounds, where it is reported that an exact calibre estimation is not possible [48–50]. In the majority of our cases, both the vertical and horizontal diameters were slightly larger than the bullet diameter. This may be attributed to a loss of cortical bone around the entrance hole, mainly due to a ring defect as discussed below. In addition, our results revealed the entry hole is bigger in larger bones. Moreover, the horizontal entry hole diameter was revealed to be bigger when soft tissue simulant was present. Interestingly, in femurs without gel, we even found a smaller horizontal entry hole than bullet diameter.

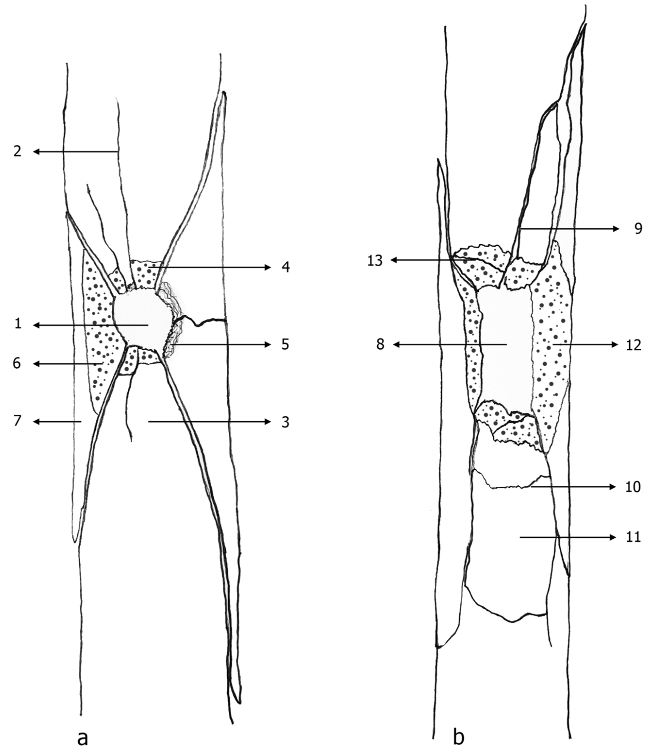

Fig. 8 Scheme of a paradigmatic entrance and exit fracture in a femur upon perpendicular impact of a 9-mm FMJ bullet shot at a handgun speed from a distance of 2 m: **a** anterior shaft aspect illustrating the following entrance traits: round entry hole (1), radiating fracture (2), v-shape (3), tip fragmentation (4), ring defect (5), wing flake defect (6), wing piece (7); **b** posterior shaft aspect illustrating the following exit traits: square exit hole (8), radiating fracture (9), transversal concentric fracture (10), stepped breakout (11), external beveling (12), layered breakage (13)

In the literature, a smaller entry hole than a bullet diameter is described as possible but less common [41]. Some authors explained this phenomenon by the elasticity of fresh bone [51, 52]. In general, our results support the evidence that an exact representation of the bullet size cannot be expected as bone is a material that can deform under force [40].

Around the entry hole, we observed distinguishable external cortical lesions. Hereby, a proper trait discrimination ensures to not confound them with external beveling of exit holes. A *ring defect* is a very superficial cortical loss at the edge of the entrance wound. Similar findings have been observed in cranial gunshots [31, 47, 53, 54]. *Tip fragmentation* is more irregular and is the consequence of bone chips that have been pushed off proximal and distal of the bullet entry. A *wing flake defect* occurs on the lateral aspects of the entry hole after a *wing flake* is pushed off upon bullet impact. Despite the link between both traits, wing flakes could not be found in all cases with wing flake defect. A potential explanation is that flakes shatter and are not recognisable anymore. In the recovery of real skeletonised remains, it is conceivable that wing flakes are difficult to find as they are small and can get easily lost. Our results indicate that cortical thickness and shaft diameter as well as soft tissue have an important influence on the presence of wing flakes. General bone chipping and delamination around the entry hole have also been reported [25]; however, there is no specific terminology that helps the reconstruction and identification of the entry hole. Although perpendicular bullet impacts in skulls usually result in smooth or sharp-edged entry holes [13, 31, 42], external bone chipping has been observed too [47, 53–56]. Regarding the trauma mechanism, bone chipping in general has been linked to increasing kinetic energy [37]. In gunshot trauma, authors have discussed bone chipping due to gases in contact shots [53], the projectile's twisting force [53, 55], a backward explosion after released kinetic energy [54, 56] and a temporary cavity-induced blowback [56].

Exit fracture

In the literature, authors reported on missing exit defects, which they explain by the fact that entry fractures cause the opposite shaft side to break before the bullet impacts there [13, 25]. In our study, all samples revealed an exit hole with radiating and concentric fractures. Nevertheless, we saw that entry-associated fractures predominantly extended laterally towards the posterior shaft aspect. This clearly influenced the shape of the exit fracture respecting the Puppe rule [57], and may explain why longitudinal concentric fractures (on the lateral shaft aspects) were less common than transversal ones.

In line with other authors, we found the exit wound was quite destructive, characterised by a substantial fragmentation resulting predominantly in a large square hole, not to be confused with the small round entry hole [36, 39, 58]. An explanation may be considered the structural damage of the bullet after entering the shaft, such as deformed circular shape and increased contact surface, leading to a high energy transmission and tissue damage [36]. Our results further showed that square exit holes correlate with a larger vertical exit hole diameter. The less common round exit hole is smaller, linked to longitudinal concentric fractures, and more likely to be found when both bone length and shaft diameter increase. The horizontal exit hole diameter, however, was shown to be larger with the presence of the soft tissue simulant.

Furthermore, we revealed additional distinctive cortical traits to identify the bullet exit. *External beveling*, as it is well known from cranial exit wounds [47, 59], was also present in our long bones. Our results indicate that it correlates with the presence of the soft tissue, cortical thickness, bone length and shaft diameter. *Layered breakage* is a trait that has previously been described in blunt force trauma [29]. The authors mentioned it to be a great indicator for the impact direction because it was exclusively found at the compression (impact) side. In comparison, we also commonly found it in gunshot trauma, though as an indicator for the exit side. *Stepped breakout* was more frequently seen in femurs than humeri. This might be traced back to the different shapes of the posterior shaft, which is rather edgy in femurs and round in humeri.

General fracture characteristics

This study confirms our previous observation of *plastic deformation* in ballistic long bone trauma [27]. It is often reported that in blunt force trauma, bone acts as viscoelastic material and thus plastic deformation occurs prior to fracture, while in gunshot trauma, bone acts as brittle material and breaks without going through the stage of plastic deformation [36, 42, 60]. Yet, it is also mentioned that limited plastic deformation can occur in gunshot trauma, too [60]. Some authors [11, 25], though, linked this observation to low-velocity ballistic impacts such as the projectiles used in the current study.

With respect to the fracture surface, by using an animal-bovine model, Adharapurapu et al. suggest that it smooths out at increasing impact energies [61]. In our human bone experimental analysis, however, we noted the fracture surface displayed bone scales, referred to as *fracture surface scaling*. The fracture margin revealed that occasionally superficial bone chips were missing, referred to as *marginal chipping*. In the literature, marginal bone chipping has also been observed in blunt force trauma, named as “knapping” [41]. It was explained that in repeated impacts, the conjoining fractures would rub against each other and cause spalling along the margins. In our study, we saw on the high-speed videos that after the bone fragments are propelled away by the temporary cavity, they are forcefully thrown back again. However, as this trait was observed in the samples without gel too, we assume marginal chipping was rather produced in the course of bullet impact than forceful retraction of the temporary cavity.

Finally, we have observed that the fracture extent was larger in femurs than humeri. This may be related to the bullet’s energy lost upon impact. Our results show that when both bone length and shaft diameter increase, the bone shatters less and the fracture lines propagate longer, which could imply a greater energy loss. In comparison, humeri revealed shorter fractures but a greater fragmentation, as noticed by smaller fragments and greater difficulty in reassembling them. In this context, support is given by the evidence that the grade of fragmentation is linked to the target size [42].

Limitations

The use of human bones for forensic experiments is associated with various limitations due to limited access and difficult tissue handling. Our sample size only allowed us to test one ballistic scenario. It can be assumed that the fracture patterns may differ to varying degrees when the ballistic variables such as bullet calibre, structure, speed and impact angle or the shooting distance are changed. Also, age- and sex-related bone proprieties may influence the fracture pattern. Furthermore, the results were obtained within an experimental setup using a test barrel and a soft tissue simulant. With respect to the latter, the underlying mechanism of how the gel exactly impacts the fracture pattern has to be further investigated. In concrete, it remains to be revealed whether the varying fracture characteristics are related to a different impact velocity after penetrating a 2-cm-thick gel layer or to another influence that soft tissue has on the bone. Furthermore, previous studies have indicated that Clear Ballistics Gel® cannot be considered equivalent to the standard 10% ballistic gelatine [28]. Authors have reported variations in Clear Ballistics Gel® concerning bullet penetration depth, temporary cavity and peak retarding forces, ultimately failing to meet the FBI calibration criteria [28]. This area warrants further investigation and should be considered in future studies investigating ballistic bone trauma.

Conclusion

With this study, we could define a distinctive ballistic fracture pattern for human long bones. The results have been achieved under the specific circumstance of a perpendicular impact of a 9-mm FMJ bullet shot at a handgun speed from a distance of 2 m. Specifically, a reliable discrimination between bullet entrance and exit was doubtlessly possible allowing to define the bullet's flight direction. The bullet entrance could be identified by a round entry hole with radiating and concentric fractures and several cortical traits such as *v-shape*, *wing piece*, *lateral notch*, *internal beveling*, *ring defect*, *tip fragmentation*, *wing flake defect* and *wing flake*. The exit hole was predominantly square and accompanied by radiating and concentric fractures. It further featured cortical traits such as *external beveling*, *layered breakage* and *stepped breakout*. In addition, general cortical traits such as *plastic deformation*, *fracture surface scaling* and *marginal chipping* were also attributed to ballistic long bone trauma. All evaluated cortical traits were reproduced in both humeri and femurs, leading to the assumption that they may be valid for other long bones, too. However, the trait's occurrence values may considerably differ between the types of bone. In this context, we found that some fracture characteristics correlate with bone properties such as shaft diameter, bone length and cortical thickness. The application of soft tissue simulant in bone trauma experiments was also revealed to influence the fracture pattern, even though the underlying effects require to be further investigated. This study provides new evidences on the ballistic fracture pattern in order to contribute to a clearer guidance on how to identify gunshot trauma when investigating fractured long bones. This is particularly relevant when forensic pathologists and anthropologists deal with skeletal remains that lack correlations with soft tissue findings. Nevertheless, due to the dynamic nature of gunshot incidents, more research is needed to evaluate to which extent the ballistic fracture pattern alters when ballistic variables and bone characteristics change.

Acknowledgements The authors are grateful to the Mossos d'Esquadra for providing the facilities, the material and the personal staff in order to realise the gunshot experiments.

Author contribution Conceptualisation: Nathalie Schwab, Ignasi Galtés; methodology: Nathalie Schwab, Jordi Monreal, Xavier Garrido, Joan Soler, Manel Vega, Pedro Brillas; formal analysis and investigation: Nathalie Schwab, Ignasi Galtés, Xavier Jordana; writing—original draft preparation: Nathalie Schwab; writing—review and editing: Ignasi Galtés, Xavier Jordana, Nathalie Schwab; visualisation: Nathalie Schwab, Ignasi Galtés, Xavier Jordana; supervision: Ignasi Galtés, Xavier Jordana.

Funding Proyectos de Generación de Conocimiento, Agencia Estatal de Investigación (PID2021-124112NB-100). Research Fund for Excellent Junior Researchers of the University of Basel, Switzerland.

Spanish National Plan for Scientific and Technical Research and Innovation,PID2021-124112NB-100,Xavier Jordana,Universität Basel.

Declarations

Ethics approval and consent to participate This study is in accordance with the ethical precepts of the Declaration of Helsinki (Fortaleza, Brazil, October 2013). It was approved by the local ethics committee (Bellvitge University Hospital, L'Hospitalet de Llobregat, Barcelona; Ref. PR416/20). All human bones were handled following the guidance for clinical use (EEC regulations 2004/23/CE and 2006/17/CE) and the legal requirements of Spain (Law 14/2007, RD 1716/2011 and RD 9/2014). The bones were donated anonymously and gathered with informed consent. All used specimens are stored in the private collection at the Catalonian Institute of Legal Medicine and Forensic Science (IMLCFC) in Barcelona, Spain (Registro Nacional de Biobancos. Ref. C.0004241).

Conflict of interest The authors declare no competing interests.

References

1. Hart GO (2005) Fracture pattern interpretation in the skull: differentiating blunt force from ballistics trauma using concentric fractures. J Forensic Sci 50:JFS2004219
2. SA Symes N Ericka ENC L'Abbé et al (2012) 17 Interpreting Traumatic A companion to forensic anthropology 39:340
3. Schwab CW (1993) Violence: America's uncivil war—presidential address, sixth scientific assembly of the eastern association for the surgery of trauma. J Trauma 35:657–665
4. Bartlett CS (2003) Clinical update: gunshot wound ballistics. Clin Orthop Relat Res® 408:28–57
5. Saayman G (2006) Gunshot wounds: medico-legal perspectives. CME: Your SA J CPD 24:131–136
6. Dougherty PJ, Sherman D, Dau N, Bir C (2011) Ballistic fractures: indirect fracture to bone. J Trauma Acute Care Surg 71:1381–1384
7. Belmont PJ Jr, Goodman GP, Zacchilli M et al (2010) Incidence and epidemiology of combat injuries sustained during "the surge" portion of operation Iraqi Freedom by a US Army brigade combat team. J Trauma Acute Care Surg 68:204–210
8. Griffiths D, Clasper J (2006) (iii) Military limb injuries/ballistic fractures. Curr Orthop 20:346–353
9. Dougherty PJ, Vaidya R, Silverton CD et al (2009) Joint and long-bone gunshot injuries. JBJS 91:980–997
10. Najibi S, Dougherty PJ (2006) Management of gunshot wounds to the joints. Tech Orthop 21:200–204
11. Berryman HE, Symes SA (1998) Recognizing gunshot and blunt cranial trauma through fracture interpretation. Forensic Osteol 2:333–352
12. O'Bc S, Berryman HE, Lahren CH (1987) Cranial fracture patterns and estimate of direction from low velocity gunshot wounds. J Forensic Sci 32:1416–1421
13. Smith OC, Pope EJ, Symes SA (2015) Look until you see: identification of trauma in skeletal material In: Hard evidence Routledge pp 190–204
14. Bland-Sutton SJ (1915) Observations on injuries of the bones of the limbs by the S. bullet. BMJ Mil Health 24:314–323
15. Bir C, Andrecovich C, DeMaio M, Dougherty PJ (2016) Evaluation of bone surrogates for indirect and direct ballistic fractures. Forensic Sci Int 261:1–7. https://doi.org/10.1016/j.forsciint.2016.01.023
16. Huelke DF, Harger JH, Buege LJ et al (1968) An experimental study in bio-ballistics. J Biomech 1:97–105. https://doi.org/10.1016/0021-9290(68)90012-2
17. Huelke DF, Buege LJ, Harger JH (1967) Bone fractures produced by high velocity impacts. Am J Anat 120:123–131
18. Huelke DF, Harger JH, Buege LJ, Dingman HG (1968) An experimental study in bio-ballistics: femoral fractures produced

by projectiles—II Shaft impacts. J Biomech 1:313–321. https://doi.org/10.1016/0021-9290(68)90025-0
19. Ragsdale BD, Josselson A (1988) Experimental gunshot fractures. J Trauma Acute Care Surg 28:S109–S115
20. Robens W, Küsswetter W (1982) Fracture typing to human bone by assault missile trauma. Acta Chir Scand Suppl 508:223–227
21. Coudane H, Grosdidier G, Borrelly J et al (1982) Experimental study of limb lesions due to hunting weapons. Acta Chir Scand Suppl 508:229–234
22. Berryman HE, Gunther WM (2000) Keyhole defect production in tubular bone. J Forensic Sci 45:483–487
23. Long WT, Chang W, Brien EW (2003) Grading system for gunshot injuries to the femoral diaphysis in civilians. Clin Orthop Relat Res® 408:92–100
24. Ryan JR, Hensel RT, Salciccioli GG, Pedersen HE (1981) Fractures of the femur secondary to low-velocity gunshot wounds. J Trauma Acute Care Surg 21:160–162
25. Martrille L, Symes SA (2019) Interpretation of long bones ballistic trauma. Forensic Sci Int 302:109890. https://doi.org/10.1016/j.forsciint.2019.109890
26. Veenstra A, Kerkhoff W, Oostra R-J, Galtés I (2022) Gunshot trauma in human long bones: towards practical diagnostic guidance for forensic anthropologists. Forensic Sci Med Pathol 18:359–367. https://doi.org/10.1007/s12024-022-00479-0
27. Schwab N, Jordana X, Soler J et al (2023) Can Synbone® cylinders and deer femurs reproduce ballistic fracture patterns observed in human long bones? J Mater Sci 58:4970–4986. https://doi.org/10.1007/s10853-023-08333-6
28. Courtney E, Courtney A, Andrusiv L, Courtney M (2017) Clear Ballistics Gel®: high speed retarding force analysis of paraffin-based alternative to gelatin-based testing of lead-free pistol bullets. In: 30th International Symposium on Ballistics. DEStech Publications, Inc.
29. Scheirs S, Malgosa A, Sanchez-Molina D et al (2017) New insights in the analysis of blunt force trauma in human bones Preliminary results. Int J Legal Med 131:867–875. https://doi.org/10.1007/s00414-016-1514-1
30. Saukko P, Knight B (2015) Knight's forensic pathology. CRC Press
31. DiMaio VJM (2015) Gunshot wounds: practical aspects of firearms, ballistics, and forensic techniques, 3rd edn. CRC Press
32. Kimmerle EH, Baraybar JP (2008) Skeletal trauma: identification of injuries resulting from human rights abuse and armed conflict. CRC Press
33. Andrews P, Fernández-Jalvo Y (2012) How to approach perimortem injury and other modifications. In: Bell LS (ed) Forensic Microscopy for Skeletal Tissues. Humana Press, Totowa, NJ, pp 191–225
34. Kieser DC, Riddell R, Kieser JA, et al (2014) Bone micro-fracture observations from direct impact of slow velocity projectiles. J Arch Mil Med 2. https://doi.org/10.5812/jamm.15614
35. Leffers D, Chandler RW (1985) Tibial fractures associated with civilian gunshot injuries. J Trauma 25:1059–1064
36. Dirkmaat D (2012) A companion to forensic anthropology. John Wiley & Sons
37. Cohen H, Kugel C, May H et al (2016) The impact velocity and bone fracture pattern: forensic perspective. Forensic Sci Int 266:54–62. https://doi.org/10.1016/j.forsciint.2016.04.035
38. Messerer O (1880) Über Elasticität und Festigkeit der menschlichen Knochen. Cotta
39. Symes SA, L'Abbé EN, Chapman EN, et al (2012) Interpreting traumatic injury to bone in medicolegal investigations. In: A companion to forensic anthropology John Wiley & Sons Ltd pp 340–389
40. Christensen AM, Passalacqua NV, Bartelink EJ (2019) Forensic anthropology: current methods and practice. Academic Press
41. Klepinger LL (2006) Fundamentals of forensic anthropology. John Wiley & Sons
42. Kieser J, Taylor M, Carr D (2012) Forensic Biomechanics. John Wiley & Sons
43. Baraybar JP, Gasior M (2006) Forensic anthropology and the most probable cause of death in cases of violations against international humanitarian law: an example from Bosnia and Herzegovina. J Forensic Sci 51:103–108
44. Besant-Matthews PE (2000) Examination and interpretation of rifled firearm injuries The pathology of trauma, 3rd edn Arnold, London 47–60
45. Sauer NJ (1998) The timing of injuries and manner of death: distinguishing among antemortem, perimortem and postmortem trauma. Forensic Osteol 2:321–331
46. Steadman DW, Basler W, Hochrein MJ, et al (2016) Domestic homicide investigations: an example from the United States. In: Handbook of Forensic Anthropology and Archaeology. Routledge, pp 351–362
47. Quatrehomme G, Işcan MY (1998) Analysis of beveling in gunshot entrance wounds. Forensic Sci Int 93:45–60. https://doi.org/10.1016/S0379-0738(98)00030-9
48. Berryman HE, Smith OC, Symes SA (1995) Diameter of cranial gunshot wounds as a function of bullet caliber. J Forensic Sci 40:751–754
49. Paschall A, Ross AH (2017) Bone mineral density and wounding capacity of handguns: implications for estimation of caliber. Int J Legal Med 131:161–166. https://doi.org/10.1007/s00414-016-1420-6
50. Ross AH (1996) Caliber estimation from cranial entrance defect measurements. J Forensic Sci 41(4):629–633
51. Tamáska L (1964) Kritische Bemerkungen zur Frage der Geschosskaliberbestimmung aus dem Durchmesser der Einschussöffnungen der Knochen. Zacchia 39:158–170
52. Pollak S, Ritt F (1992) Vergleichende Untersuchungen an Einschusslücken in Rumpf-und Extremitätenknochen mit vorwiegend spongiöser Struktur. Beitr Gerichtl Med 50:363–363
53. Spitz WU, Fisher RS (1980) Medicolegal Investigation of Death, Charles C. Thomas, Springfield, IL
54. Coe JI (1982) External beveling of entrance wounds by handguns. Am J Forensic Med Pathol 3:215
55. Baik S-O, Uku JM, Sikirica M (1991) A case of external beveling with an entrance gunshot wound to the skull made by a small caliber rifle bullet. Am J Forensic Med Pathol 12:334–336
56. Peterson BL (1991) External beveling of cranial gunshot entrance wounds. J Forensic Sci 36:1592–1595
57. Madea B, Staak M (1988) Determination of the sequence of gunshot wounds of the skull. J Forensic Sci Soc 28:321–328
58. Huelke DF, Darling JH (1964) Bone fractures produced by bullets. J Forensic Sci 9:461–469
59. Quatrehomme G, Yaşar İşcan M (1997) Bevelling in exit gunshot wounds in bones. Forensic Sci Int 89:93–101. https://doi.org/10.1016/S0379-0738(97)00121-7
60. Wedel VL, Galloway A (2013) Broken bones: anthropological analysis of blunt force trauma (2nd Ed.). Charles C Thomas Publisher
61. Adharapurapu RR, Jiang F, Vecchio KS (2006) Dynamic fracture of bovine bone. Mater Sci Eng, C 26:1325–1332

Publisher's Note Springer Nature remains neutral with regard to jurisdictional claims in published maps and institutional affiliations.

Springer Nature or its licensor (e.g. a society or other partner) holds exclusive rights to this article under a publishing agreement with the author(s) or other rightsholder(s); author self-archiving of the accepted manuscript version of this article is solely governed by the terms of such publishing agreement and applicable law.

6. DISCUSSION

In good preserved cadavers, skin and soft tissue injuries typically show characteristic features allowing conclusions on the applied mechanical force such as gunshot, blunt force, sharp force or other impacts [23]. In gunshot trauma, the ballistic characteristics of entrance and exit skin wounds are widely accepted and applied in routine forensic investigations, while less precise morphological information is given for bones. The interpretation and reconstruction of ballistic bone trauma is particularly challenging when dealing with long bones as conclusive data is scarce. To resolve such uncertainty, realistic experiments are of great importance.

This work is based on an exclusive study in which real human bones were used, as well as carefully selected alternative models. The findings reveal new insights into how gunshot trauma in long bones can be interpreted and reconstructed. The first part of the work deals with the validity of alternative models in comparison to human bones. The second part characterises the distinct ballistic fracture pattern in human long bones disclosed in this study.

6.1. The development of the experimental setup

To gain more knowledge on the ballistic fracture pattern, an experimental approach was designed permitting the reproduction of gunshot long bone trauma under controlled circumstances and in an as realistic manner as possible. This is why, entire fresh human bones, alongside alternative models, were fired with real ammunition at a realistic impact velocity that simulates a shot from a handgun.

In order to determine reproducible and comparable fracture characteristics, one gunshot scenario was selected in this research. This implied to shoot the shaft, as this area has a relatively thick cortical wall and thus allows better the characterisation of cortical traits than the cancellous rich area near the epiphysis.

To guarantee the replication of the same trauma circumstance across a diverse sample size, precise targeting has been considered mandatory. In line with other authors [45] a test barrel was deemed to be the best choice to shoot under uniform conditions as it ensures more consistently precise shots than firing with a gun by hand. Furthermore, all biological bones were dissected from the soft tissue to consistently identify and indicate the impact point on the shaft. In accordance with other authors, a simulant was then applied to replace the soft tissue [45, 69, 74, 81]. Although soft tissue simulants are isotropic and cannot entirely reproduce the heterogeneous tissue characteristics of a living body, they are still widely used to simulate the ballistic effects of soft tissue during gunshot [82].

In this regard, the standard soft tissue simulant is calibrated 10% ballistic gelatine [78]. However, this standard simulant has a rather blurred aspect. In comparison, Clear Ballistics Gel®, a newer simulant which has come into broad use recently, is characterised by its excellent clarity and transparency [78]. Since it was intended to analyse the fracture propagation during gunshot on the high-speed videos, Clear Ballistics Gel® was preferred over 10% ballistic gelatine. Besides that, the preparation and handling of Clear Ballistics Gel® is less complicated than of standard ballistic gelatine [78].

Nevertheless, in this study the experience was made that after surrounding the bones with Clear Ballistics Gel®, air bubbles would form around the shafts. This drastically hampered the fracture observation on the recordings. After reporting this issue to the manufacturer, the answer was given this was a common problem when applying the gel with objects. The best way to get rid of those bubbles would be to place the gel and bone in the oven allowing the heat to work out those bubbles by bringing them to the surface. However, the decision was made to not follow this suggestion in order to not expose the fresh bones and surrogates to a temperature of 100°C. To overcome the missing data on the fracture propagation, additional human bones without the application of a soft tissue simulant were included to the study. This eventually allowed an accurate visualisation and analysis of the propagating fracture on the high-speed videos.

In further regard to choose an accurate soft tissue simulant, a previous study has claimed that Clear Ballistics Gel® cannot be considered equivalent to the standard 10% ballistic gelatine [78]. The authors have reported variations in Clear Ballistics

Gel® concerning bullet penetration depth, temporary cavity, and peak retarding forces, ultimately failing to meet the FBI calibration criteria. In any case, to which extent these differences influence the fracture pattern of direct impacts remains unclear and has to be further studied.

The thickness of the soft tissue simulant on the target side was 2 cm for each specimen. This value was also chosen in the gunshot experiments of other authors [45, 69]. To fill the hollow interior of the Synbone® cylinders, simulating bone marrow, was also in line with the literature [69].

For this study, metal cups with a simple tree-point screw system were constructed and mounted on a table in order to stabilised the long bones upright. In other experiments with 10% ballistic gelatine, bone models were usually completely immerged in the blocks and did not require further stabilisation [45, 69, 74, 81].

In order to calculate the bullet's energy loss during the sample penetration, a light barrier was used. Although it was possible to measure the velocity in most shots, not all data points could be obtained. The regrettable absence of velocity data could be traced back to bullet and bone fragments causing interferences with the light barrier. This methodological issue, however, is an important finding as it suggests that a light barrier might not be the best method to measure the exit speed in gunshot experiments with bones. The analysis of the high-speed images could probably serve as a suitable alternative method for calculating the loss of velocity during bone penetration [69]. This however requires a previous preparation allowing to determine the exact distances on the footages. In this study, difficulties were encountered in using the recordings retrospectively for an accurate assessment of the projectile velocity, as no precise metric information could be derived from the images.

6.2. The evaluation of long bone trauma models

Alternative models for trauma experiments are of great interest due to the restricted possibilities of using human specimens for forensic research. Despite different tissue and material, a suitable alternative is thought to exhibit properties such as elasticity, strength and energy absorption similar to human tissue [17]. Moreover, useful models should ensure reproducibility [45]. This thesis provides conclusions on whether Synbone® cylinders and red deer femurs are suitable to macroscopically reproduce detailed ballistic fracture patterns in human long bones.

6.2.1. The similarities of the trauma models

On the first sight, the ballistic fractures in human, synthetic and animal bones appeared similar. All samples presented comminuted fracture and showed a stellate pattern at the impact side. All models allowed the assessment of the impact direction and bullet trajectory, since entrance and exit side could be identified and distinguished from each other. In all model groups, a beveled exit defect with radiating fracture lines was found. This allowed the conclusion that the fracture on the posterior shaft side was produced by a direct projectile impact. As a standard feature to distinguish between entrance and exit, it is well known that bone bevels out in the direction in which the projectile travels [83]. In cranial bones, the entry wound classically presents an internal beveling, whereas external beveling is a typical characteristic of the exit wound [84, 85]. In this thesis, internal beveling of the entrance defect and the already mentioned external beveling of the exit defect were reproduced in all sample groups. Furthermore, in all model groups the exit fractures were dominated by a vast fragmentation and thus larger than the bullet entry. This has already been observed by other researchers [86]. In accordance with claims about the particular importance of the entry wound assessment [18], the impact side in all model groups provided more characteristic traits to identify gunshot trauma than the exit side.

6.2.2. The dissimilarities of the trauma models

A detailed fracture pattern analysis showed that both the surrogate and animal models differed significantly from human bones. When comparing the two alternative models, the clusters of entry, exit, and general cortical traits in the animal model were found to be more similar to human bone than the Synbone® surrogates.

In a ballistic study comparing human craniums with Synbone® plates and spheres, Smith et al. noted similar entry but different exit wound features between the models [87]. Unlike these findings, in the long bone models of this study especially the entrance fracture presented differences between the model groups. Traits were observed that revealed to be distinct for human bones. They were described as wing flake, wing flake defect and ring defect. The aspect of v-shape, as already observed by Martrille et al. [38], and tip fragmentation, a term defined in this thesis, were reproduced in all sample groups. However, both traits appeared significantly more often in human and animal bones than in Synbone® surrogates. Y-branching, depressed ring and bullet wipe revealed to be characteristic Synbone® entrance traits. According to the literature, the presence or absence of a depressed ring may help to identify the type of ammunition in terms of fully jacket or lead bullets [68, 70]. However, this finding may not be applicable in human bones, since they could not be reproduced there. Another unique Synbone® finding is the bullet wipe that may be associated with the presence of a depressed ring. In other words, the anterior surface around the bullet entry in the surrogates appeared depressed but mostly intact. In contrast, in human and animal bones a loss of cortical bone around the bullet entry was always seen. The main difference on the impact side of the red deer femurs was that especially the medial and lateral aspects of the bullet entry were shattered and could not be reassembled. This did not allow the same precise evaluation of the entrance traits compared to human bones and Synbone® surrogates. Focusing on calibre estimation, studies on cranial bones have revealed that the minimum diameter of the entry hole allows the discrimination between "small" and "large" calibres, whereas a precise determination is difficult [88–90]. In this study, significant differences between the entry size in the models were found. The human bones reproduced bigger entry holes, while the Synbone® surrogates featured mostly smaller entry holes than the projectile used. This may be explained by the different entry hole traits, ring defect in human bones versus depressed ring in Synbone® surrogates. While the first represents a cortical loss of bone, the latter can be regarded as an inward folding of the material. Again, the deer bones could not be used to evaluate the entry hole size.

With respect to the exit fracture, there were also some dissimilarities found between the three models. Layered breakage revealed to exclusively occur in human bones. Interestingly, this trait has formerly been associated to the compression side of blunt force trauma in fresh human long bones [64]. The Synbone® femur cylinders mostly presented a square hole like in human bones, whereas the majority of the humerus cylinders showed a round exit hole. The deer bones did not allow the assessment of the bullet exit shape.

In accordance with the literature, the distinct fracture patterns found in this study may essentially be attributed to differences in the underlying material [68, 87], but also to differences in the external geometry and internal microarchitecture.

6.2.3. The problem of the Synbone® surrogates

Surrogate material such as polyurethane does not feature the microstructural complexity of real bone based on its components and their arrangement in space [91]. Consequently, it has been expressed that polyurethane is not a suitable alternative for studies investigating bone trauma below a very general and superficial level [87]. Yet, other authors have claimed that the Synbone® surrogates can be used as a substitute. Those authors have found that the Snybone® material features a similar resistance to porcine bone [68, 69]. In contrast, this study's results on the bullet's energy lost upon impact indicated that the resistance to the projectile is significantly lower in Synbone® cylinders than in human and deer bones. Furthermore, the data suggests that the Synbone® surrogates are more brittle than real bone. This assumption is made because plastic deformation, referred to as to the persistent deformation of bone prior fracturing [83], was exclusively found in real bones. In comparison to the Synbone® polyurethane cylinders, bone consists of a mineral phase (hydroxyapatite) embedded in an organic matrix (mainly type I collagen) [65]. Whilst the former makes the bone rigid and stiff, the latter contributes to its toughness and gives it a certain flexibility reducing brittleness and allowing some resistance to fracture [92]. In further comparison to Synbone®, real bone is a fluid-imbibed material whose water is not only present in the vascular system and canaliculi, but also structurally bound in the collagen matrix [93]. This water content has also been regarded as critical to the mechanical behavior [83]. It was found that drying out of a bone is related to a loss of elasticity and plasticity [64, 94]. In this context, fracture characteristics have been linked to the elasticity, cohesiveness and density of bone [95]. It is known that the less flexible the tissue the greater the damage because more energy is transferred to the stretch mechanism [96, 97]. Further support for the assumption that the Synbone® surrogates are more brittle than real bone is given by the finding that transverse fractures occurred more frequently in the Synbone® surrogates than human bones. In the literature, transverse lines are typically associated to fractures in dry, brittle bone [98].

Next to different material properties, also the geometrical variability of the models, in particular dissimilar cortical thickness and the complex shape of real bone has to be considered as cause for the different fracture patterns. In accordance with Smith et al [87], these factors also influence the resistance through thinner and thicker bone areas and thus fracture propagation. Theoretically, Synbone® also manufactures anatomical models. However, the ones especially developed for ballistic testing were geometrically simplified. These simplified cylinders have been developed to reduce the effect of heterogeneous tissues during research and hence should guarantee reproducibility. In this study, however, there were some differences observed in the detailed fracture patterns among the Synbone® models. Some entrance traits such as v-shape, y-branching, tip fragmentation and ring defect only occurred irregularly. Also the exit hole revealed to appear round or square shaped. Furthermore, I found a considerable variability of the fracture extent among the humerus cylinders. In contrast to the findings of Henwood et al. [68], however, there were no fractures observed reaching the cut edges of the cylinders. Since fracture lines run along the least resistance [35], a potential explanation for the observed inconsistencies among the Synbone® models may lay in a certain degree of heterogeneity of the polyurethane wall. As an indicator for this heterogeneity, there were void lacunas of up to 2.5 mm found in some samples. This assumption finds further support by the observation of irregular fragment shapes in the Synbone® models. Henwood et al. made an analogous observation, reporting on a sudden change of fracture direction in Synbone® surrogates that could not be observed in real bones from pigs [68]. The authors claimed that the fracture lines change the direction when they reach a different pore density. However, they also express some reluctance to accept this interpretation because not all fracture lines showed a response to the change in pore density. Ultimately, it was observed that the wall of the Synbone® surrogates would split apart which was referred to as wall splitting. This trait could not be found in the human and animal models and may thus have nothing to do with real ballistic bone fractures.

6.2.4. The problem of the animal model

Authors have argued that animal bones remain the essential alternative model for human bone trauma since synthetic material is too different to biological tissue [99]. As mentioned above, all bones have a mineral and organic component. Yet, it has to be considered that the histological structure of bone tissue differs between the species [100, 101]. This complicates the matter of substituting human bones with animal bones. The deer femurs tested in this study fragmented massively into very small pieces and chips upon gunshot. The fractures could not be as efficiently reconstructed and thus not all parts as precisely evaluated as human bones and Synbone® cylinders. This massive destruction was considered as a main drawback of the animal model. Interestingly, this finding differs from results by Kieser et al. who found radiating fracture lines producing a butterfly-shaped fracture at the impact side of the anterior mid-shaft of fresh mature female deer femurs [73]. Their findings resemble more the fracture pattern found in the human bones than in the deer bones of this thesis. This difference might be particularly traced back to the impact energy of 0.013 to 5.35 J of the spherical steel projectiles used in the experiments by Kieser, compared to the impact energy of 517.97 J in this study. This assumption may be supported by the literature reporting that bone behaves more like brittle material under high velocity impacts [102, 103].

Since the grade of comminution is not only associated to the amount of transferred energy but also to a small target size [83], an additional influence might be related to the smaller size of the deer bones used in this study (Iberian subspecies from Catalonia, Spain). They featured an average length of 22.4 cm and an average diaphyseal width of 1.9 cm. It is assumed they were smaller than the ones used by Kieser et al. from New Zealand, who reported in an earlier study an average bone length of 27.6 cm and a mid-diaphyseal width of 2.7 cm [74]. The relation between the grade of comminution and a small target size may further be supported by the experience in this study, that human humeri compared to human femurs shattered in smaller fragments and hence were more difficult to assemble. Kieser et al. reported deer femurs being a suitable model to substitute human femurs [72]. The deer femurs used in this study were considerably smaller and from this point of view they might rather substitute human humeri. This can find further support by the observation that energy loss in human humeri and deer femurs were quite similar. With respect to the material properties, the deer bones seem to have a comparable toughness as human humeri. Similar to human bones, also the deer bones featured plastic deformation.

6.3. The human fracture pattern

As revealed through the evaluation of ballistic trauma models, neither the synthetic nor the animal model sufficiently reproduced the characteristics of the human fracture pattern. This finding makes those alternative models unsuitable to replace human bones for further fracture investigations. Consequently, for the classification of a ballistic fracture pattern in long bones, only human models were used. To this purpose, the sample size was increased from 14 to a total of 29 human bones. Hereby, 10 femurs and 10 humeri were shot with ballistic gel and 6 femurs and 3 humeri were shot without ballistic gel. The purpose of shooting bones without the gel was to improve the evaluation of the fracture propagation on the high-speed recordings. This condition, additionally allowed to assessing the influence of soft tissue on the fracture pattern.

The sound macro-morphological examination of the ballistic fractures allowed the characterisation of the fracture type as well as detailed cortical traits. Those were divided into bullet entrance, bullet exit and general cortical traits. The first two thus permitted to identify the shooting direction and bullet path. In forensic death investigations, such additional information besides the diagnosis of a gunshot wound is highly valuable for the reconstruction of the event [43]. Figure 12 illustrates the scheme of paradigmatic diaphyseal gunshot fracture resulting from the gunshot scenario tested in this thesis. In all sample groups, a similar ballistic fracture pattern was found. However, the occurrence values of some traits differed between the groups. The results support the relevance of using a soft tissue simulant, but are not entirely in line with the assumption that the biomechanics behind gunshot trauma are similar in all tubular bones [61]. A detailed discussion of the traits and their correlation to ballistic gel and bone properties is provided in the following paragraphs.

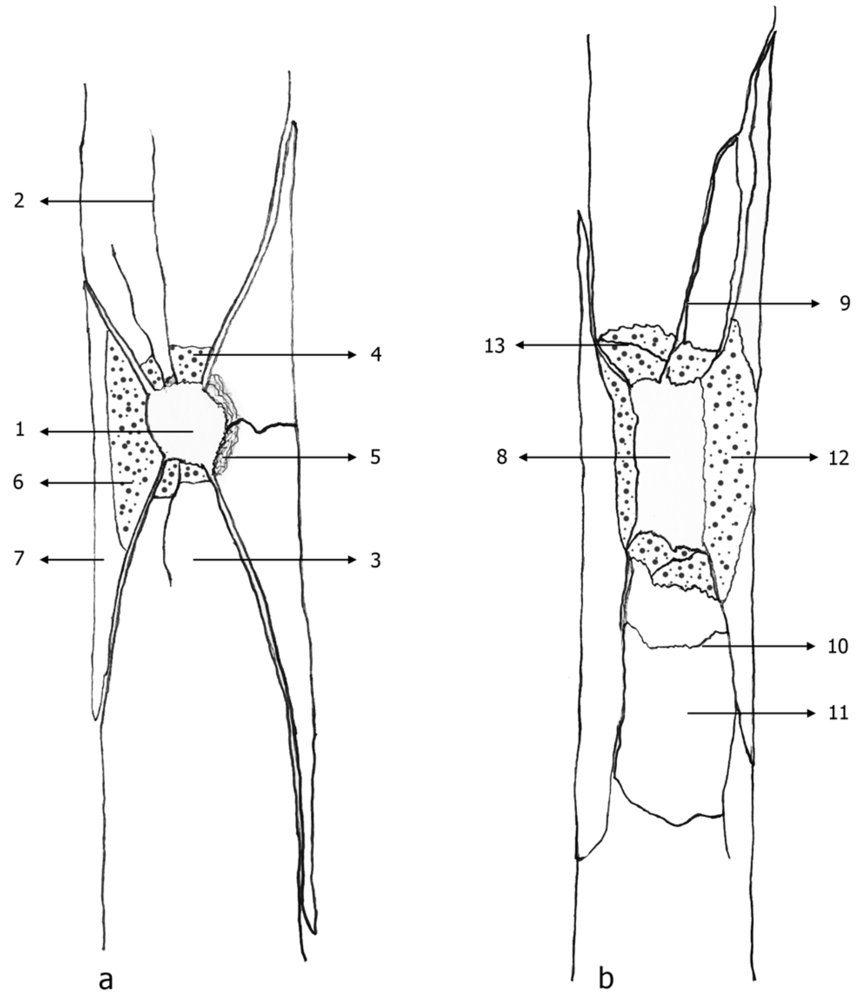

Fig. 12 Scheme of a paradigmatic entrance and exit fracture in a femur upon perpendicular impact of a 9 mm FMJ bullet shot at a handgun speed from a distance of 2 m: **a** anterior shaft aspect illustrating the following entrance traits: round entry hole (1), radiating fracture (2), v-shape (3), tip fragmentation (4), ring defect (5), wing flake defect (6), wing piece (7), **b** posterior shaft aspect illustrating the following exit traits: square exit hole (8), radiating fracture (9), transversal concentric fracture (10), stepped breakout (11), external beveling (12), layered breakage (13).

6.3.1. The general fracture type

All samples presented comminuted fracture, which is consistent with the review by Veenstra et al. revealing comminuted fracture is the most frequent diaphyseal fracture in gunshot trauma [60]. In order to characterise the fracture type more accurately, the appearance at the impact side was considered.

In the literature the fracture type in ballistic long bone trauma is commonly classified as stellate pattern, indicating that multiple fractures radiate from the entry hole. Sometimes the fracture type has also been referred to as butterfly fracture [44, 47, 56, 73]. Yet, there is a controversy in using this term as it implies a different fracture mechanic occurring classically in blunt force trauma [1]. There, a real butterfly fracture is thought to initiate on the tension side of the shaft, which is opposite to the impact side [103, 104]. In contrast, ballistic fractures initiate at the impact side. Hence, some authors also use the term false butterfly fracture to describe this reverse phenomenon [103, 105]. Lately, lower gunshot velocities have also been linked to other patterns such as spiral, oblique or bore-hole fractures [44, 50, 54, 73, 105].

In this study, the impact side revealed an entry hole with radiating and concentric fractures, similar to the findings by Martrille & Symes and Smith et al. [37, 38]. As these fracture components also appear in skulls, Smith et al. claimed that long bone and cranial gunshot trauma is comparable. In general, the formation of radiating and concentric heaving fractures is strongly related to large amounts of kinetic energy [33, 37, 38, 106]. Principally, radiating fractures without concentric ones can occur when they are sufficient to relieve the pressure [107]. In contrast, concentric fractures do not occur solely. In cranial gunshot trauma concentric fractures were related to the increased intracranial pressure and blast effect upon bullet penetration [107]. Long bones can also be considered as hollow organs with a solid wall. Thus, increased pressure in the shaft and cavity formation are thought to be part of the ballistic fracture mechanism [83].

In cranial gunshot trauma, radiating and concentric fractures are usually visible at the impact side [33]. Authors described the concentric form after the radiating ones and end perpendicularly at them [33, 35]. The fracture image reminds of a spiderweb and thus is referred to as spiderweb-like pattern [33]. In long bones, the concentric fractures were often not visible on the frontal view since they appeared mostly lateral on the shaft. Hence, they were less commonly transversal ones on the anterior aspect. Soft tissue simulant even revealed to reduce their appearance. In addition, the concentric fractures typically merged with the radiating ones instead of ending perpendicularly at them. As a consequence, the definition of a classical spiderweb-like pattern maybe not entirely accurate for ballistic long bone trauma.

In summary, a stellate pattern was considered to be the most suitable to describe the fracture type revealed in this study.

6.3.2. The entrance fracture pattern

In line with the postulation that particularly the bullet impact region is of high conclusive value [18, 79], the entrance fracture provided more characteristics than the exit facture.

V-shape

The v-shape is formed by oblique radiating fracture lines. It defines the anterior silhouette of the shaft. Its tip points towards the bullet impact. In this study, v-shape was formed in all human bones. This characteristic could also be recognised in a work from Baraybar & Gasior who analysed long bone fractures of real gunshot victims [42].

Wing piece

The wing piece is a bone fragment formed by the fusion of radiating and concentric fractures on the lateral shaft aspect(s). It affects the hole cortical wall, whilst only the extremes run out superficially. The aspect facing the entry hole may contain part of the ring defect or a wing flake defect. A wing piece can be entire, but also broken into two or more fragments. It is mostly detached from the shaft, yet easy to recognise among other fragments due to its characteristic shape. Martrille & Symes described it as a pie shaped fragment that can be confused with wings of a butterfly fracture [38]. In this study it was identified in all human bones. On the high speed-videos it was shown that the wing piece was laterally blasted off the shaft. This is in line with Di Maio, who explained when a bullet penetrates a bone, it creates a temporary cavity causing the bone fragments to be propelled laterally [18].

Lateral notch

A lateral notch is a prominent notch-like defect on the fracture surface of the lateral shaft aspect(s) after the break out of a lateral wing piece. As the wing piece's extremes typically run out superficially, they leave behind this corresponding and easily visible cortical defect. This trait was defined in this thesis, as it has not been described in the literature before. Furthermore, it can be characterised as very common one as it appeared in all human samples with the exception of one humerus. In the literature, it has been unreported to date.

Round entry hole

A round entry hole is the bullets initial entry defect that visually appears round. This was found in all human bones and has already been well reported in perpendicular impacts [38, 107].

Entry hole size

This quantitative variable showed the entry hole size did not precisely reflect the bullet diameter. Comparable findings exist for cranial gunshot wounds, where it is reported that an exact calibre estimation is not possible [88–90]. In the majority of this study's cases, both the vertical and horizontal diameter were slightly larger than the bullet diameter. This may be attributed to a loss of cortical bone around the entrance hole, mainly due to ring defect. In addition, the results revealed the entry hole is bigger in larger bones. Moreover, the horizontal entry hole diameter was revealed to be bigger when soft tissue simulant was present. Interestingly, in femurs without gel there were even smaller horizontal entry hole diameters measured than the bullet diameter. In the literature, a smaller entry hole than bullet diameter is described as possible but less common [107]. Some authors explained this phenomenon by the elasticity of fresh bone [108, 109]. In general, the results of this thesis support the evidence that an exact representation of the bullet size cannot be expected as bone is a material that can deform under force [106].

Internal beveling

Internal beveling is a funnel shape in the cortical wall with the larger part on the internal aspect. Beveling in general is a standard feature to distinguish between bullet entrance and exit. It has been linked to bone shards knocking off in the bullet's flight direction [18, 28, 35, 84, 110, 111]. The literature on cranial bones revealed the entry wound classically presents an internal beveling, whereas external beveling is a typical characteristic of the exit wound as discussed later on [84, 85]. In this study all specimens exhibited internal beveling.

Radiating fracture lines

Radiating fracture lines run from the entry hole toward the epiphyses and the posterior aspect of the shaft. They were consistently produced in all samples and have been discussed above in the section on the general fracture type.

Concentric fracture lines

Concentric fractures lines are curvilinear fractures facing with their concave aspect towards the entry hole. They were part of all entrance fractures in human bones and have also been discussed previously in the section on the general fracture type.

Ring defect

A ring defect is a very superficial, circular or partial circular loss of cortical bone on the margin of the entry hole. Its appearance reminds of an abrasion ring. Similar findings, have been observed in cranial gunshots [18, 84, 112, 113]. A ring defect may be interrupted by other entrance patterns such as tip fragmentation. This trait was featured in all human bones.

Tip fragmentation

Tip fragmentation is a superficial, external loss of cortical fragment(s) at the tip of the bone around the entry hole. Compared to the ring defect it is irregular and only appears proximal and / or distal of the bullet entry. It is the consequence of bone chips that have been pushed off. The transition to the intact cortical bone is sharply defined by quite chiselled edges. In case oblique fractures separate the bone, tip fragmentation on bone parts next to each other create the image of a stepped circular margin around the bullet entry. In the literature this trait has not yet been reported. It was defined in this thesis and revealed to be a very common trait as it appeared in all human bones with the exception of one femur and humerus.

Wing flake defect

A wing flake defect occurs on the lateral aspect(s) of the entry hole after a wing flake is pushed-off upon bullet impact. Its shape is very characteristic and thus easy to recognise. This cortical lesion was defined in this thesis, as it has not been otherwise specified in the literature.

Wing flake

A wing flake is a loose trapezoidal chip of cortical bone that resembles spread wings. It originates from the lateral aspect(s) of the entry hole. Its shape is similar to the wing piece, but it is usually much smaller and most importantly, it is only a cortical chip and does not affect the hole cortical wall. This trait is yet unreported in the literature. Despite the link between both traits, wing flakes could not be found in all cases with wing flake defect. A potential explanation is that flakes shatter and are not recognisable anymore. Moreover, this study revealed that the cortical thickness and shaft diameter as well as soft tissue have an important influence on the presence of wing flakes. With respect to the first two correlations, wing flakes were more common in femurs than humeri. In the recovery of real skeletonised remains, it is conceivable that wing flakes are difficult to find as they are small and can get easily lost.

A comment on bone chipping

The above-described cortical traits ring defect, tip fragmentation, wing flake and wing flake defect can be traced back to the phenomenon of bone chipping. They appear around the entry hole and can be clearly distinguished from one another by a careful examination. Hereby, a proper traits discrimination ensures to not confound them with external beveling of exit holes. In comparison with the literature, general bone chipping and delamination around the bullet entry in long bones have already been reported without a deeper specification [38]. Although perpendicular bullet impacts in skulls usually result in smooth or sharp-edged entry holes [18, 37, 83], external bone chipping has been observed too [84, 112–115]. Regarding the trauma mechanism, bone chipping in general has been linked to increasing kinetic energy [103]. In gunshot trauma, authors have discussed bone chipping due to gases in contact shots [112], the projectile's twisting force [112, 114], a backward explosion after released kinetic energy [113, 115] and a temporary cavity induced blowback [115]. Other authors have related the phenomenon of bone chipping to the impact of a full metal jacket projectiles [70]. This area clearly deserves more attention for further research in future.

6.3.3. The exit fracture pattern

In the literature, authors reported on missing exit defects, which they explain by the fact that entry fractures cause the opposite shaft side to break before the bullet impacts there [37, 38]. In this study, all samples revealed an exit hole with radiating and concentric fractures allowing the conclusion that they were directly produced by the projectile. Nevertheless, the entry associated fractures predominantly extended laterally towards the posterior shaft aspect. This clearly influenced the shape of the exit fracture taking into account the Puppe rule that fracture lines stop at preexisting ones [116]. Moreover, this may explain why longitudinal concentric fractures (on the lateral shaft aspects) were less common than transversal ones. Analogue to the entrance, also for the exit defect distinct cortical traits were identified.

Square exit hole

A square exit hole is the bullets exit defect that visually appears edgy or square. In line with other authors, the exit wound was quite destructive, characterised by a substantial fragmentation resulting predominantly in a large square hole, not to be confused with the small round entry hole [1, 86, 105]. As explanation may be considered the structural damage of the bullet after entering the shaft, such as deformed circular shape and increased contact surface, leading to more energy transmission and tissue damage [1]. The results of this thesis further showed that square exit holes correlate with a larger vertical exit hole diameter. The less common round exit hole is smaller, linked to longitudinal concentric fractures, and more likely to be found when both bone length and shaft diameter increases. The horizontal exit hole diameter, however, was shown to be larger with the presence of the soft tissue simulant.

External beveling

External beveling is a funnel shape in the cortical wall with the larger part on the external aspect. As already mentioned above, this trait is well known from cranial exit wounds. It was also present in the long bones of this study. The results further indicated that this trait correlates with the presence of soft tissue, cortical thickness, bone length and shaft diameter.

Radiating fracture lines

Radiating fracture lines run from the exit defect towards the epiphyses and the anterior aspect of the sample. They were part of the exit fracture in all samples.

Concentric fracture lines

Concentric fractures lines are curvilinear fractures facing with their concave aspect towards the exit hole. They were found in all samples.

Layered breakage

Layered breakage is a layered pattern on the fracture surface of the cortical bone. This trait has previously been described in blunt force trauma [64]. The authors mentioned it to be a great indicator for the impact direction because it was exclusively found at the compression (impact) side. In comparison, in this study it was also commonly found in gunshot trauma, though as an indicator for the bullet exit side.

Stepped breakout

Stepped breakout appears as similarly shaped fragments that break out in steps on the posterior shaft aspect. It is the consequence of a sequence of multiple transversal concentric fractures around the exit hole. In the literature, this trait has not been reported to date. In this research, it has been more frequently seen in femurs than humeri. This might be traced back to the different shape of the posterior shaft, which is rather edgy in femurs and round in humeri. In future studies, it may be interesting to shoot femurs from behind in order to get an exit fracture on the rounded anterior shaft aspect. In doing so, it could be tested whether this trait is truly related to the bullet exit or to anatomical characteristics such as the irregular shape of the line aspera.

6.3.4. The general fracture characteristics

It was revealed that some of the characteristics were neither attributable to the entrance nor exit fracture. They, however, constitute reproducible and easily evaluable characteristics that can be found in ballistic long bone trauma.

Plastic deformation

Plastic deformation is a persistent deformation of bone. As mentioned above, plastic deformation can be explained by the organic component of bone that gives the tissue some degree of flexibility and resistance to fracture. But, not only intrinsic factors influence the bone's fracture biomechanics. It is thought that in response to different mechanical stressors bone reacts differently. In principle, plastic deformation is strongly associated with low-velocity impacts, such as blunt force trauma. There, it has often been reported that bone behaves like a ductile material by deforming prior to fracturing, while in gunshot trauma, bone acts as a brittle material and breaks without going through the stage of plastic deformation [1, 77, 83]. Yet, the consistent finding of this characteristic in each bone can be supported by other authors who have already pointed out that limited plastic deformation can occur in gunshot trauma, too [77]. Some authors [35, 38], though, linked this observation to ballistic impacts at rather low velocities.

Fracture surface scaling

Fracture surface scaling describes tiny bony scales on the fracture surface. It was observed in all human bones. This trait was defined in this thesis as it has not been described before. As an interesting comparison, Adharapurapu et al. suggested that the fracture surface smooths out at increasing impact energies [117]. Yet, it has to be considered that those authors studied bovine models and not human bones.

Marginal chipping

Marginal chipping appears as superficial bone chips that are occasionally missing on the fracture margin. In this study, it was found in all human bones. In the literature, marginal bone chipping has been observed in blunt force trauma, named as "knapping" [107]. It was explained that in repeated impacts the conjoining fractures would rub against each other and cause spalling along the margins. In this study, it was seen on the high-speed videos that after the bone fragments were propelled away by the temporary cavity, they were forcefully thrown back again. However, as this trait was observed in the samples without gel too, it is assumable that marginal chipping was rather produced in the course of the bullet impact than forceful retraction of the temporary cavity.

Fracture extent

Finally, it was observed that the fracture extent was larger in femurs than humeri. This may be related to the bullet's energy lost upon impact. The results showed that when both bone length and shaft diameter increase, the bone shatters less and the fracture lines propagate longer, which could imply a greater energy loss. In comparison, humeri revealed shorter fractures but a greater fragmentation, as noticed by smaller fragments and greater difficulty in reassembling them. In this context, support is given by the evidence that the grade of fragmentation is linked to the target size [83].

6.3.5. Differentiation from other types of trauma

The revealed characteristics represent a distinct ballistic fracture pattern in human long bones. The data suggests that with a comprehensive fracture pattern analysis a reliable distinction from other type of trauma may be made.

As discussed above, blunt force trauma can feature few individual traits similar to ballistic trauma such as radiating fracture lines, layered breakage, plastic deformation and marginal chipping [64, 77, 107]. However, when these few traits are interpreted within the bigger picture of the fracture, potential doubts should be resolved.

As mentioned in the introduction, confusion has also been reported in distinguishing gunshot wounds from perforations with pointed objects such as arrows, since both have been associated with round entry holes [30–32]. However, crossbow injuries are thought to not produce radiating or concentric fractures, and particularly to not result in as complex fractures as gunshots wounds [87, 106]. Since the arrows usually travel at lower velocities, they transfer less energy to the tissue and do not produce the blast effect of a penetrating bullet.

More difficult, though, might be the distinction from other impacts at ballistic trauma speeds such as blast injuries resulting from penetrating fragments and shrapnel. There is limited data on the corresponding fracture patterns, but it has been reported that they can lead to similar fractures as high velocity bullets, including the formation of radiating and concentric fractures [106].

In contrast, other types of trauma such as sharp force may be less problematic to distinguish from gunshot. In specific, sharp force typically leaves distinct (cut) marks on the bone surface such as straight line incisions, punctures, gouges and / or clefts [106]. In comparison, such traits could not be found in this study.

6.4. Practical guidance for the analysis of ballistic long bone trauma

Based on the experience gained during this research, a practical guidance for the interpretation and reconstruction of ballistic long bone trauma can be proposed. Figure 13 shows a sequential procedure for the trauma analysis. Hereby, the principles of the forensic anthropological investigation of skeletal remains were respected, including a comprehensive recovery, gentle cleaning from adherent soft tissue and assembling of all bone fragments to identify the type of bone and reconstruct the facture [61, 77].

When applying the results of this research, it must be considered that the characteristics relate to diaphyseal fractures. It is conceivable that gunshots towards the metaphysis or epiphysis may result in different fracture patterns because in this area the cortical wall is thinner. Hence, the fracture location on a long bone should be taken into account during the analysis.

The experience made in this study was that long bones shattered severely upon gunshot. The resulting fragments varied in size that ranged down to the extent of sand grains. Those tiny fragments could not be incorporated into the fracture reconstruction. With regard to the forensic fieldwork, it is very likely that small fragments may not be recovered. Yet, the cortical traits described in this thesis are predominantly not depend on the recovery and assembling of tiny fragments. When comparing humeri with femurs, the experience was however made that the analysis of humeral fractures was more challenging as they generally shattered into smaller fragments.

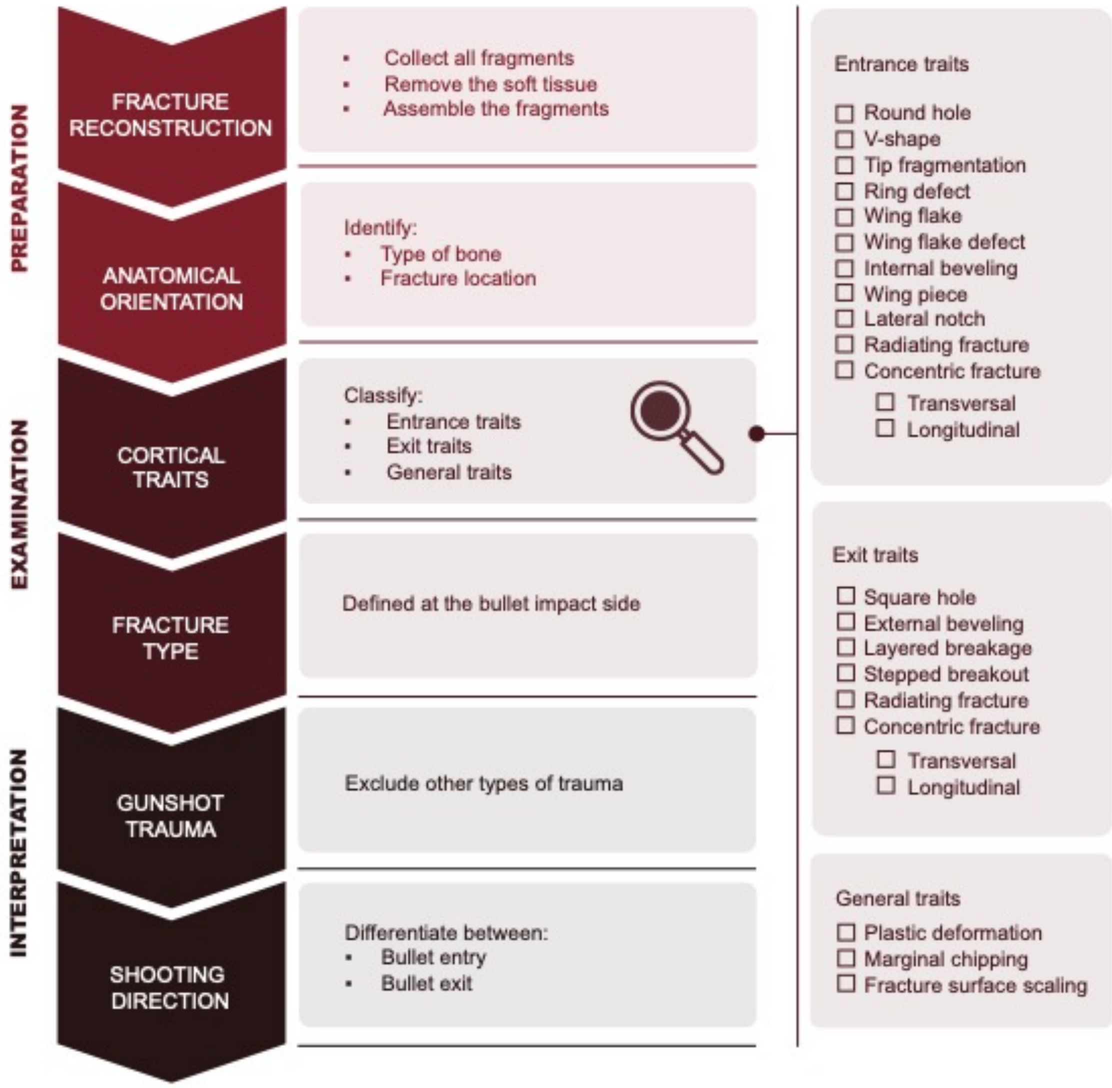

Fig. 13 Approach for the analysis of ballistic long bone trauma.

After the fracture reconstruction, it is recommended to check the cortical bone for any in this thesis revealed trait and classify them as entrance, exit and general characteristic. This will further allow the determination of the general fracture type and the identification of the bullet impact direction.

A further comment may address forensic imaging, which is a widely applied method when investigating skeletal remains [61]. In this respect, it is quite conceivable that the defined macroscopic fracture pattern can also be visualised using high-resolution technology such as computed tomography. However, to what extend the cortical traits are recognisable with different radiological methods may be investigated in future studies.

6.5. The thesis' scientific impact on the forensic fieldwork

The results of this research may find application in the forensic pathological and anthropological examination of skeletal injuries. As mentioned, the interpretation and reconstruction of long bone fractures can be very challenging. This applies in particular to cases where skeletal remains are severely damaged or incompletely recovered, and no additional information on the trauma mechanism can be obtained from the skin or soft tissue.

Such complicated conditions can occur during a routine legal medical examination of a deceased individual, whose body is skeletonised, decomposed, burned, mutilated or otherwise unrecognisable. Beyond that, the examination of badly preserved human remains recovered from mass graves is a fundamental task in the emerging field of humanitarian forensic actions. In this context, exhumations after armed conflicts are more common since investigations into war crimes are becoming more demanded. The relevance of such investigations is given by the International Criminal Tribunal for the Former Yugoslavia which was later expanded to include Rwanda. Exhumations were conducted to determine cause and circumstances of death during the respective genocides [118, 119].

The ballistic fracture pattern characterised in this thesis may contribute to the identification and reconstruction of gunshots to long bones in both everyday forensic investigations and forensic humanitarian operations. Hereby, the results might even help to shed light on events long in the past. In summary, the outcome of this thesis may contribute to deliver reliable evidence for national and international truth commissions.

6.6. Limitations

The use of human bones for forensic experiments is associated with various limitations due to limited access and difficult tissue handling. Although it was a unique opportunity to use real human bones for experimental forensic research, the sample size only allowed to testing one ballistic scenario. Hence, the results of this study represent fracture patterns in the diaphysis, produced by a 9 mm full metal jacket projectile with an impact speed of 360 m/s. It can be assumed that the fracture patterns may differ to varying degrees when the ballistic variables such as bullet calibre, structure, speed and impact angle or the shooting distance are changed. Also, age and sex related bone proprieties may influence the fracture pattern.

In regard to the evaluation of alternative bone models, a further limitation related to the sample size concerned the number of animal models tested. However, within this group a 100% congruence of the presence or absence of the evaluated fracture patterns was found. Another limitation of the first part of this thesis was that the different trauma models were evaluated macroscopically. To receive further information on the material behaviour of each model, it might be useful to investigate the differences from a microstructural point of view.

With respect to the study design, the results were obtained within an experimental setup using a test barrel and a soft tissue simulant. Regarding the latter, the underlying mechanism of how the gel exactly influences the fracture pattern has to be further investigated. In particular, it remains to be revealed whether the varying fracture characteristics between gel and no gel samples are related to a different impact velocity after penetrating a 2 cm thick gel layer or to another influence that soft tissue has on the bone. Furthermore, authors have indicated that Clear Ballistics Gel® cannot be considered equivalent to the standard 10% ballistic gelatine [78]. To which extent the different soft tissue simulants influence the fracture pattern also warrants further research.

7. CONCLUSIONS

The following conclusions can be drawn from the results obtained under the special conditions of a distant range, vertical shot with a 9 mm FMJ bullet at handgun velocity:

1. The ballistic fracture patterns produced in the Synbone® surrogates and animal bones tested in this study seemed to be a fair general approximation of those seen in human long bones. They all presented a stellate pattern at the impact side. However, the detailed analysis of the fracture traits revealed a broad range of dissimilarities, warranting special caution when extrapolating ballistic fracture patterns from alternative models to human long bones.

2. The Synbone® surrogates did on the one hand not reproduce all characteristics observed in human bones, and on the other hand featured characteristics such as y-branching, depressed ring, bullet wipe, round exit hole and wall splitting that were not typical for human bones. This leads to the assumption that the polyurethane material may provide an alternate failure mechanism than real bone.

3. The animal model appeared to be more suitable than Synbone®, in terms of both, qualitative and quantitative fracture characteristics. However, the main drawback of the deer femurs seemed to be the massive fragmentation that did not allow a same precise fracture reconstruction and assessment as the human bones. Hence, the shape and size of the entry and exit holes, and the fracture characteristics at the lateral shaft aspects could not be evaluated.

4. In the human long bones, a distinct ballistic fracture pattern was characterised indicating that a secure interpretation of gunshot trauma seems to be possible. In addition, the defined cortical traits suggest that the bullet direction can be determined, which can be of great value for forensic event reconstructions.

5. The bullet entrance in human long bones could be identified by a round entry hole with radiating and concentric fractures and several cortical traits, including v-shape, wing piece, lateral notch, internal beveling, ring defect, tip fragmentation, wing flake defect and wing flake.

6. The exit hole in human long bones was predominantly square and accompanied by radiating and concentric fractures. It further featured cortical traits such as external beveling, layered breakage and stepped breakout.

7. General cortical traits such as plastic deformation, fracture surface scaling and marginal chipping were additionally attributed to gunshot trauma in human long bone.

8. The results further suggest that a similar fracture pattern might be reproduced in other long bones, too. Among all analysed characteristics only stepped breakout and the fracture extent showed a significant difference between femurs and humeri (both were greater in femurs). Nonetheless, bone properties seem to influence the fracture pattern. In concrete, the cortical thickness and shaft diameter correlated with the occurrence of wing flake, wing flake defect, external beveling and a larger horizontal entry hole diameter. The shaft diameter and bone length correlated with a larger vertical entry hole diameter, a not squared exit hole and a greater occurrence of longitudinal concentric fractures at the exit.

9. In regard to the application of a soft tissue simulant, the results showed a positive correlation with the occurrence of wing flake, wing flake defect, external beveling and the size of the horizontal exit hole diameter. In comparison, a negative correlation was shown for transversal concentric fractures at the bullet entry. This seems to indicate that soft tissue may influences the fracture pattern in gunshot trauma, even though the underlying effects require to be further investigated.

10. This study provides further insights into the ballistic fracture pattern in human long bones aiming to contribute to a clearer orientation during the investigation of gunshot injuries. This is particularly relevant when forensic pathologists and anthropologists deal with skeletal remains that lack correlations with soft tissue findings. Nevertheless, due to the dynamic nature of gunshot incidents, future research is needed to evaluate to which extent the fracture pattern alters when ballistic variables and bone characteristics change.

8. REFERENCES

1. Dirkmaat D (2012) A companion to forensic anthropology. John Wiley & Sons
2. Schwab CW (1993) Violence: America's uncivil war—presidential address, sixth scientific assembly of the eastern association for the surgery of trauma. J Trauma 35:657–665
3. Bartlett CS (2003) Clinical update: gunshot wound ballistics. Clinical Orthopaedics and Related Research® 408:28–57
4. Saayman G (2006) Gunshot wounds: medico-legal perspectives. CME: Your SA Journal of CPD 24:131–136
5. Dougherty PJ, Sherman D, Dau N, Bir C (2011) Ballistic fractures: indirect fracture to bone. Journal of Trauma and Acute Care Surgery 71:1381–1384
6. Jena AB, Sun EC, Prasad V (2014) Does the Declining Lethality of Gunshot Injuries Mask a Rising Epidemic of Gun Violence in the United States? J Gen Intern Med 29:1065–1069. https://doi.org/10.1007/s11606-014-2779-z
7. Maqungo S, Kauta N, Held M, et al (2020) Gunshot injuries to the lower extremities: Issues, controversies and algorithm of management. Injury 51:1426–1431. https://doi.org/10.1016/j.injury.2020.05.024
8. Papadopoulos IN, Kanakaris NK, Danias N, et al (2013) A structured autopsy-based audit of 370 firearm fatalities: Contribution to inform policy decisions and the probability of the injured arriving alive at a hospital and receiving definitive care. Accid Anal Prev 50:667–677. https://doi.org/10.1016/j.aap.2012.06.018
9. Riddez L (2014) Wounds of war in the civilian sector: principles of treatment and pitfalls to avoid. Eur J Trauma Emerg Surg 40:461–468. https://doi.org/10.1007/s00068-014-0395-6
10. Turgut K, Gür A, Güven T, Oğuztürk H (2019) Evaluation of factors related to mortality caused by firearm injury: a retrospective analysis from Malatya, Turkey. Archives of Iranian medicine 22:80–84
11. Global Firearms Holdings. https://www.smallarmssurvey.org/database/global-firearms-holdings. Accessed 13 Jun 2024
12. Global Burden of Disease 2016 Injury Collaborators, Naghavi M, Marczak LB, et al (2018) Global Mortality From Firearms, 1990-2016. JAMA 320:792–814. https://doi.org/10.1001/jama.2018.10060
13. Werbick M, Bari I, Paichadze N, Hyder AA (2021) Firearm violence: a neglected "Global Health" issue. Global Health 17:120. https://doi.org/10.1186/s12992-021-00771-8

14. Oberwittler D (2019) Lethal Violence: A Global View on Homicide. In: Oxford Research Encyclopedia of Criminology and Criminal Justice. Oxford University Press

15. Mahoney PF (2005) Ballistic trauma: a practical guide, 2. ed. Springer, London [Heidelberg]

16. Heard BJ (2008) Handbook of Firearms and Ballistics: Examining and Interpreting Forensic Evidence, 1st ed. Wiley

17. Coupland RM, Rothschild MA, Thali MJ (2011) Wound Ballistics. Springer, Berlin, Heidelberg

18. DiMaio VJM (2015) Gunshot Wounds: Practical Aspects of Firearms, Ballistics, and Forensic Techniques, Third Edition. CRC Press

19. Hollerman JJ, Fackler ML, Coldwell DM, Ben-Menachem Y (1990) Gunshot wounds: 1. Bullets, ballistics, and mechanisms of injury. AJR Am J Roentgenol 155:685–690. https://doi.org/10.2214/ajr.155.4.2119095

20. Cooper GJ, Ryan JM (1990) Interaction of penetrating missiles with tissues: some common misapprehensions and implications for wound management. Br J Surg 77:606–610. https://doi.org/10.1002/bjs.1800770604

21. Fackler ML (1988) Wound Ballistics: A Review of Common Misconceptions. JAMA 259:2730–2736. https://doi.org/10.1001/jama.1988.03720180056033

22. Courtney A, Courtney M (2012) Physical mechanisms of soft tissue injury from penetrating ballistic impact. DFRL US Air Force Academy

23. Saukko P, Knight B (2015) Knight's forensic pathology. CRC press

24. Sorg MH, Haglund WD (1996) Forensic Taphonomy: The Postmortem Fate of Human Remains. Boca Raton

25. Symes SA, L'Abbé EN, Stull KE, et al (2014) Taphonomy and the timing of bone fractures in trauma analysis. In: Manual of forensic taphonomy. CRC Press Boca Raton, Florida, pp 341–365

26. Andrews P, Fernández-Jalvo Y (2012) How to Approach Perimortem Injury and Other Modifications. In: Bell LS (ed) Forensic Microscopy for Skeletal Tissues. Humana Press, Totowa, NJ, pp 191–225

27. Cappella A, Amadasi A, Castoldi E, et al (2014) The Difficult Task of Assessing Perimortem and Postmortem Fractures on the Skeleton: A Blind Text on 210 Fractures of Known Origin. Journal of Forensic Sciences 59:1598–1601. https://doi.org/10.1111/1556-4029.12539

28. Sauer NJ (1998) The timing of injuries and manner of death: distinguishing among antemortem, perimortem and postmortem trauma. Forensic osteology: advances in the identification of human remains 2:321–331

29. Najibi S, Dougherty PJ (2006) Management of gunshot wounds to the joints. Techniques in Orthopaedics 21:200–204

30. Zátopková L, Hejna P (2011) Fatal suicidal crossbow injury--the ability to act. J Forensic Sci 56:537–540. https://doi.org/10.1111/j.1556-4029.2010.01666.x

31. Karger B, Sudhues H, Kneubuehl BP, Brinkmann B (1998) Experimental arrow wounds: ballistics and traumatology. J Trauma 45:495–501. https://doi.org/10.1097/00005373-199809000-00011

32. Pomara C, D'Errico S, Neri M (2007) An unusual case of crossbow homicide. Forensic Sci Med Pathol 3:124–127. https://doi.org/10.1007/s12024-007-0006-5

33. Hart GO (2005) Fracture pattern interpretation in the skull: differentiating blunt force from ballistics trauma using concentric fractures. Journal of Forensic Sciences 50:JFS2004219

34. Symes SA, Ericka N, L'Abbé ENC, et al (2012) 17 InterpretingTraumatic. A Companion to Forensic Anthropology 39:340

35. Berryman HE, Symes SA (1998) Recognizing gunshot and blunt cranial trauma through fracture interpretation. Forensic osteology: advances in the identification of human remains 2:333–352

36. O'BC S, Berryman HE, Lahren CH (1987) Cranial fracture patterns and estimate of direction from low velocity gunshot wounds. Journal of Forensic sciences 32:1416–1421

37. Smith OC, Pope EJ, Symes SA (2015) Look until you see: identification of trauma in skeletal material. In: Hard evidence. Routledge, pp 190–204

38. Martrille L, Symes SA (2019) Interpretation of long bones ballistic trauma. Forensic Science International 302:109890. https://doi.org/10.1016/j.forsciint.2019.109890

39. Belmont Jr PJ, Goodman GP, Zacchilli M, et al (2010) Incidence and epidemiology of combat injuries sustained during "the surge" portion of operation Iraqi Freedom by a US Army brigade combat team. Journal of Trauma and Acute Care Surgery 68:204–210

40. Griffiths D, Clasper J (2006) (iii) Military limb injuries/ballistic fractures. Current Orthopaedics 20:346–353

41. Dougherty PJ, Vaidya R, Silverton CD, et al (2009) Joint and long-bone gunshot injuries. JBJS 91:980–997

42. Baraybar JP, Gasior M (2006) Forensic anthropology and the most probable cause of death in cases of violations against international humanitarian law: an example from Bosnia and Herzegovina. Journal of forensic Sciences 51:103–108

43. Woźniak KJ, Moskała M, Grabherr S. Gunshot trauma. In: Grabherr S, Grimm JM, Heinemann A, editors. Atlas of postmortem angiog- raphy. Springer; 2016. p. 453–90.

44. Bland-Sutton SJ OBSERVATIONS ON INJURIES OF THE BONES OF THE LIMBS BY THE S. BULLET.

45. Bir C, Andrecovich C, DeMaio M, Dougherty PJ (2016) Evaluation of bone surrogates for indirect and direct ballistic fractures. Forensic Science International 261:1–7. https://doi.org/10.1016/j.forsciint.2016.01.023

46. Huelke DF, Harger JH, Buege LJ, Dingman HG (1968) An experimental study in bio-ballistics: Femoral fractures produced by projectiles—II Shaft impacts. Journal of Biomechanics 1:313–321. https://doi.org/10.1016/0021-9290(68)90025-0

47. Huelke DF, Harger JH, Buege LJ, et al (1968) An experimental study in bio-ballistics. Journal of Biomechanics 1:97–105. https://doi.org/10.1016/0021-9290(68)90012-2

48. Huelke DF, Buege LJ, Harger JH (1967) Bone fractures produced by high velocity impacts. American Journal of Anatomy 120:123–131

49. RAGSDALE BD, JOSSELSON A (1988) Experimental gunshot fractures. Journal of Trauma and Acute Care Surgery 28:S109–S115

50. Robens W, Küsswetter W (1982) Fracture typing to human bone by assault missile trauma. Acta chirurgica Scandinavica Supplementum 508:223–227

51. Coudane H, Grosdidier G, Borrelly J, et al (1982) Experimental study of limb lesions due to hunting weapons. Acta chirurgica Scandinavica Supplementum 508:229–234

52. Berryman HE, Gunther WM (2000) Keyhole defect production in tubular bone. Journal of Forensic Sciences 45:483–487

53. Long WT, Chang W, Brien EW (2003) Grading system for gunshot injuries to the femoral diaphysis in civilians. Clinical Orthopaedics and Related Research® 408:92–100

54. RYAN JR, HENSEL RT, SALCICCIOLI GG, PEDERSEN HE (1981) Fractures of the femur secondary to low-velocity gunshot wounds. Journal of Trauma and Acute Care Surgery 21:160–162

55. Witschi TH, Omer GE (1970) The treatment of open tibial shaft fractures from Vietnam War. J Trauma 10:105–111. https://doi.org/10.1097/00005373-197002000-00002

56. Leffers D, Chandler RW (1985) Tibial fractures associated with civilian gunshot injuries. The Journal of trauma 25:1059–1064

57. Rose SC, Fujisaki CK, Moore EE (1988) Incomplete fractures associated with penetrating trauma: etiology, appearance, and natural history. J Trauma 28:106–109. https://doi.org/10.1097/00005373-198801000-00016

58. Tornetta P, Tiburzi D (1994) Anterograde interlocked nailing of distal femoral fractures after gunshot wounds. J Orthop Trauma 8:220–227. https://doi.org/10.1097/00005131-199406000-00007

59. Rodrigues RL, Sammer DM, Chung KC (2006) Treatment of complex below-the-elbow gunshot wounds. Ann Plast Surg 56:122–127. https://doi.org/10.1097/01.sap.0000196414.70178.ff

60. Veenstra A, Kerkhoff W, Oostra R-J, Galtés I (2022) Gunshot trauma in human long bones: towards practical diagnostic guidance for forensic anthropologists. Forensic Sci Med Pathol 18:359–367. https://doi.org/10.1007/s12024-022-00479-0

61. Kimmerle EH, Baraybar JP (2008) Skeletal trauma: identification of injuries resulting from human rights abuse and armed conflict. CRC press

62. Madea B (2007) Case histories in forensic medicine. Forensic Science International 165:111–114. https://doi.org/10.1016/j.forsciint.2006.05.012

63. Madea B, Saukko P, Musshoff F (2007) Tasks of research in forensic medicine - different study types in clinical research and forensic medicine. Forensic Sci Int 165:92–97. https://doi.org/10.1016/j.forsciint.2006.05.009

64. Scheirs S, Malgosa A, Sanchez-Molina D, et al (2017) New insights in the analysis of blunt force trauma in human bones. Preliminary results. Int J Legal Med 131:867–875. https://doi.org/10.1007/s00414-016-1514-1

65. Galloway A, Zephro L (2005) Skeletal Trauma Analysis of the Lower Extremity. pp 253–277

66. Mateos Cachorro A (1999) Botella, M. O; Alemán, I. y Jiménez, S. A (2000). Los huesos humanos. Manipulación y alteraciones

67. Forensic and Ballistic Archives. In: SYNBONE. https://www.synbone.com/product-category/biomechanics-generics/forensic-and-ballistic/. Accessed 13 Jun 2024

68. Henwood BJ, Appleby-Thomas G (2020) The suitability of Synbone® as a tissue analogue in ballistic impacts. J Mater Sci 55:3022–3033. https://doi.org/10.1007/s10853-019-04231-y

69. Kneubuehl BP, Thali MJ (2003) The evaluation of a synthetic long bone structure as a substitute for human tissue in gunshot experiments. Forensic Science International 138:44–49. https://doi.org/10.1016/j.forsciint.2003.08.003

70. Henwood BJ, Oost TS, Fairgrieve SI (2019) Bullet Caliber and Type Categorization from Gunshot Wounds in *Sus Scrofa* (Linnaeus) Long Bone. J Forensic Sci 64:1139–1144. https://doi.org/10.1111/1556-4029.14004

71. Zhang X, Xu C, Wen Y, Luo S (2015) The experimental and numerical study of indirect effect of a rifle bullet on the bone. Forensic Sci Int 257:473–480. https://doi.org/10.1016/j.forsciint.2015.10.032

72. Kieser DC, Kanade S, Waddell NJ, et al (2014) The deer femur – A morphological and biomechanical animal model of the human femur. Bio-Medical Materials and Engineering 24:1693–1703. https://doi.org/10.3233/BME-140981

73. Kieser DC, Riddell R, Kieser JA, et al (2014) Bone Micro-Fracture Observations From Direct Impact of Slow Velocity Projectiles. J Arch Mil Med 2:. https://doi.org/10.5812/jamm.15614

74. Kieser DC, Carr DJ, Leclair SC, et al (2013) Clothing increases the risk of indirect ballistic fractures. J Orthop Surg Res 8:42. https://doi.org/10.1186/1749-799X-8-42

75. Kieser DC, Carr DJ, Leclair SCJ, et al (2013) Gunshot induced indirect femoral fracture: mechanism of injury and fracture morphology. J R Army Med Corps 159:294–299. https://doi.org/10.1136/jramc-2013-000075

76. Liebschner MA (2004) Biomechanical considerations of animal models used in tissue engineering of bone. Biomaterials 25:1697–1714

77. Wedel VL, Galloway A (2013) BROKEN BONES: Anthropological Analysis of Blunt Force Trauma (2nd Ed.). Charles C Thomas Publisher

78. Courtney E, Courtney A, Andrusiv L, Courtney M (2017) Clear Ballistics Gel®: High Speed Retarding Force Analysis of Paraffin-Based Alternative to Gelatin-based Testing of Lead-Free Pistol Bullets. In: 30th International Symposium on Ballistics. DEStech Publications, Inc.

79. Schwab N, Jordana X, Soler J, et al (2023) Can Synbone® cylinders and deer femurs reproduce ballistic fracture patterns observed in human long bones? J Mater Sci 58:4970–4986. https://doi.org/10.1007/s10853-023-08333-6

80. Schwab N, Jordana X, Monreal J, et al (2024) Ballistic long bone fracture pattern: an experimental study. Int J Legal Med 138:1685–1700. https://doi.org/10.1007/s00414-024-03191-6

81. Kieser DC, Carr DJ, Leclair SC, et al (2013) Remote ballistic fractures in a gelatine model - aetiology and surgical implications. J Orthop Surg Res 8:15. https://doi.org/10.1186/1749-799X-8-15

82. Jussila J, Police Technical Centre H Finland, Second Department of Surgery (2004) Wound ballistic simulation: assessment of the legitimacy of law enforcement firearms ammunition by means of wound ballistic simulation by Jorma Jussila. University of Helsinki, Helsinki

83. Kieser J, Taylor M, Carr D (2012) Forensic Biomechanics. John Wiley & Sons

84. Quatrehomme G, İşcan MY (1998) Analysis of beveling in gunshot entrance wounds. Forensic Science International 93:45–60. https://doi.org/10.1016/S0379-0738(98)00030-9

85. Quatrehomme G, Yaşar İşcan M (1997) Bevelling in exit gunshot wounds in bones. Forensic Science International 89:93–101. https://doi.org/10.1016/S0379-0738(97)00121-7

86. HUELKE DF, DARLING JH (1964) BONE FRACTURES PRODUCED BY BULLETS. J Forensic Sci 9:461–469

87. Smith MJ, James S, Pover T, et al (2015) Fantastic plastic? Experimental evaluation of polyurethane bone substitutes as proxies for human bone in trauma simulations. Legal Medicine 17:427–435. https://doi.org/10.1016/j.legalmed.2015.06.007

88. Berryman HE, Smith OC, Symes SA (1995) Diameter of cranial gunshot wounds as a function of bullet caliber. Journal of Forensic Sciences 40:751–754

89. Paschall A, Ross AH (2017) Bone mineral density and wounding capacity of handguns: implications for estimation of caliber. Int J Legal Med 131:161–166. https://doi.org/10.1007/s00414-016-1420-6

90. Ross AH (1995) Caliber estimation from cranial entrance defect measurements

91. Augat P, Schorlemmer S (2006) The role of cortical bone and its microstructure in bone strength. Age Ageing 35 Suppl 2:ii27–ii31. https://doi.org/10.1093/ageing/afl081

92. Wang M, Gao X, Abdel-Wahab A, et al (2015) Effect of micromorphology of cortical bone tissue on crack propagation under dynamic loading. EPJ Web of Conferences 94:03005. https://doi.org/10.1051/epjconf/20159403005

93. Nyman JS, Roy A, Shen X, et al (2006) The influence of water removal on the strength and toughness of cortical bone. J Biomech 39:931–938. https://doi.org/10.1016/j.jbiomech.2005.01.012

94. Pineri MH, Escoubes M, Roche G (1978) Water--collagen interactions: calorimetric and mechanical experiments. Biopolymers 17:2799–2815. https://doi.org/10.1002/bip.1978.360171205

95. Schmitt K-U, Niederer PF, Cronin DS, et al (2014) Trauma Biomechanics: An Introduction to Injury Biomechanics. Springer Science & Business Media

96. Sellier KG, Kneubuehl BP, Haag LC (1995) Wound Ballistics and the Scientific Background: The American Journal of Forensic Medicine and Pathology 16:355. https://doi.org/10.1097/00000433-199512000-00013

97. Fackler ML (1996) Gunshot wound review. Ann Emerg Med 28:194–203. https://doi.org/10.1016/s0196-0644(96)70062-8

98. Wheatley BP (2008) Perimortem or postmortem bone fractures? An experimental study of fracture patterns in deer femora. J Forensic Sci 53:69–72. https://doi.org/10.1111/j.1556-4029.2008.00593.x

99. Muschler GF, Raut VP, Patterson TE, et al (2010) The Design and Use of Animal Models for Translational Research in Bone Tissue Engineering and Regenerative Medicine. Tissue Engineering Part B: Reviews 16:123–145. https://doi.org/10.1089/ten.teb.2009.0658

100. Hillier ML, Bell LS (2007) Differentiating human bone from animal bone: a review of histological methods. J Forensic Sci 52:249–263. https://doi.org/10.1111/j.1556-4029.2006.00368.x

101. Dominguez VM, Crowder CM (2012) The utility of osteon shape and circularity for differentiating human and non-human Haversian bone. Am J Phys Anthropol 149:84–91. https://doi.org/10.1002/ajpa.22097

102. Einhorn TA (1992) Bone strength: the bottom line. Calcif Tissue Int 51:333–339. https://doi.org/10.1007/BF00316875

103. Cohen H, Kugel C, May H, et al (2016) The impact velocity and bone fracture pattern: Forensic perspective. Forensic Science International 266:54–62. https://doi.org/10.1016/j.forsciint.2016.04.035

104. Messerer O (1880) Über Elasticität und Festigkeit der menschlichen Knochen. Cotta

105. Symes SA, L'Abbé EN, Chapman EN, et al (2012) Interpreting Traumatic Injury to Bone in Medicolegal Investigations. In: A Companion to Forensic Anthropology. John Wiley & Sons, Ltd, pp 340–389

106. Christensen AM, Passalacqua NV, Bartelink EJ (2019) Forensic anthropology: current methods and practice. Academic Press

107. Klepinger LL (2006) Fundamentals of forensic anthropology. John Wiley & Sons

108. Tamáska L (1964) Kritische Bemerkungen zur Frage der Geschosskaliberbestimmung aus dem Durchmesser der Einschussöffnungen der Knochen. Zacchia 39:158–170

109. Pollak S, Ritt F (1992) Vergleichende Untersuchungen an Einschusslücken in Rumpf-und Extremitätenknochen mit vorwiegend spongiöser Struktur. BEITRAGE ZUR GERICHTLICHEN MEDIZIN 50:363–363

110. Besant-Matthews PE (2000) Examination and interpretation of rifled firearm injuries. The pathology of trauma, 3rd edn Arnold, London 47–60

111. Steadman DW, Basler W, Hochrein MJ, et al (2016) Domestic homicide investigations: an example from the United States. In: Handbook of Forensic Anthropology and Archaeology. Routledge, pp 351–362

112. Spitz WU, Fisher RS (1980) Medicolegal Investigation of Death, Charles C. Thomas, Springfield, IL

113. Coe JI (1982) External beveling of entrance wounds by handguns. The American Journal of Forensic Medicine and Pathology 3:215

114. Baik S-O, Uku JM, Sikirica M (1991) A case of external beveling with an entrance gunshot wound to the skull made by a small caliber rifle bullet. The American Journal of Forensic Medicine and Pathology 12:334–336

115. Peterson BL (1991) External beveling of cranial gunshot entrance wounds. Journal of forensic sciences 36:1592–1595

116. Madea B, Staak M (1988) Determination of the sequence of gunshot wounds of the skull. Journal of the Forensic Science Society 28:321–328

117. Adharapurapu RR, Jiang F, Vecchio KS (2006) Dynamic fracture of bovine bone. Materials Science and Engineering: C 26:1325–1332

118. Blewitt GT (1997) The role of forensic investigations in genocide prosecutions before an international criminal Tribunal. Med Sci Law 37:284–288. https://doi.org/10.1177/002580249703700402

119. Cordner S, Tidball-Binz M (2017) Humanitarian forensic action — Its origins and future. Forensic Science International 279:65–71. https://doi.org/10.1016/j.forsciint.2017.08.011